Cationic and Anionic Dual Polymer Pairs for Mature Fine Tailings Flocculation and Dewatering

by

Ying Zhu

A thesis submitted in partial fulfillment of the requirements for the degree of

Master of Science

in

Materials Engineering

Department of Chemical and Materials Engineering
University of Alberta

ABSTRACT

The accumulation of oil sands tailings poses serious environmental issues in Alberta, Canada. In the tailings ponds, the fine clays and residual bitumen form the so-called mature fine tailings (MFT) which contain 30~40 wt% fine solid particles primarily below 44 μm in size, 1~3 wt% residual bitumen with the balance water. Without any physical or chemical treatment, the MFT remains as a stable suspension in tailings ponds indefinitely. Adding a polymer as a process aid to treat the oil sands tailings has been investigated for many years to cause fine solids to flocculate and thus accelerate dewatering. However, the performance of single polymer treatment is generally unsatisfactory. Recent studies in sewage treatment suggest that a dual polymer method, in which two different polymers are added in sequence, has a better flocculation performance.

In this study, the use of dual polymer pairs in the flocculation and dewatering of MFT was investigated. A cationic polydiallyldimethylammonium chloride (polyDADMAC) polymer (Alcomer 7115, from BASF) and an anionic linear polyacrylamide polymer (A3335, from SNF) were found to be an effective combination in MFT dewatering treatment by filtration. The effects of polymer dosage, filtration pressure and the sequence of polymer addition were studied. Capillary suction time (CST) and specific resistance to filtration (SRF) were measured to evaluate the dewaterability of treated MFT. From the experimental data, MFT treated with the polymer combination of Alcomer 7115 and A3335 can give low CST results around 50 s, compared with around 3000 s of untreated MFT. Also the SRF was decreased from a magnitude of 10^{14} m/kg to 10^{12} ~ 10^{13} m/kg, indicating treated MFT being relatively much easier to dewater. Cryogenic scanning

electron microscopic (Cryo-SEM) images of the treated MFT were taken to show the morphology of the MFT with or without treatment with either a single polymer or dual polymer pairs. The results demonstrated that the pore sizes are larger when the dual polymer pairs were used, implying higher dewaterability of MFT in this case.

Acknowledgements

I would like to thank my supervisor Dr. Qi Liu for his excellent guidance and most patient help on both my courses and graduate research at University of Alberta.

I would like to thank Dr. Xiaoli Tan, research associate of IOSI and co-Principal Investigator of this project, for his valuable advice on my research and numerous help to solve my academic questions.

I would like to thank the lab technicians of IOSI: Lisa Brandt, Jeremiah Bryksa, Yahui Zhang, Brittany Mackinnon and intern student Mubaraka Husain for all of the lab assistance they provided.

I would like to thank Simon Yuan (Syncrude) and Babak Jajuee (Imperia Oil) for the feedback and technical advice they gave.

Finally, I would like to thank Natural Resources Canada (NRCan) and Imperia Oil Limited for the financial support provided to carry out this work.

Table of Contents

List of Tables

List of Figures

1 Introduction

1.1 Oil Sands in Alberta

It has been proven that Alberta's oil sands are the third-largest crude oil reserve in the world after Saudi Arabia and Venezuela [1]. Alberta's oil sands are distributed under about 142,200 km^2 of land in Athabasca, Cold Lake and Peace River areas in northern Alberta and contain about 1.7 trillion barrels of bitumen in place [2] [3] (Figure 1.1).

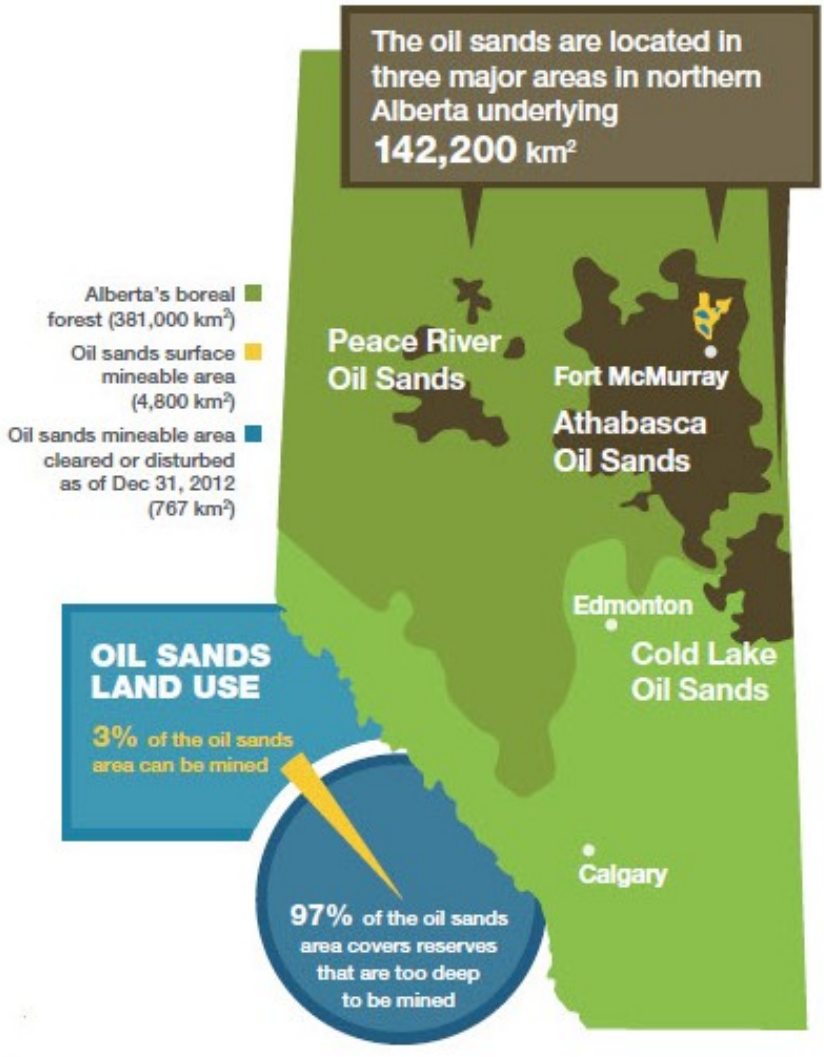

Figure 1.1 Distribution of oil sands in northern Alberta [4].

There are two different methods of producing oil from oil sands: open-pit mining and in-situ methods. Open-pit mining is used to mine the oil sands that are close to the surface and the mined oil sands ores are treated by the hot water extraction process to recover the bitumen. In-situ methods produce bitumen that is deep-buried in the ground using specialized extraction techniques, such as steam-assisted gravity drainage (SAGD). Approximately 80% of Alberta's oil sands are recoverable using in-situ production, while only 20% (which impacts only 3% of the surface area of the oil sands region [5]) can be recovered by mining [6].

From the first commercial production of oil from the Alberta oil sands in 1967, at about 12,000 bbl/day [7], the production rate reached 1.9 million bbl/day in 2014 [8], and is expected to reach 5.3 million bbl/day by 2030 [9].

1.2 Oil Extraction Processes

Oil sands are a natural mixture of sands, clay, various minerals, water and bitumen. It is believed that the sand grains in oil sands are surrounded by a layer of water and a film of bitumen. The bitumen content of Alberta oil sands ranges from 0 to 19 wt%, with an average content of 12 wt%. The content of water ranges from 3 to 13 wt% depending on the types of oil sands ores. The balance of the oil sands mass are mineral materials, which are mainly quartz, silts and clay [10]. The structure of Alberta oil sands makes the bitumen in the oil sands extractable by the Clark hot water extraction (CHWE) process. Nowadays, the typical operating slurry temperature is about 40~55°C [11].

In the open-pit mining operation, the oil sands are mined using shovels and trucks. The mined oil sands are crushed and mixed with caustic (NaOH) warm water to liberate the

bitumen from the sands/clays. Vigorous mechanical mixing as well as long hydrotransport pipelines are utilized, resulting in further lump size reduction. Bitumen is released from sand grains during mixing or inside hydrotransport pipelines. After air is introduced, air bubbles attach to bitumen. The aerated bitumen floats to the top and forms bitumen froth. Then the bitumen froth is skimmed off from the slurry in primary separation vessels (PSV). Small amount of bitumen droplets, which is usually un-aerated and remaining in the slurry, is further recovered by induced air flotation in mechanical floatation cells and tails oil recovery vessels, or cyclo-separators [12]. The process is shown in Figure 1.2. A typical overall bitumen recovery in commercial operations is about 88~95 %.

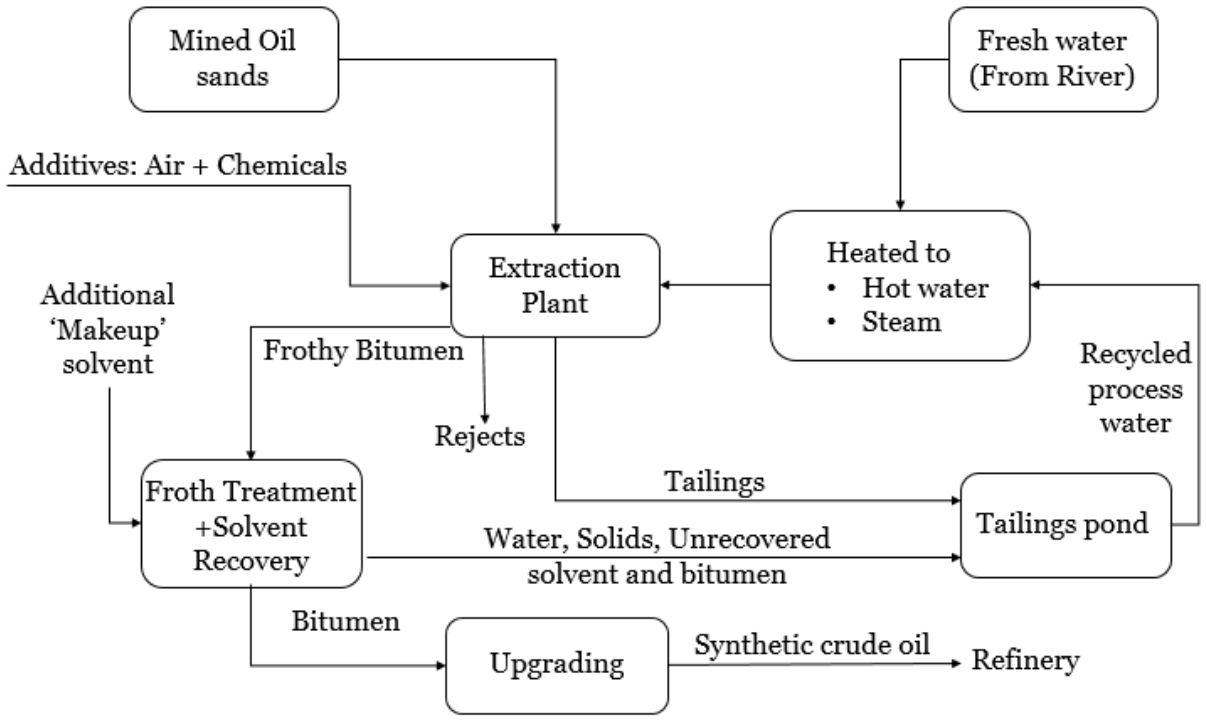

Figure 1.2 Schematic flowsheet of hot water extraction process for oil sands.

The bitumen froth normally contains 60 wt% bitumen, 30 wt% water and 10 wt% solids [11]. After de-aeration, the bitumen froth is mixed with solvents to obtain a sufficient

density difference between water and bitumen as well as to reduce the viscosity of bitumen. This expedites the separation of water and solids from bitumen using inclined plate settlers, cyclones or centrifuges. The clean mixture of diluent and bitumen is then sent to upgraders.

1.3 Oil Sands Tailings

1.3.1 Compositions and Properties of Oil Sands Tailings

After bitumen extraction, the remaining mixture of water, coarse sands, fine clays and residual bitumen is defined as tailings and discharged into tailing ponds for solid-liquid separation. During separation, the clarified water can be recycled from the pond and used in the extraction circuit. Coarse sand particles precipitate quickly and form beaches, while remaining fine tails with a solids content of 6~10 wt% accumulate in the tailing ponds. Those fine tails settle quickly to 20 wt% solid, and reach 30 wt% over a few years, which is the so-called mature fine tailings (MFT).

MFT contains 30~40 wt% of fine solids with a diameter below 44 μm, and 1-3 wt% of residual bitumen, with balance water. It will remain in a fluid state for decades because of its extremely slow consolidation rate [13], which is mainly caused by the stable gel-like structure.

1.3.2 Environmental Issues Posed by Mature Fine Tailings

With the high production rate of bitumen, the accumulation of tailings requires large area tailing ponds, which has a detrimental impact on landscape. This is a concern because currently there is no technology to reclaim the tailings. About 1.5 barrels of MFT are

accumulated in tailings ponds per barrel of bitumen produced [14]. Up to now, the existing tailings ponds occupied 176 km^2 (67 mi^2) land in northern Alberta [15]. And in the next few decades, due to the anticipated increase in production rate, the accumulation of MFT is expected to grow at an increasing rate.

Besides the impact to landscape, a more serious problem is the environmental pollution it caused. The toxic materials contained in the tailings, including naphthenic acids, polycyclic aromatic hydrocarbons, phenolic compounds, ammonia, mercury and other trace metals [16], pose risks to wildlife and aquatic organisms. Moreover, the pollutants reported to be emitted from oil sands tailings ponds, volatile organic compounds (VOCs), greenhouse gases (including carbon dioxide (CO_2) and methane (CH_4)), and reduced sulfur compounds (RSCs) (including hydrogen sulfide (H_2S)) [17], can react near the ponds to produce secondary pollutants or can be transported further away [18]. The effect of those pollutants are still largely unknown. However, more and more investigation indicate that those pollutants are fatal to surrounding living organisms.

In addition, 2~3 m^3 water are needed to produce every one barrel of bitumen. Due to the current rate of bitumen production, the demand of water is massive. Current tailings treatment technologies allow the recycle of about 75% of the process water, so that 25% of the required water is still drawn from fresh water supply, which amounts to 0.5~0.75 m^3 (or about 3~5 barrels) per barrel of produced bitumen [19]. Therefore, the treatment of mature fine tailings is required so that the large amount of water held by it can be released and then reused, with a target of potentially 100% water recycle.

1.4 Objectives of Research and Description of Thesis

1.4.1 Objectives of Research

It is hypothesized that dual-polymer treatment for mature fine tailings is more effective than current single-polymer treatment. The objective of this thesis is to seek polymer pairs to assess the dewatering effect in dual-polymer treatment, as well as to convert fluid MFT into stackable solids through dual-polymer treatment and filtration methods.

1.4.2 Hypothesis of Mechanism for Dual-polymer Treatment

The addition of polymer flocculants/coagulants to an aqueous suspension of solid particles would lead to the formation of connected aggregate structures of many particles (flocs) by polymer bridging/charge neutralization. The formation of the flocs with porous structure will benefit dewatering [20] [21]. The idea of dual polymer treatment is to take advantage of interaction of two different polymers thus to obtain flocs of MFT with higher porosity and suitable mechanical strength, which allows easier water removal. The working mechanism of dual-polymer treatment for MFT was hypothesized as shown in Figure 1.3.

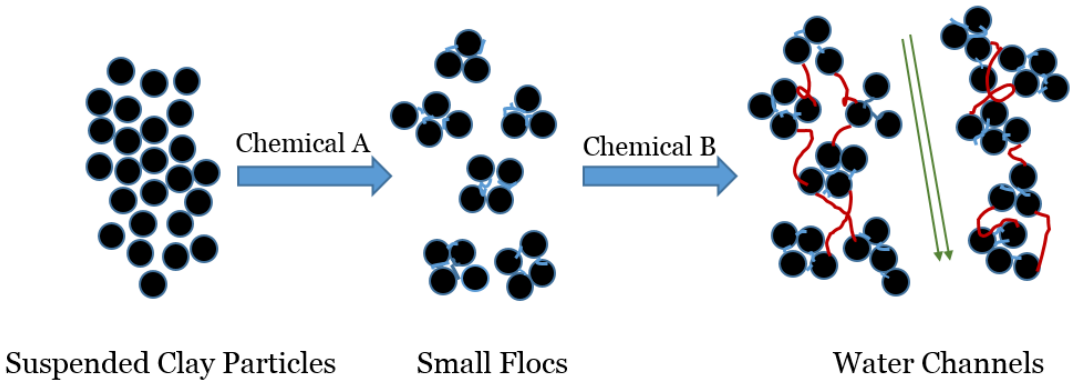

Figure 1.3 Schematics of dual-polymer treatment mechanism.

The addition of the first chemical would bring fine particles together and form small flocs. With the addition of the second chemical, it would further aggregate the fine particles as well as those small flocs into larger flocs, forming porous structure. And the pores can be considered as water channels during dewatering (filtration) process. Therefore, larger pore size would lead to better filterability of MFT.

1.4.3 Description of Thesis

The idea of dual-polymer treatment was inspired by sewage treatment technologies. Recent studies in sewage treatment suggest that a dual polymer method has a better flocculation performance and leads to better water clarity in dewatering treatment of wastewater. As the current single polymer treatment for MFT is not satisfactory, and as there are many similarities between sewage treatment and MFT treatment, dual-polymer treatment is investigated for MFT dewatering.

Performance parameters such as capillary suction time (CST) and specific resistance to filtration (SRF) that are used to evaluate dewatering performance in wastewater treatment are adopted to assess the dewaterability of MFT. A series of experiments were conducted to justify the usability of those parameters to indicate the dewaterability of MFT.

Polymer treatment is actually a process of flocculation. A key factor of flocculation is mixing, which is mainly affected by stirring time, stirring speed, the type of impellers used as well as the ratio of impeller diameter to container diameter. Based on the understanding of flocculation and preliminary experimental results, a general procedure

for dual polymer treatment was developed, which was found to be most effective under our lab conditions.

Different combinations of chemicals were tested until a polymer pair, consisting of a cationic polyDADMAC polymer (Alcomer 7115, from BASF) and an anionic linear polyacrylamide polymer (A3335, from SNF), was found which gave best dewaterability of MFT. Based on these two polymers, a series of experiments were conducted to find an optimum dosage for the treatment. Filtration tests were carried out after the treatment to remove water and to increase the final solid content of filter cakes, as well as to study the specific resistance of treated MFT. The highest solid content in the MFT after filtration is around 64 wt%, which is higher than that obtained using other MFT treatment technologies. Filtration tests assisted by pressure and vacuum were compared to further understand the dewatering effect of dual polymer treatment. Cryogenic scanning electron microscopic (cryo-SEM) images were obtained to visualize the structure of MFT as well as single-polymer and dual-polymer treated MFT, to verify the validity of proposed mechanism for dual-polymer treatment.

Based on the phenomena observed during polymer treatment experiments and filtration tests, other specific types of polymers (α-cellulose, geopolymers, chitin, etc.) were investigated aiming at obtaining higher solid contents in treated MFT.

2 Literature Review

2.1 High Water Holding Capacity of MFT

As mentioned in introduction, MFT is a stable suspension with 1~3 wt% residual bitumen, 30~40 wt% fine particles with the remainder being water. Therefore, around 60~70 wt% of the mass of MFT is trapped water, which suggests that MFT has a high water holding capacity. And this can be attributed to several reasons, outlined in the following.

2.1.1 The Effect of Ultrafine Solids

Numerous research attributed this high water holding capacity of MFT to the presence of ultrafine solids (<0.3 μm) [22]–[24]. There are two major types of ultrafine solids contained in MFT: hydrophilic ultrafine solids (HUS) and biwetted ultrafine solids (BUS). Both of these two types of ultrafine solids are responsible for the stable gel formation in MFT. The BUS are associated with various amount of strongly bounded organic material (SOM). Biwetted particles seem to aggregate rapidly in dilute suspensions in electrolyte solutions, as the settlement of sludge below 6 wt% solids is rapid. But they enhance the gel-forming propensity in concentrated suspensions---once the solids content rises above 30 wt% the gel-structure is difficult to break [25]. However, it has been found that the presence of ultrafine particles of appropriate sizes is a necessary but not adequate condition for the formation of MFT [26].

2.1.2 The Effect of Residual Bitumen

In earlier studies, SEM images were presented to show that bitumen existed in the MFT as free droplets of 1~10 μm in diameter. Researchers found that some of those droplets also contaminate the edges of clays, which may contribute to the stability and high water holding capacity of MFT structure. Moreover it has been found that the presence of residual bitumen can be detrimental to the hydraulic conductivity of MFT [27] [28], since free bitumen droplets can block the pores between particles, thus trapping water inside and hindering the consolidation of MFT (Figure 2.1).

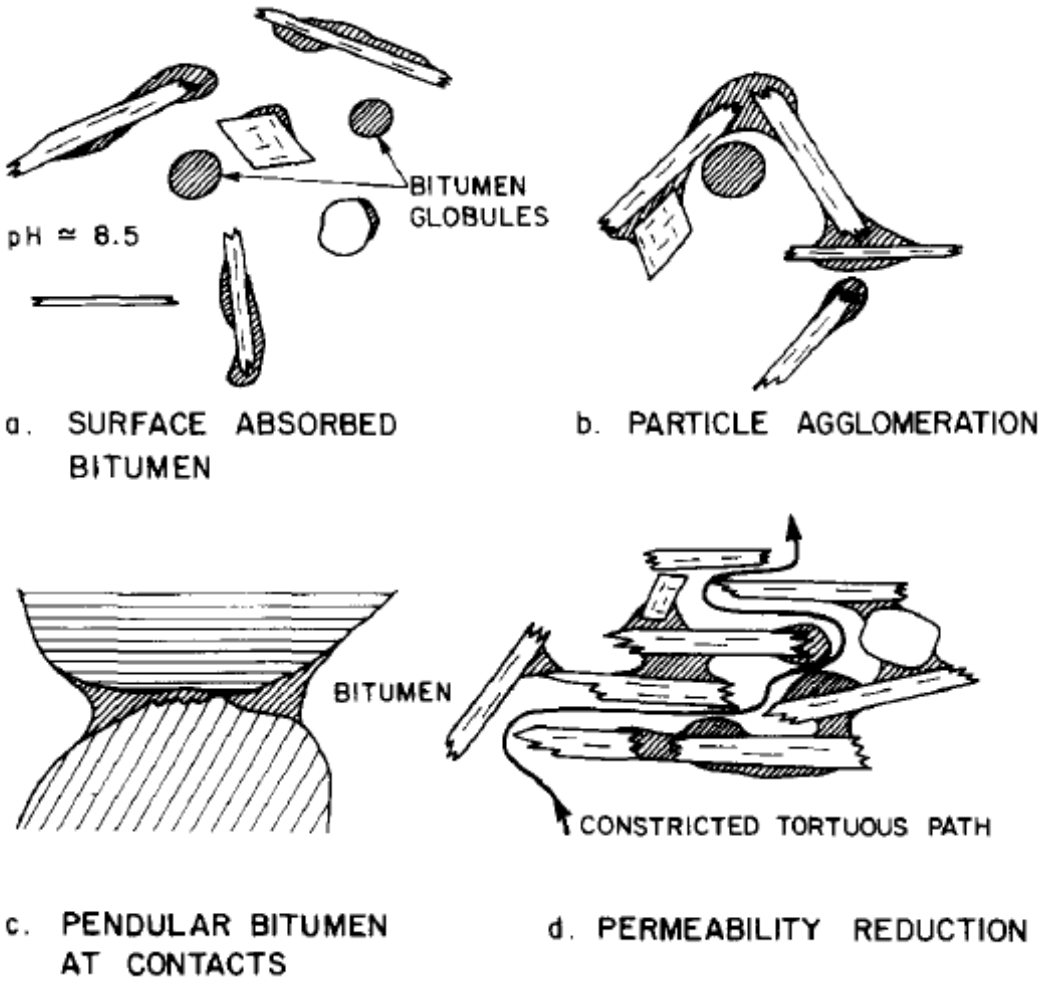

Figure 2.1 Effect of bitumen on particle settlement and permeability [27].

In other studies, it was believed that the stable structure is due to the presence of water-soluble asphaltic acids in the bitumen, which act as clay dispersants [10].

2.1.3 Summary

Both ultrafine solids and residual bitumen play an important role in the formation of stable gel-like structure of MFT. However, at present, the distributions of clay particles or ultrafine solids, the nature of the organics, and the effect of residual bitumen are poorly understood. Hence, findings suggest that the stability and high water retention of MFT is due to the combined effects of the presence of fine solids and the effect of residual bitumen [29]. Further investigation is required to find out which factor(s) played a more significant role.

2.2 Current Technologies for Tailings Treatment

Due to those serious environmental issues the oil sands tailings brought forth, technologies aiming to reduce tailings volumes are investigated. Over the last few decades, significant efforts have been made to develop effective technologies to dewater and consolidate oil sands tailings [10] [30], which led to the exploitation of many methods for the treatment of tailings. Several major technologies are discussed in the following sections.

2.2.1 Natural Process

During natural process, tailings are pumped into tailings ponds directly to be densified by gravitational consolidation and sedimentation. Therefore this processing method is also called sedimentation or consolidation. After separating solids from tailings stream,

the supernatant is recycled to the extraction process. Natural processing method is low-cost. However, large areas of land are required to treat large quantities of tailings. Furthermore, this technology accepts that the MFT will consolidate over a very long time period in the order of hundreds of year. As a consequence, natural methods can hardly solve MFT problem considering current situations.

2.2.2 Composite Tailings (CT)/ Non-segregating Tailings (NST)

Composite/consolidated tailings process involves mixing coarse sands and coagulant (commonly used coagulant is gypsum) with MFT to generate non-segregating tailings which can be pumped to ponds. In several years, the fines consolidate and a soft deposit is formed. The main factors that affect the formation of non-segregating tailings are, contents of fine solids, mineralogy, water chemistry and particle size distribution [31]. For one cubic meter of MFT, after mixed with certain volume of coarse sands, it generates about 2.2 m^3 (contains about 57 wt% solids) of fresh CT. And after the process, it can be consolidated to 1.2 m^3 (contains about 80 wt% solids) of CT deposit [32]. This technology densifies MFT to a relatively high solid content in a reasonable time. However, a few challenges still remain to be overcome before it can be put in wide industrial application. Firstly, there is insufficient sand to treat all MFT with CT process. Secondly, CT remains to be fluid so tailings dams are still required. Moreover, the water released from this process is detrimental to bitumen recovery when recycled back to extraction process, as the addition of gypsum increases the calcium ion content in recycled water [33].

2.2.3 Thickened Tailings/Paste Technology

In thickened tailings process, both the extraction fine tails and beach run-off streams are introduced into a process vessels called thickeners, as showed in Figure 2.2.

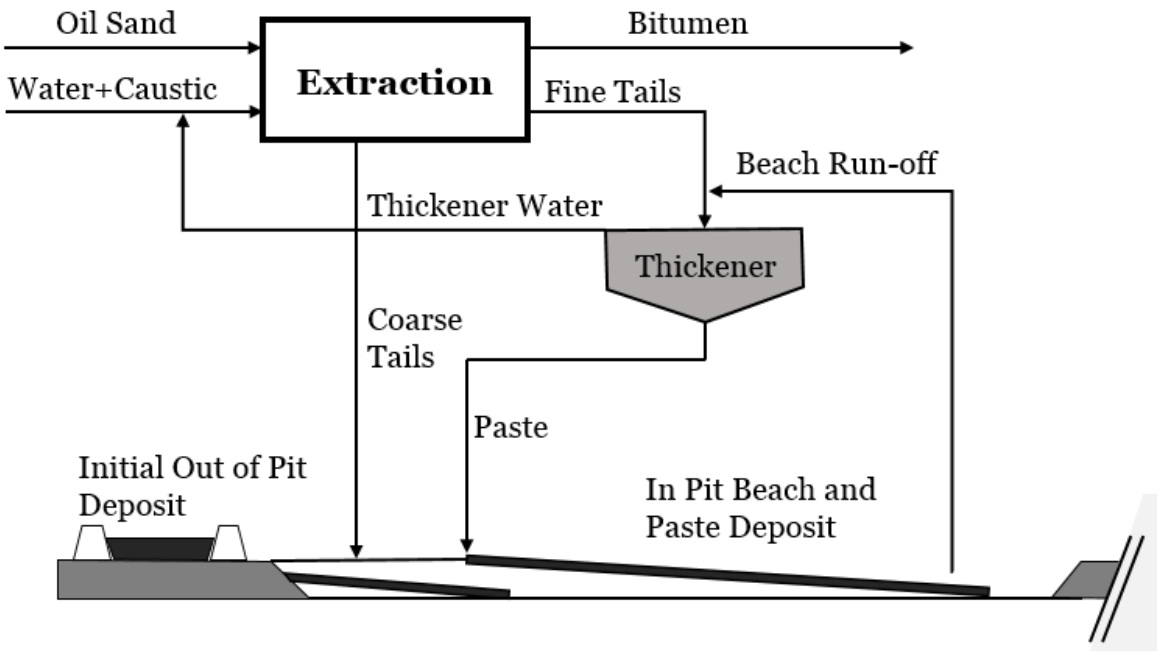

Figure 2.2 Schematic flowsheet of Thickened Tailings Disposal Concept [34].

During the operation chemicals are added to coagulate/flocculate fine particles into larger particles in order to enhance gravity settling of solids in water, thus increasing the density of bottom flow of the thickener. High molecular weight, medium charge anionic polymers, such as partially hydrolyzed polyacrylamide (for example: Percol 727, Percol 336) have been used for flocculating fine particles and have shown good results on dewatering of MFT [34].

The underflow contains most of the coarse sand, and most of water carrying most of fines goes to the overflow. Clarified water from the thickener is recycled back to extraction for

re-use. The target of thickener operation is to densify tailings to a solid content of 45~55 wt%, and pumped to store behind engineered containment [35]. Slurry density obtained from normal practice is about 30 wt% solids, and with the addition of sands a higher density can be obtained [32]. The advantages of this technology are that the rapidly released processed water can be reused immediately in the extraction process, and it shortens the time of gravity settling from years to half an hour. However, the thickened tailings process/paste technology has not been applied to treating MFT.

2.2.4 Emerging Technologies for Tailings Treatment

As the limitations of CT technologies are more and more noticeable, and the legacy MFT continues to grow, new technologies are studied. They focus on solidifying fine tailings directly, without making mixtures of fines and coarse sands before treatment.

One of those technologies is in-line thickening with thin lift dewatering, which involves in-line treatment of MFT using an anionic polyacrylamide flocculant, followed by thin layer deposition [32] [35] [36]. A significant disadvantage of this method is that after a layer reached a certain solid content, it needs to be removed from the surface and transported to another deposition point, which adds complexity and extra cost to the process. Also, very large areas are required to operate the thin-lift drying process.

Centrifugation is another technology in development for MFT treatment [35]–[37]. Before processing, MFT is required to be diluted to a certain concentration, then the diluted MFT is mixed with a polyacrylamide solution before feeding into a centrifuge. The “cake” after centrifuge can reach a solid content of 55~60 wt%. Although the separation forces is thousands of times higher than gravitational force, the high cost of this process

makes it less attractive. Besides, testing at full scale is needed to properly evaluate the potential of this technology.

2.2.5 Summary

Each of those technologies, conventional or new, has certain advantages. However, up to now, no technologies are proven to be effective in converting fluid mature fine tailings into stackable tailings. Furthermore, most of the technologies involved in using flocculent to bring fine particles together. Nevertheless, to achieve a good flocculation of MFT, the MFT needs to be diluted first, which significantly limited the overall applicability of those technologies.

2.3 Flocculation

Through the studies of the properties and structure of MFT, as well as tailings treatment practice, clay particles (fine particles) are always found to be among the crucial factors affecting the dewaterability of MFT. The addition of a flocculant not only becomes a major process in most technologies for tailings treatment, but it is also widely used in minerals industry, pulp and paper industry and wastewater treatment. Commonly used flocculants include cationic, anionic and non-ionic organic macromolecules [38].

2.3.1 Mechanisms of Flocculation

There are three major mechanisms for flocculation brought about by adding flocculants: 1) bridging, 2) charge neutralization, 3) electrostatic patch models [39]. During bridging flocculation, the loops and tails of a polymer molecule are attached to more than one particles/aggregates, thus bringing them together to form large aggregates, as shown in

Figure 2.3 (a). Therefore, high molecular weight of the used polymer is required so that segments of the polymer are long enough to pass the electrostatic barrier of the particles. Charge neutralization mechanism acts on particles by reducing their electric double layer repulsion due to adsorption of highly charged polyelectrolytes on particles carrying opposite charges. The electrostatic patch flocculation is caused when polymers of very high charge density interact with oppositely charged particles of low charge density. Thus the net residual charge of polymer patch on one particle can attach to the bare part of another particle oppositely charged, as shown in Figure 2.3 (b).

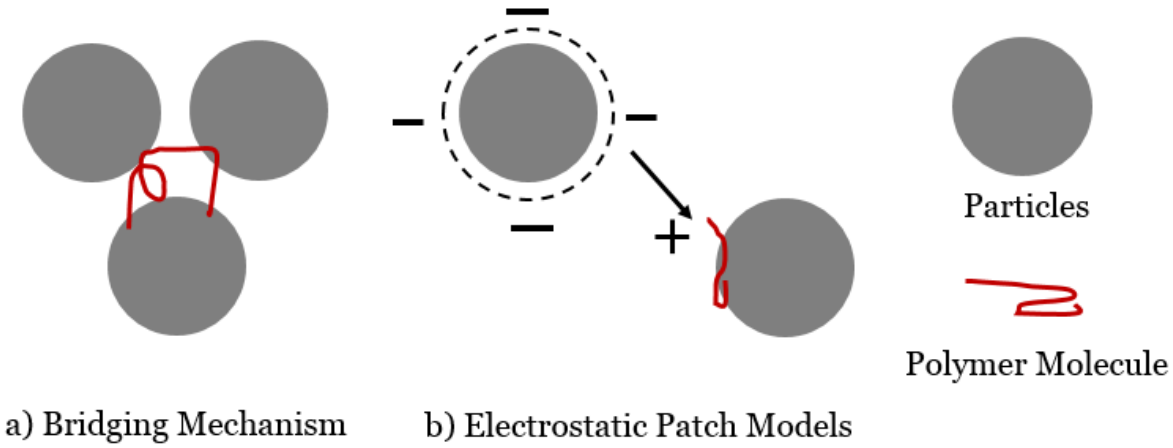

Figure 2.3 Schematics of a).bridging mechanism b).electrostatic patch models.

2.3.2 Stages of Flocculation Processes

The addition of polymers to a suspension is to destabilize the suspension by forming large aggregates thus to separate solids from liquid. The flocculation process usually involves following stages [40]:

1) Mixing of the polymer molecules with particles.

2) Attachment of polymer chains on particles (adsorption).

3) Re-conformation of the attached chains from their initial state to an eventual equilibrium.

4) Flocculation of particles either by bridging or by charge effects.

5) Break-up of flocs.

The stages of the flocculation process are shown in Figure 2.4.

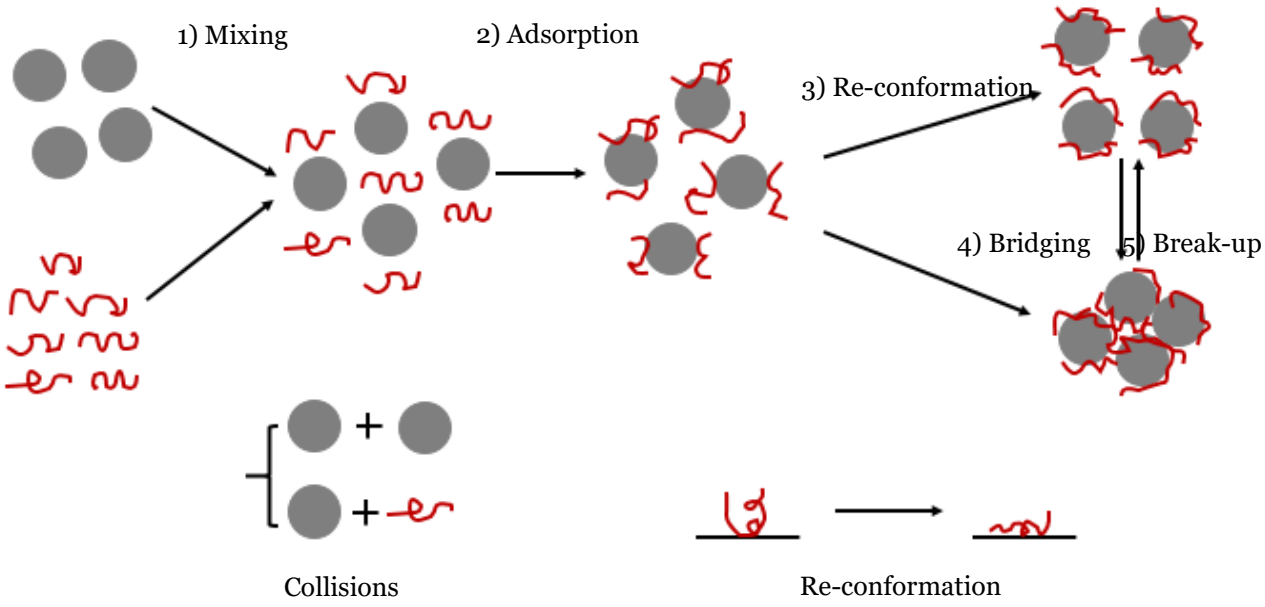

Figure 2.4 Schematics of flocculation with adsorbed polymers.

In practice, these stages do not necessarily happen in a certain sequence, and they can happen simultaneously and are often competing against each other. This makes the flocculation process complicated and difficult to analyze directly. Therefore, it is important to understand the flocculation mechanisms and study the key factors that have significant influence on each stage. One of the most crucial factors among those is the time period each stage undergoes. Other factors such as mixing, polymer molecular

weight, polymer concentration, background electrolyte concentration and particle concentration [41], are important for flocculation too.

2.3.3 Effect of Mixing

Due to their high molecular weight, polymer flocculants usually form very viscous stock solutions. Proper mixing is required to disperse such solutions uniformly into suspension rapidly, and to induce collisions between particles and polymer molecules. Inadequate mixing causes a local overdose of the polymers, resulting in steric stabilization which is thought to be the origin of residual haze and poor filterability in flocculated suspensions [42], also it does not allow flocs to grow sufficiently large in the time period available. On the other hand, excessive agitation causes breakage of flocs, leading to a reduction of possible maximum floc sizes [43]. It is interesting to note that some studies indicated that certain degree of floc breakage can in fact improve the dewaterability of MFT [44]. Clearly, for each individual system, there appears to be an optimum mixing scheme (time and intensity) [45] [46].

2.3.4 Effect of Polymer Dosages and Molecular Weight

Polymer dosage has a direct effect on the final size and structure of flocs, thus determines the dewaterability to some degree. A low polymer dosage may not be sufficient to bridge fine particles to form flocs (adsorption). While an excessive polymer dosage may cause steric stabilization of the particles. Only the optimum dosage of polymer will give a best polymer adsorption rate, which corresponds to optimum flocculation, as shown in Figure 2.5. The optimum flocculation occurs when the flocculant dosage is such that it causes less than complete coverage of particles. This is because the incomplete surface coverage

ensures that there are unoccupied surface sites for polymer adsorption during collision [47].

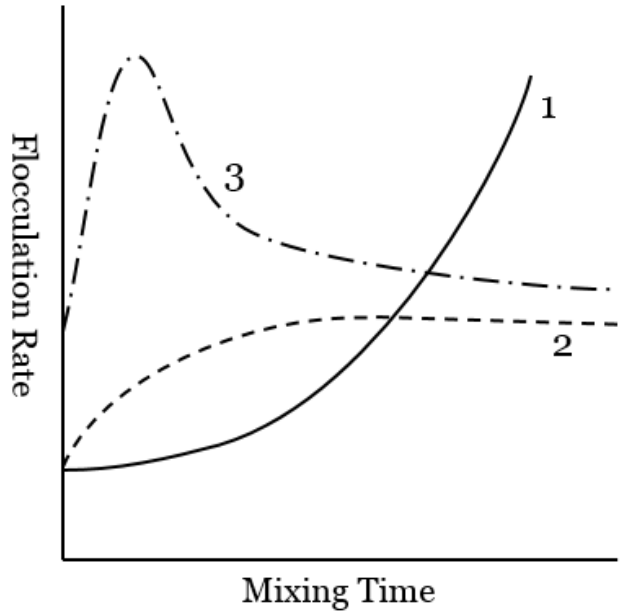

Figure 2.5 Schematics of flocculation rate of polymers 1. "Optimum" polymer dosage with dilute suspension; 2. Higher than optimum dosage with dilute suspension; 3. Sub-optimal dosage with concentrated suspension [40].

For bridging flocculation, higher molecular weight is advantageous, as the molecules are large enough to extend beyond the range of electrostatic repulsion and to reach particles, which makes it easier for polymer adsorption [48]. Also, high molecular weight flocculants can link more particles together, leading to larger flocs. It was found that the collision frequency will be higher for larger particles [49]. As a result, relatively larger particles tend to be flocculated more readily than smaller particles, leaving the latter suspended, which leads to high supernatant turbidity after sedimentation. Further investigation found that a sequential addition of low and high molecular weight polymers provides best results for flocculation as well as high clarity of supernatant [50].

2.3.5 Conformation of Adsorbed Polymers

Once polymers are adsorbed, they can re-conform on the particle surface. The re-conformation depends on the polymer-particle interaction (Figure 2.6). If the polymer has a flat conformation, it may not extend far enough from the particle surface to bridge with particles. A flat conformation can also block further polymer adsorption thus hinder the overall flocculation process [51]. A study found that the adsorption of anionic polyacrylamide on the alumina surface is in a flat conformation initially, but over time, as more polymers are adsorbed, the conformation becomes more extended. This is due to the repulsion force between polymer molecules [52]. Another study carried out on kaolinite showed that particles bridged by polymers with higher charge density have smaller polymer "loops" and "tails", while the particles flocculated by lower charge density polymers have further extended "loops" and "tails" [53]. The latter produces larger flocs and allows a faster settling rate. Possible conformations of polymer molecules adsorbed at solid/water interface are showed in Figure 2.6.

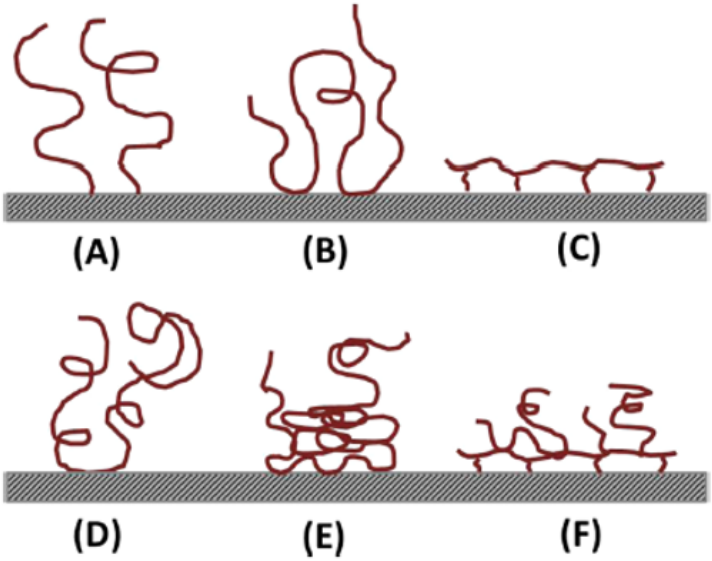

Figure 2.6 Possible conformations of polymer molecules adsorbed at solid/water interface: (A) single point attachment (weak binding); (B) loop adsorption; (C) flat multiple site attachment (strong adsorption); (D) random coil (high molecular weight polymers); (E) non-uniform segment distribution; and (F) multilayer adsorption [52].

2.3.6 Summary

Flocculation in practice is a complicated process involving many sub-steps. These sub-steps do not necessarily occur in sequence but are simultaneous and competing with each other. Moreover, flocculation process cannot be analyzed directly. Parameters used to monitor the process are usually indirect measurements. As a result, the choice of polymers in any particular application is largely an arts rather than science [54].

2.4 Current Development of Polymer Treatment of MFT

Most MFT treatment studies or practices involve the use of one additive and/or dilution. Problems associated with water recycling and further consolidation of the fluid fine tailings limit the implementation of those technologies on an industrial scale. Therefore,

new and emerging technologies are aimed at treating MFT without dilution or any pre-processing.

2.4.1 Polymers Used in MFT Treatment

Various polymers, both natural and synthetic, have been tested as flocculants to treat MFT. Biopolymers, mainly polysaccharides, are usually biodegradable, non-toxic, and shear-stable [55]. Also another big advantage of biopolymer is that they have very wide sources and of low cost. However, compared to natural polymers, synthetic polymers are much more effective in flocculation applications due to the fact that they can be tailored according to the needs of the applications [56]. Among synthetic polymers, those commonly used ones are poly(ethylene oxide) in the nonionic category, poly(diallyldimethylammoniumchloride) or in short polyDADMAC in the cationic category, as well as polyacrylamide and poly(styrenic sulfonic acid) in the anionic category [56]. Polyacrylamide can be easily hydrolyzed resulting in anionic charge. It is well known that polyacrylamide and its copolymers are used as good flocculants in mineral and pulp & paper industry. Nevertheless, a drawback of polyacrylamide is that it can be easily degraded by shear.

The study in this thesis is mainly based on the use of two synthetic polymers: A cationic polydiallyldimethylammonium chloride (polyDADMAC) polymer Alcomer 7115 and an anionic linear polyacrylamide polymer A3335, which were found to be very effective in MFT treatment.

2.4.2 Modification of Single Polymer Flocculation for MFT

Most of the studies on MFT treatment were focusing on single polymer treatment [19], [57]–[59]. Conventional single polymer treatment is not effective for tailings with high fines content such as MFT. Derived from sewage treatment, recent studies suggest that a dual polymer method, in which two different polymers are added in sequence, has a better flocculation performance and leads to better water clarity in dewatering treatment [60] [61]. It has been shown that the use of a combination of low and high molecular weight polymers gives better dewatering characteristics of aerobically digested activated sludge [61]. Data in the literature also suggested that dual-polymer flocculants of opposite charge give a higher final solid content of filter cake compared to dual flocculants of like charge [62].

In consideration of the similarities between wastewater treatment and fine tailings treatment, the dual polymer treatment method is investigated for oil sands tailings. A novel study from Syncrude [50] investigated the use of combinations of coagulation (C) and flocculation (F) for diluted fine tailings treatment. In most studies, the term coagulation and flocculation are used interchangeably. Here, coagulation refers to charge neutralization process while flocculation indicates bridging process. The researchers from Syncrude conducted experiments on a coagulation process followed by a flocculation and then again by a coagulation (denoted as CFC), to compare with a flocculation process followed by a coagulation stage and then again a flocculation (FCF), as well as to flocculation process followed only by a coagulation stage (FC). Their results showed that the FCF sequence gave large final floc size, resulting in fast initial settling rates.

2.4.3 Summary

Although there are a few reported studies on using dual polymers in dewatering, the majority of them have been empirical studies. The mechanisms of the complicated dual-polymer treatment system are not well understood. In the case of MFT, almost no systematic investigation was conducted to thoroughly assess the dewatering effect of dual polymers on undiluted MFT.

3 Materials and Methods

3.1 MFT Samples and Reagents

3.1.1 MFT Samples

The MFT sample used in this study was collected in 2010 from the same depth of a same Syncrude tailings pond, and packed in different buckets. The MFT in each bucket was homogenized with a Makita 6013BR hand-held agitator before sub-sampling to smaller buckets (around 550 g MFT in each small buckets) for experiments. The MFT sample was analyzed by Dean-Stark extraction and was found to contain 35.6 wt% solids, 2.7 wt% bitumen and 61.7 wt% water. Quantitative X-Ray Diffraction (QXRD) analysis shows that it consists of 27.4 wt% quartz, 2.6 wt% K-feldspar, 3.2 wt% siderite, 36.0 wt% kaolinite and 30.7 wt% illite. Also the particle size distribution is characterized by volume distribution using Mastersizer 3000: the volume median diameter (Dv50) is 7.4 μm, 10 % of distribution of fine particles that are smaller than 1.3 μm, and 90 % of distribution of them are smaller than 35.1 μm.

3.1.2 Reagents

Different pairs of chemicals were tested, as shown in Table 3.1. Sodium dodecyl sulfate, sodium dodecyl benzenesulfonate and sodium lignosulfonate are from Sigma-Aldrich and are of reagent grade; Alcomer 7115 and Magnafloc series (Magnafloc 5250, Magnafloc 156 and Magnafloc 336) are from BASF; A3335 is from SNF provided by Imperial Oil; Lignin is from West Fraser Mills; Cellulose nanocrystals are from AITF and Celquat is from Akzo Nobel. All these polymer samples are commercial grades.

Other reagents with a potential to improve the dewaterability of MFT treated with this combination (Alcomer 7115 and A3335) were tested as well. Among those reagents, α-Cellulose and Chitin powder is from Sigma-Aldrich, the latter is of practical grade; sodium silicate is manufactured by Fisher Scientific and of technical grade; sodium hydroxide is from Fisher Scientific and of ACS reagent grade; sporosarcina pasteurii bacteria solutions were provided by Civil and Environmental Engineering, University of Alberta.

Table 3.1 Chemicals tested

<table>
<tr><th>Chemical A</th><th>Chemical B</th></tr>
<tr><td>–</td><td>Anionic polyacrylamide polymers (Magnafloc series) (MW: 15-22 million g/mol)</td></tr>
<tr><td>Sodium dodecyl sulfate</td><td rowspan="8">Anionic linear polyacrylamide polymer (A3335) (MW:17 million g/mol)</td></tr>
<tr><td>Sodium dodecyl benzenesulfonate</td></tr>
<tr><td>Lignin</td></tr>
<tr><td>Sodium lignosulfonate</td></tr>
<tr><td>Cellulose nanocrystals</td></tr>
<tr><td>Cationic Cellulose derivatives (Celquat) (MW: 50,000 – 90,000 g/mol)</td></tr>
<tr><td>Cationic polyDADMAC polymers (Alcomer 7115) (MW: 200, 000 - 400,000 g/mol)</td></tr>
</table>

The typical procedure was to add the chemicals (polymers) with a lower molecular weight (MW) to generate small flocs, followed by the high MW polymers. Of all the combinations of chemicals listed above, a polymer pair of Alcomer 7115 and A3335 was found to give the best dewatering performance of MFT, in terms of CST and net water release. For comparison purposes, in later tests, the addition sequence of the Alcomer 7115 and A3335

was changed to observe any possible benefits. In this thesis, the dual-polymer treatment description was mostly specifically focused to MFT treated with Alcomer 7115 and A3335.

3.2 Equipment

3.2.1 Flocculation System

Polymer treatment (flocculation) tests were conducted using a Heidolph RZR 2052 control overhead stirrer, with a pitch blade turbine (PBT) impeller, and a 2 L beaker (detailed description of why PBT impeller and 2 L beaker were chosen is in Appendix A). An adjustable stand was used to support the beaker in order to adjust the distance between impeller and the bottom of the beaker, which was set to 2.5 cm. The overhead stirrer was connected through a USB cable to a computer where the Watch & Control software was installed. The stirring speed can be adjusted, and both the stirring speed and the torque can be monitored through the software interface. The equipment used for the flocculation test is shown in Figure 3.1.

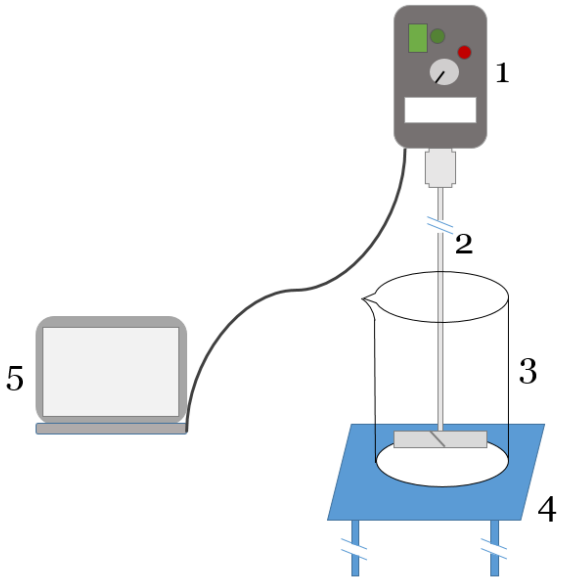

1. Overhead Stirrer
2. Pitch Blade Turbine impeller
3. 2 L Beaker
4. Adjustable Stand
5. PC interface

Figure 3.1 Equipment for flocculation tests.

In a typical flocculation test, 500 g MFT was introduced to the 2 L beaker. The adjustable stand was then raised so that the impeller was at a fixed position of 25 mm from the bottom of the beaker. The stirrer was then started after setting it to a desired rpm. Changes in torque and stirring speed with time are monitored and recorded by the software throughout the treatment process.

3.2.2 Pressure Filtration System

A small amount of flocculant treated MFT sample was taken for CST measurements. The remaining treated MFT sample was then transferred into a filtration system. The filter paper for both pressure and vacuum filtration was Millipore 142 mm diameter hydrophilic glass fiber filter paper with a 0.7 μm pore size. The pressure filtration system is shown in Figure 3.2. The filter is connected to a compressed air line, which provides the designed pressure by applying compressed air on the surface of treated MFT. A beaker was placed beneath the bottom drain (the adjustment of the bottom drain is described in Appendix B), and the weight of the beaker was monitored by a weighing scale which was connected to a computer. A Balance Link software installed in the computer recorded the weight reading every 15 seconds. The data could be exported to a data analysis and plotting software (such as Origin) for analysis.

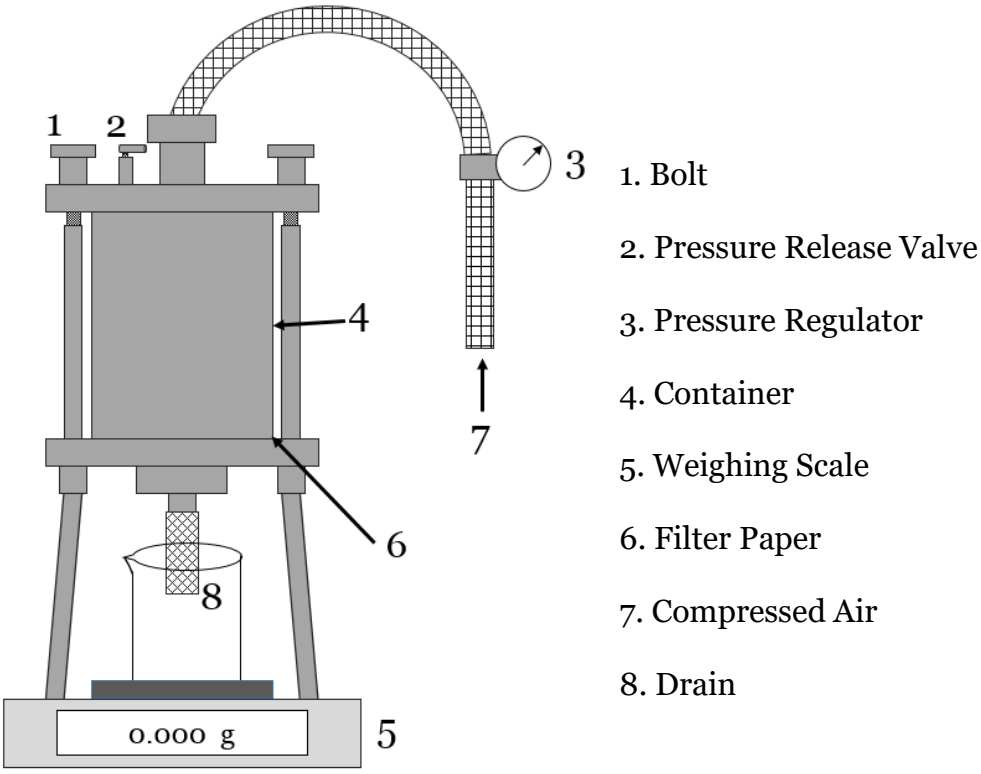

Figure 3.2 Schematic drawing of pressure filtration system.

3.2.3 Vacuum Filtration System

The setup of the vacuum filtration system is shown in Figure 3.3. A porcelain Buchner funnel, used to hold MFT, was held by a steel frame. Filter paper was cut to fit the area of the funnel. A graduated cylinder was placed underneath the funnel. A rubber stopper was used to seal the joint. As shown in Figure 3.3, the graduated cylinder was connected to a condensation trap, which was connected to a vacuum pump. After introducing treated MFT into the funnel, two layers of lab parafilms were used to close the opening of the funnel to avoid evaporation. Filtrate volume was read every 1 min for the first 30 min of filtration, and every 5 min afterwards.

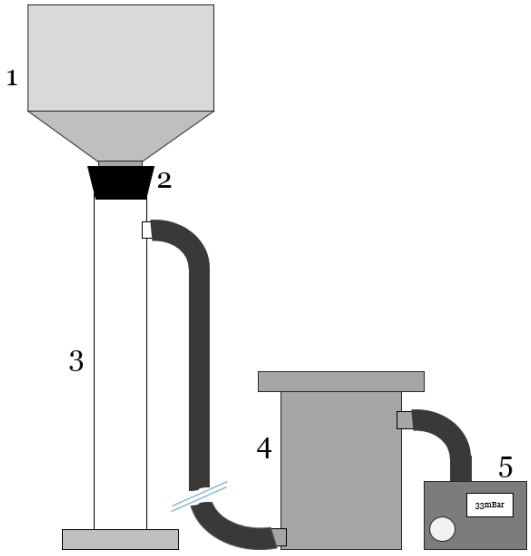

1. Porcelain Funnel
2. Rubber Stopper
3. Graduate Cylinder
4. Condensation trap
5. Vacuum Pump

Figure 3.3 Schematic drawing of vacuum filtration system.

After filtration, the wet filter cakes were weighed immediately, and then transferred to a VWR Symphony vacuum oven to dry. The drying process lasted around 12 hours at a temperature of 75°C and under a vacuum pressure of 80 kPa. The solid content of the filter cake is calculated from the dry and wet weight of the filter cake:

$$\text{Solid content} = \frac{Mass\ of\ Dry\ Cake}{Mass\ of\ Wet\ Cake} \times 100\% \qquad (3.1)$$

3.3 Evaluation Methodologies

3.3.1 Capillary Suction Time (CST)

The measurement of capillary suction time (CST) was developed by Gale and Baskerville [63] to study the filterability of sewage sludge. This technique had been adopted in sewage treatment gradually [64] since CST test was considered to be an easy and quick method to determine sewage dewaterability [65]. CST measurements have also been used

in assessing dewaterability of other sludge [66] [67]. It is one of the most commonly used tests to determine sludge dewaterability [68].

The CST apparatus used was type 319 multi-purpose CST with 5 single radius test heads from Triton Electronics Ltd, as shown in Figure 3.4. The apparatus consists of two transparent perspex plates. The lower plate has a recessed depth so that a filter paper can fit in, while the upper plate connected with the electrical timer has recession at both longitudinal direction so it can be placed on top of the lower plate. The upper plate has a round opening in the center so it can hold a stainless steel funnel. At the bottom of the upper plate, there are two concentric round tracks with two probes in the inner track and one probe in the outer track to detect interface flow.

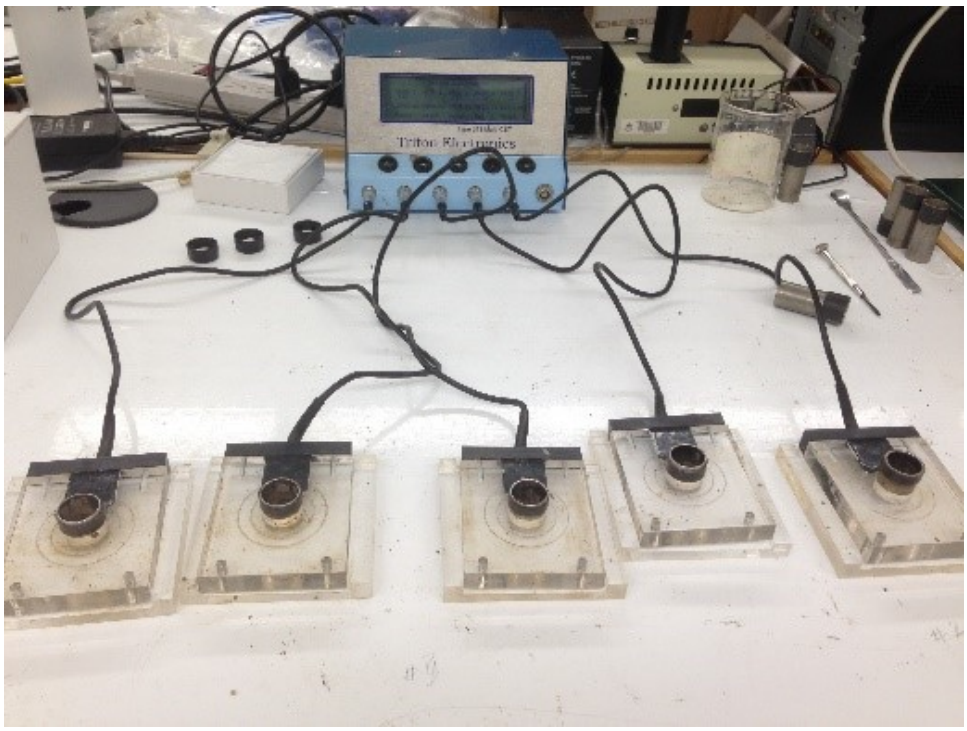

Figure 3.4 Type 319 Multi-CST apparatus.

The schematic drawing showing the structure of the stainless steel funnel seat is shown in Figure 3.5.

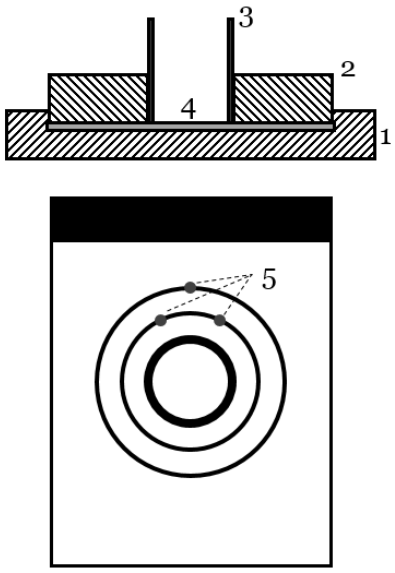

1. Lower Plate
2. Upper Plate
3. Stainless Steel Funnel
4. Filter Paper
5. Probes

Figure 3.5 Schematic drawing of the stainless steel funnel seat.

The measurement starts when sludge is poured into the stainless steel funnel. Water begins to flow through the filter paper and form a moving circle in the filter paper. When the moving circle reaches the edge of probes located at the inner track on the bottom of the upper plate, electrical signal will be sent to the timer to start timing. The timing ends when moving circle reached the probe at the outer track. The capillary suction time can be read from the electrical timer directly.

The principle of the apparatus is based on capillary suction pressure of a porous medium. When a treated sludge is poured into the funnel, a certain height of the sediment bed will be formed. Depending on the stability of the sludge, the height of sediment bed varies. Once a porous medium such as a filter paper is put underneath the funnel, water inside the sludge will begin to drain through the sediment bed into the filter paper to form a

moving circle. The movement of water in the porous medium (filter paper) mainly relies on the height of sediment bed, the permeability of sediment bed and the water-holding capacity of the solids in the sludge [69] [70]. The sediment bed formed by a stable/well-dispersed sludge is expected to be lower and more compact with narrower pores spaces, compared with unstable/aggregated suspension. Thus the more stable the sludge is, the longer the CST.

The original MFT used contained 35.6 wt% solids, and the fine solids in MFT have very high water-holding capacity. The settling of the fine solids in MFT is extremely slow. Hence, when placed into the stainless steel funnel, the sediment bed formed is of low height and high density. The CST result of the original MFT was 2800 - 3500 s. After treatment with polymer flocculants, the fine solids form flocs with larger pores, and in the meantime, the stability of MFT is broken thus it loses part of the water-holding capacity. As a result, the polymer-treated MFT is supposed to give lower CST than the original untreated MFT. In this thesis, the CST results are averages from three to four of CST tests.

3.3.2 Specific Resistance to Filtration

Specific resistance to filtration (SRF) and CST are the two most widely applied tests to characterize the filterability of sludge [71] [72]. Compared with CST, which is simple and inexpensive to operate, the measurement of SRF is more complicated, time consuming and more expensive to complete [73]–[75]. However, CST values obtained are unable to predict the physical properties of sample and changes during the dewatering process. While originated from classical filtration theory developed by Ruth [76]–[79], the SRF form a theoretical model incorporating the parameters of the filtration process [80], so

that it can be used to characterize the dewaterability of sludge under vacuum, pressure or a centrifugal force field [81]. Even though the parameters used in the SRF models were derived from classical filtration theory and do not comprehensively describe dewatering behaviors, the SRF is extensively used in characterizing dewaterability of sludge [71] [72] [75] [81] [82].

As the name implies, the SRF is used to represent a resistance to filtration. This resistance includes an apparatus resistance as well as a sludge resistance [83]. Here the latter is the studying object. In the process of separating solid and liquid, the SRF of a filter cake represents the difficulty with which a liquid filtrate can permeate through the filter cake [84]. As a result, the SRF has a physical meaning of measuring the resistance to filtration for a unit mass of filter cake per unit filter area [85]. Therefore, a smaller SRF value indicates easier and faster filtration [81] [86].

Under a constant pressure difference, the liquid contained in the sludge would pass through the filter medium with small pores to prevent particles from penetrating, which would otherwise provide resistance to liquid passage. As the filtration progresses, solid particles were retained on the surface of the filter medium, forming filter cake as shown in Figure 3.6 [87]. The cake thickness increased from 0 to L_c until filtration stopped, accordingly the filtrate volume increased from 0 to V mL.

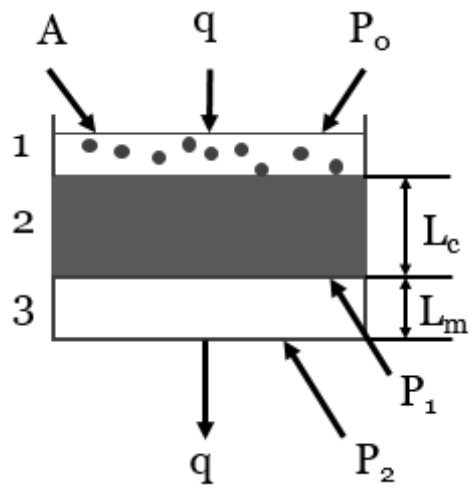

1 Tailings
2 Filter Cake
3 Filter Medium
A Filter Area
q Flow Rate
P_o Inlet Pressure
P_1 Pressure on Filter Medium
P_2 Pressure under Filter Medium
L_C Thickness of Filter Cake
L_m Thickness of Filter Medium

Figure 3.6 Schematics of liquid filtrate going through filter medium under pressure filtration.

According to Ruth's theory, the filtrate flow rate (q) is proportional to the pressure difference ΔP (ΔP equals to the pressure difference between P_o and P_2) applied through the filter cake and the filter medium, and inversely proportional to the summation of resistances of the filter cake (R_c) and filter medium (R_m), and the viscosity of liquid filtrate [75] [85] [88] [89]. The combination of the above yields the equation:

$$q = \frac{dV}{dt} = \frac{A\Delta P}{\mu(R_c + R_m)} \qquad (3.2)$$

For a given filter medium and slurry, the resistance of filter medium R_m is a constant value with a unit of m^{-1}. The cake resistance R_c is proportional to the filtrate volume V and inversely proportional to the filter area A [90] [91], so that R_c can be described as:

$$R_c = rw\frac{V}{A} \qquad (3.3)$$

Where r is the specific cake resistance to filtration (m/kg), and w is the concentration of the slurry (kg/m3).

Substituting Eq. (3.3) into Eq. (3.2) gives:

$$\frac{dV}{dt} = \frac{\Delta P}{\frac{\mu}{A}(rw\frac{V}{A} + R_m)} \tag{3.4}$$

Eq. (3.4) can be written in another way:

$$\frac{dV}{dt} = \frac{\Delta P(A^2)}{\mu rwV + \mu R_m A} \tag{3.5}$$

For the experiments described in this work, the pressure difference was constant throughout the filtration process. Integration of Eq. (3.4) or Eq. (3.5) leads to the classical filtration equation:

$$\frac{t}{V} = \frac{\mu rw}{2\Delta PA^2}V + \frac{\mu R_m}{\Delta PA} \tag{3.6}$$

Eq. (3.6) illustrates that a plot of t/V versus V would provide a straight line with a slope a and intercept b, which are:

$$a = \frac{\mu rw}{2\Delta PA^2} \tag{3.7}$$

$$b = \frac{\mu R_m}{\Delta PA} \tag{3.8}$$

The specific cake resistance to filtration and the filter medium resistance can be expressed as:

$$r = \frac{2\Delta P A^2}{\mu w} a \qquad (3.9)$$

$$R_m = \frac{\Delta \mathrm{PA}}{\mu} b \qquad (3.10)$$

The detailed derivation of the above equations can be found in many textbooks or publications [58] [84] [87] [92]–[94].

Since the change of filtrate volume with time can be recorded, a straight line can be easily generated from the plot of t/V versus V. Thus the values of a and b can be obtained, which can be used to calculate the specific cake resistance and the resistance of filter medium. Furthermore, once their values are obtained, values can be substituted into Eq. (3.6), which can be adopted to set the t time as a cycle of operation [58].

For pressure filtration tests in this thesis research, the filter area (A) was the inside area of the metal funnel, which is 0.0121 m^2. The applied filtration pressure was constant at 150 kPa, 300 kPa, or 600 kPa. The viscosity of liquid filtrate was very close to the viscosity of water, which has been verified by several viscosity tests in a rheometer, hence here μ was considered to be 0.8937 Pa·s. As for the value of w, in batch filtration, w is the concentration of the slurry (kg/m^3), which should be a constant [71] [95].

As mentioned earlier, a Balance Link software was used to record the changes of filtrate mass with time. The filtrate has very similar physical properties as water, including viscosity and density. Therefore, assuming the density of filtrate to be 1000 kg/m^3, it was

easy to convert filtrate mass data from the recording to volume data. Origin 2015 was used to analyze the data and complete the linear fitting.

The following shows an example to demonstrate the detailed operation to calculate SRF. In the following experiment, 1 kg/t lignosulfonate (at a stock concentration of 2.0 wt%) and 1 kg/t A3335 (at a stock concentration of 0.4 wt%) were added sequentially to treat 500 g MFT. The treated MFT was then filtered under a constant applied pressure of 300 kPa. The filtrate volume versus time curve is shown in Figure 3.7. Based on the volume and time data, a plot of t/V versus V could be obtained, as shown in Figure 3.8.

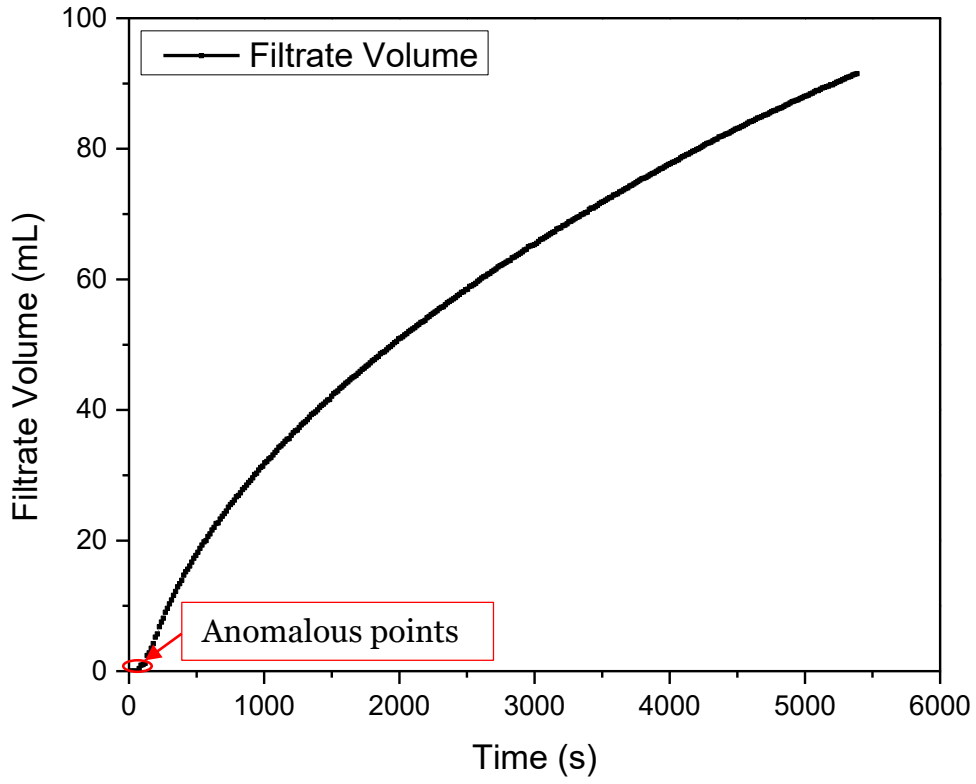

Figure 3.7 Filtrate volume versus time curve of MFT treated with 1 kg/t lignosulfonate and 1 kg/t A3335.

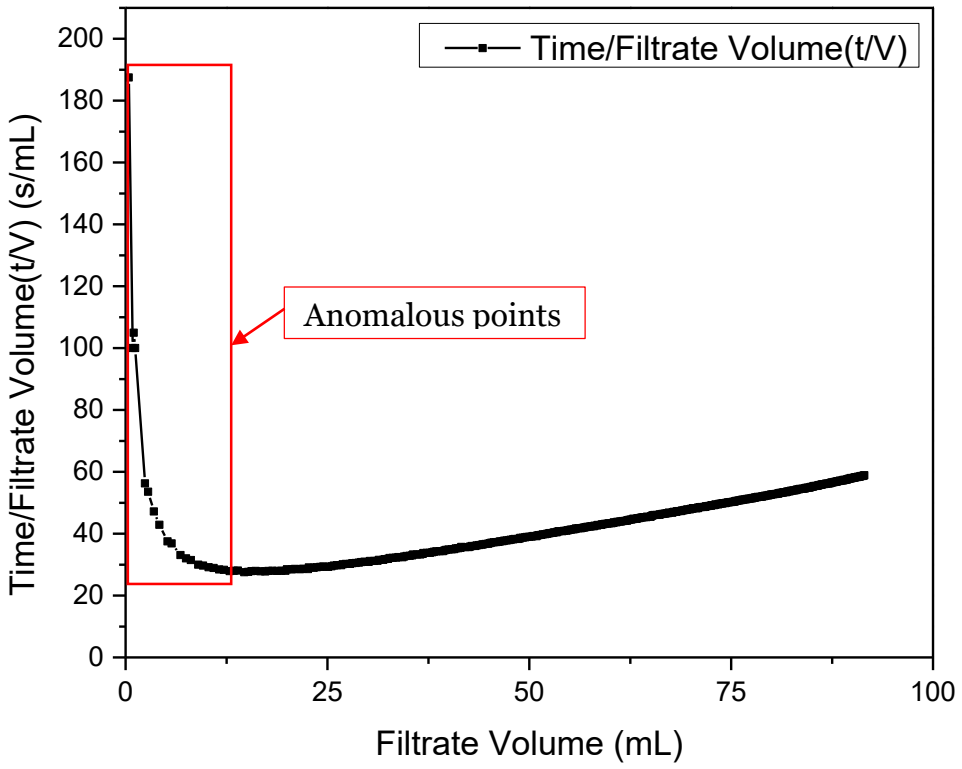

Figure 3.8 t/V versus volume curve of MFT treated with 1 kg/t lignosulfonate and 1 kg/t A3335.

In both Figure 3.7 and Figure 3.8, anomalous points at the initial stage of filtration which neither fit the parabolic curve in the *V-t* plot nor the linear *t/V-V* graph were observed. This might be because the pressure was increasing at the initial stage of filtration [93], or other reasons as shown in Figure 3.9, and this stage should be avoided in data analysis. For the *t/V-V* plot, non-linearity probably would appear at the end of the fitting, too, as explained in Figure 3.9.

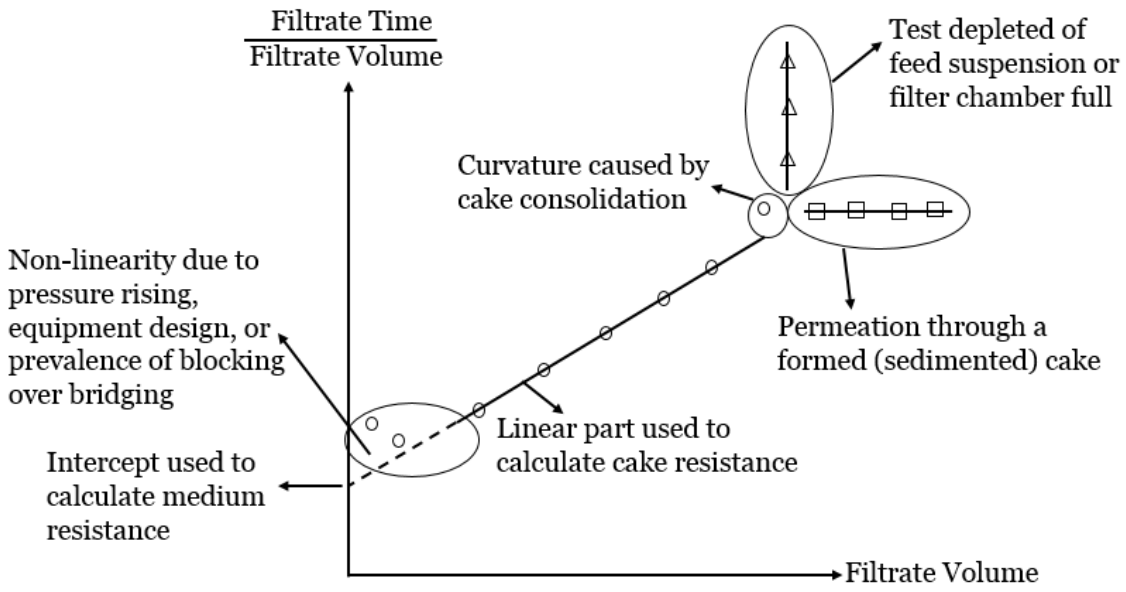

Figure 3.9 Possible reasons for non-linearity at the end of fitting curve [96].

Figure 3.10 shows the linear fitting generated based on the modified t/V versus V curve. The slope and intercept of the line were shown in the graph with fitting parameters, as can be seen in Figure 3.10. R^2 value was calculated to judge if the fitting was acceptable.

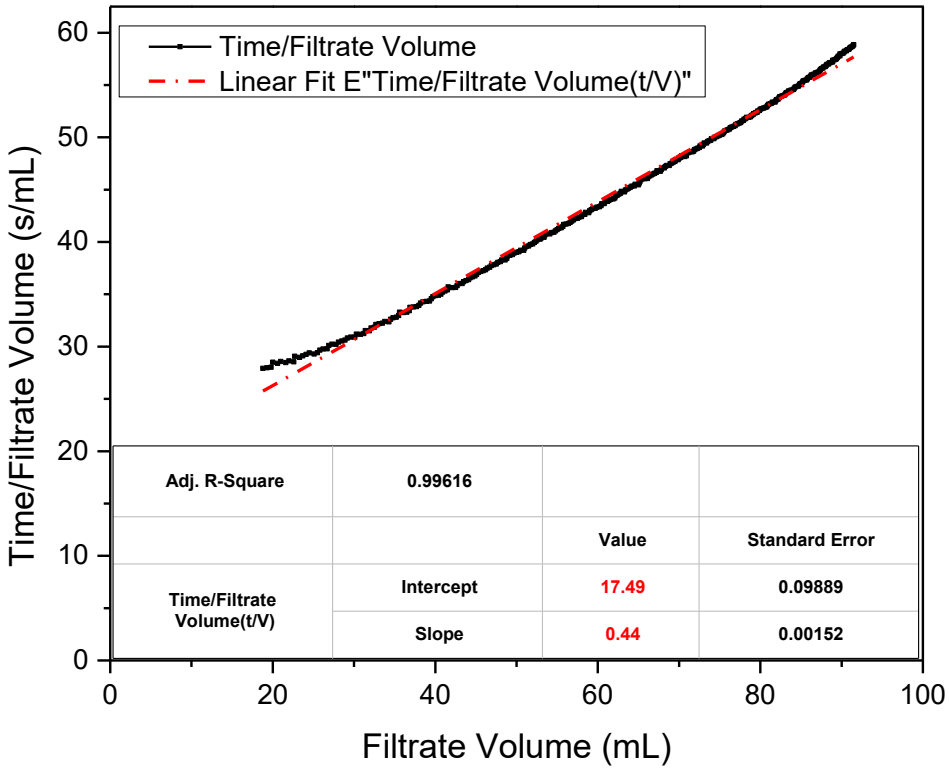

Figure 3.10 Linear fitting of modified t/V versus V curve of MFT treated with 1 kg/t lignosulfonate and 1 kg/t A3335.

The mass of solid cake per unit filtrate volume w was:

$$w = \frac{178g}{435mL} = \frac{178\times10^{-3}}{435\times10^{-6}} = 409.2kg/m^3 \qquad (3.11)$$

According to the data obtained above, slope a is 0.44 s/mL², which is 0.44×10¹² s/m⁶, substituting into Eq. (3.9):

SRF: $$r = \frac{2\times(300\times10^3 - 101\times10^3)\times(0.0121^2)}{(0.8937\times10^{-3})\times409.2}\times0.44\times10^{12} = 7.05\times10^{13}\,m/\text{kg} \qquad (3.12)$$

Substituting b (17.49 s/mL, which is 17.49×10^6 s/m^3) into Eq. (3.10), the resistance of the filter medium (filter paper) is:

$$R_m = \frac{(300\times10^3 - 101\times10^3)\times0.0121}{(0.8937\times10^{-3})}\times17.49\times10^6 = 4.71\times10^{13}\,m^{-1} \quad (3.13)$$

Eq. (3.12) gives the value of SRF of the filter cake. Since SRF values are comparable from one experiment to another, there was an approximated evaluation of relative ease of filtration based on the magnitude of the specific resistance, as shown in Table 3.2.

Table 3.2 Relative ease of filtration based on the magnitude of SRF [96].

Ease of separation	r (m/kg)
Very easy	$\leq10^9$
Easy	10^{10}
Moderate	10^{11}
Difficult	10^{12}
Very Difficult	$\geq10^{13}$

As one of the main methods to evaluate filterability of treated MFT, thereby to evaluate the polymer treatment, SRF was calculated for experiments described in the following chapters, in the same way as it was described above.

3.3.3 Cryo-SEM Images of Flocs Structure

Cryogenic scanning electron microscopy (cryo-SEM) is a commonly used characterization technique in life sciences. There are many similarities between samples in petroleum industry and those in life sciences, although cryo-SEM technique is less common in petroleum industry [97] [98]. Here this technique was used to observe the porous structure of MFT with or without polymer treatment.

The scanning electron microscope used was Zeiss EVO LS15 EP-SEM equipped with LaB6 electron source, and has a resolution of around 100 nm at the highest magnification. It is equipped with a Bruker energy dispersive X-ray spectroscopy (EDS) system with a silicon drift detector with a resolution of 123 eV and a 10 mm^2 window area. It is also equipped with a cold stage and in environmental mode, which is able to image hydrated samples.

To compare the porous structure between untreated MFT, single polymer treated MFT and dual polymers treated MFT, images of untreated MFT samples, MFT treated with 1 kg/t A3335, MFT treated with 4 kg/ton Alcomer 7115, and MFT treated with 4 kg/t Alcomer 7115 and 1 kg/t A3335 were obtained. For cryogenic sample preparation, each sample was placed into a copper sample stub. First a rapid freezing of sample was conducted using liquid nitrogen to maintain the morphology or relationship between various components. Then the frozen sample was fractured by a blade. Followed by the sublimation of water under controlled conditions. Afterwards, the sample was coated with gold. The coated sample was transferred into the SEM chamber for observation [99].

3.4 Optimization of Procedures

To make the treatment effective, parameters need to be optimized. As mentioned in chapter 2, except those fixed parameters (dimensions of beaker and impeller, type of impeller, properties of MFT), other parameters remained to be optimized are stirring speed and stirring time.

3.4.1 Optimum Stirring Speed

To optimize stirring speed, single polymer treatment was tested with A3335 (stock solution was at 0.4 wt%) provided by Imperial Oil. CST tests were conducted to evaluate the flocculation outcome. The polymer dosage used was 1 kg/t. And CST results were measured every 30 s after injecting polymer solutions under different stirring speed (150 rpm, 200 rpm, 250 rpm, 300 rpm, 400 rpm, and 500 rpm), as shown in Table 3.3.

CST results showed that for each stirring speed, there was an optimal stirring time window, corresponding to a minimum CST value. After comparing CST results at a certain stopping time but from different stirring speeds, it was clear that a stirring speed of 300 rpm showed the lowest CST, indicating best dewatering performance of MFT. Results obtained when repeating those experiments demonstrated the same trend, which confirmed that 300 rpm was the optimum stirring speed under the experimental conditions.

Table 3.3 Comparison of CST of different stopping time for single polymer treatment.

Stop Time (s) / CST (s) / Stirring Speed (rpm)	30	60	90	120
150	---	1107	846	907
200	1094	953	890	915
250		592	516	720
300	---	367	426	578
400	---	576	528	631
500	790	560	570	687

3.4.2 Optimum Stirring Time

Also, CST results showed that optimal operating time window under the experimental conditions with a stirring speed of 300 rpm is from 0 s to 60 s. To further optimize experimental conditions, the change of torque was used as an indicator to monitor flocculation. As the added polymers bridge the particles together, the torque increases. Therefore, the peak value of torque can be used to indicate the maximum bridging flocculation of MFT caused by the polymers.

Furthermore, for better water release, large flocs need to be broken to release trapped water. Hence, the point that torque reached its peak value was used as the start time point, and the stirring time after that was referred as the required time window.

A time window of 15 s and 30 s was tested and each was tested three times. The CST results are shown in Table 3.4.

Table 3.4 CST results of different time window.

CST (s) / Stop Time (s)	Trial 1	Trial 2	Trial 3
15	233	146	142
30	458	289	332

From Table 3.4, it can be seen that if MFT was treated with single polymer A3335, the optimal operating window is around 15 s after torque reached its peak value.

3.4.3 General Procedure for Dual-Polymer Treatment

Based on the preliminary experimental results on single polymer treatment and an understanding of bridging flocculation, a general procedure for dual-polymer treatment was developed, as shown in Figure 3.11, which was found to be most effective in the experiments carried afterwards.

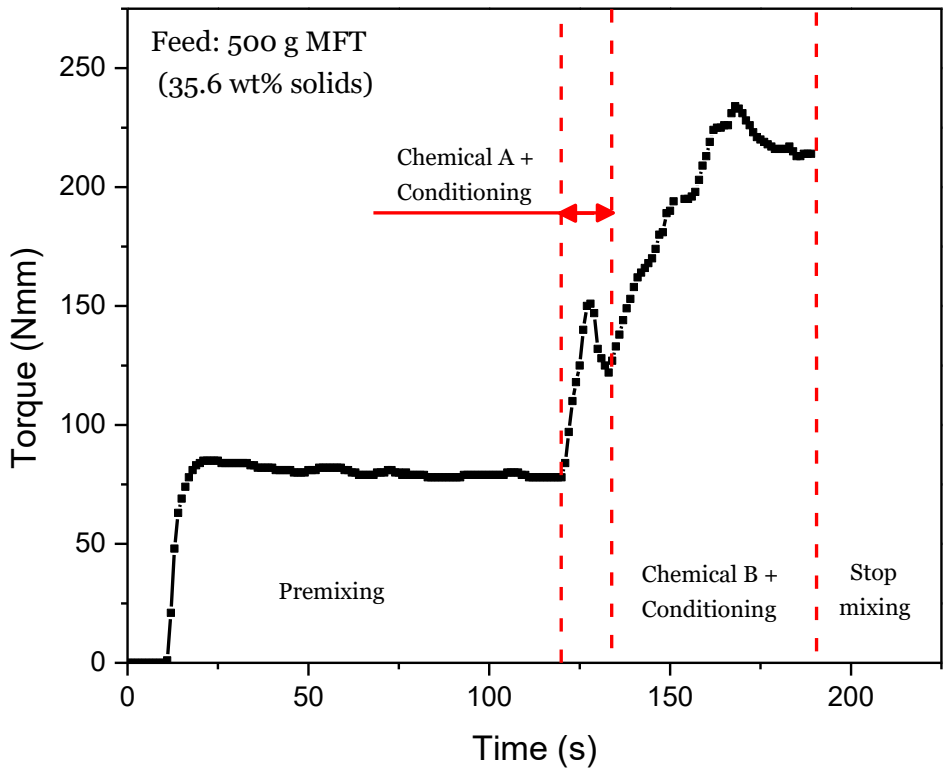

Figure 3.11 General procedure for dual-chemical treatment of MFT.

It took a few seconds for the impeller to ramp to 300 rpm. A timer was started after the stirring speed reached 300 rpm, and the MFT sample was stirred for 120 s to homogenize the sample before adding chemical A. The second chemical (chemical B) was added when the peak torque was reached after adding chemical A. Stirring was stopped 15 s after the torque reached its peak value after adding chemical B.

4 Dewatering of MFT using Alcomer 7115 and A3335

Based on the results of preliminary screening, a cationic polymer Alcomer 7115 and an anionic polymer A3335 were chosen to study the dewatering effect of dual-polymer treatment for MFT. The chosen Alcomer 7115 cationic polymer (called Alcomer 7115 in this thesis) is polydiallyldimethylammonium chloride (polyDADMAC) with a molecular weight of 200,000 to 400,000 g/mol and high charge density, supplied by BASF. A3335 is a linear polyacrylamide which has an average molecular weight of 17×10^6 g/mol and an anionic charge density of 30%, manufactured by SNF and provided by Imperial Oil. All the experiments described in this chapter followed the general protocol for dual polymer treatment, shown in Figure 3.11. Alcomer 7115 (at a stock concentration of 2.0 wt%) was used as the first polymer, followed by A3335 (at a stock concentration of 0.4 wt%). It is expected that the addition of Alcomer 7115 will bring the fine particles together to form small flocs. The addition of A3335 can further aggregate those small flocs into large flocs with porous structure, thus improving the dewaterability of MFT.

4.1 Pressure Filtration

Pressure filtration under a pressure of 150 kPa, 300 kPa or 600 kPa was conducted after the dual-polymer treatment.

4.1.1 CST and SRF as Indicators for MFT Treatment

Table 4.1 shows the CST results as well as the SRF results of MFT treated with dual polymers and filtered under a pressure of 150 kPa. The dosage of Alcomer 7115 was varied

between 0.5 and 4 kg/t, while the dosage of A3335 was fixed at 1 kg/t at all Alcomer 7115 dosages.

Table 4.1 CST and SRF results of dual-polymer tests under 150 kPa.

Dosage of Polymers	CST(s)	SRF($\times 10^{13}$ m/kg)
0.5 kg/t Alcomer + 1 kg/t A3335	494	2.98
1 kg/t Alcomer + 1 kg/t A3335	454	2.35
2 kg/t Alcomer + 1 kg/t A3335	717	1.54
3 kg/t Alcomer + 1 kg/t A3335	336	1.19
4 kg/t Alcomer + 1 kg/t A3335	311	0.85

Recorded filtrate volume as a function of time is shown in Figure 4.1. Linear fittings were generated based on the filtrate volume versus time curve, as shown in Figure 4.1. The slopes of the linear fitting curves indicate filtration rates.

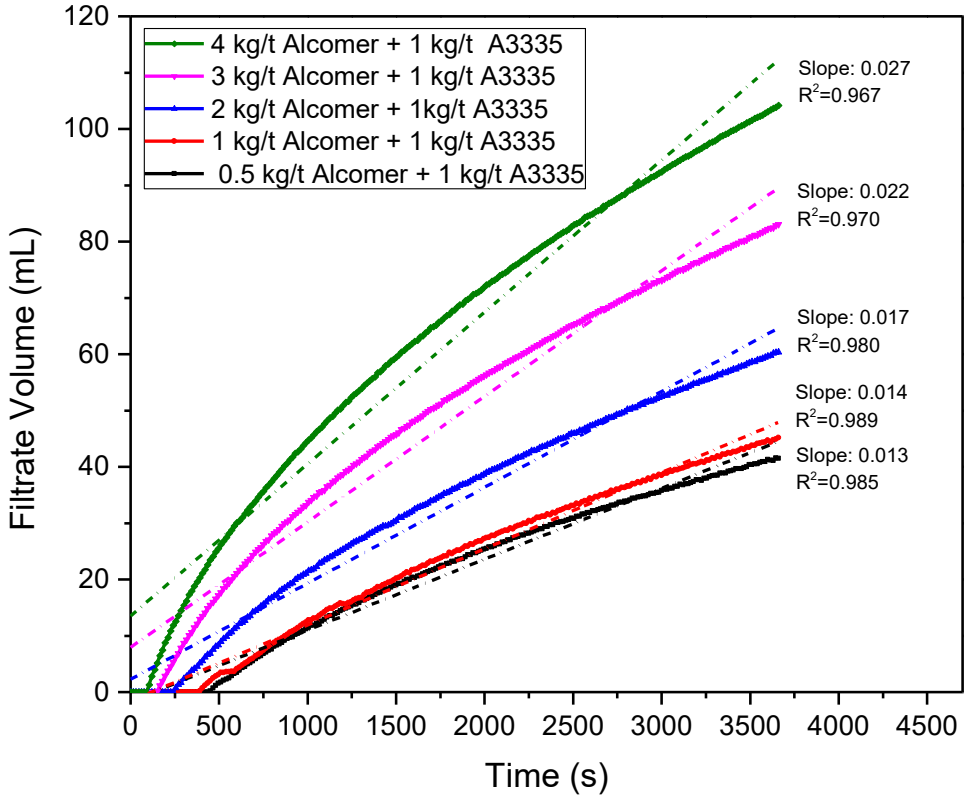

Figure 4.1 Filtrate volume as a function of time.

Data in Table 4.1 show that the CST for the test using 2 kg/t Alcomer 7115 and 1 kg/t A3335 was significantly higher than the rest. This dosage combination was repeated three times, and the results are shown in Table 4.2:

Table 4.2 CST results of MFT treated with 2 kg/t Alcomer 7115 and 1 kg/t A3335

No.	1	2	3
CST (s)	418	713	1019
Average CST (s)		717	

The measured CST at this particular dosage combination varied widely. At this point it is not clear the reason for the variation. In the plot of filtration rate versus CST (Figure 4.2), it can be clearly seen that this particular dosage combination (the red dot) is out of line from the rest of the data. Therefore, the CST value of that experiment was left out in the filtration rate versus CST modeling in Figure 4.2.

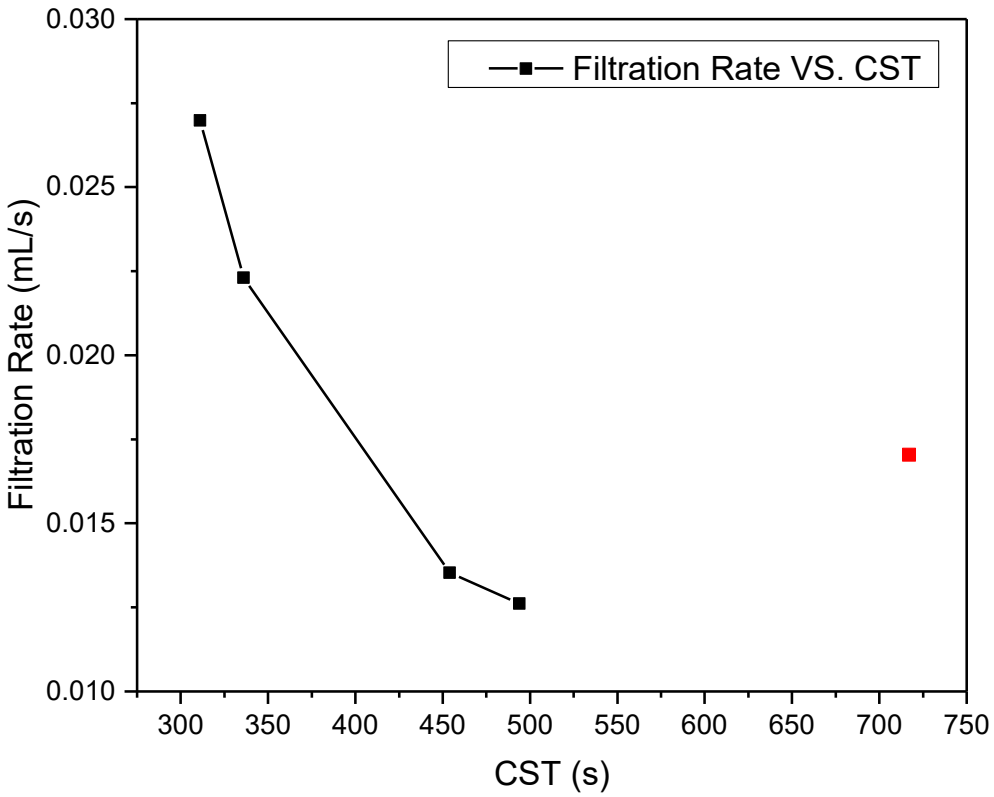

Figure 4.2 Different filtration rates under different CST.

Figure 4.3 shows the changes of filtration rate with SRF. As can be seen, the higher the SRF, the slower the filtration rate. This agrees with the definition of SRF, and thus proves that SRF can be used as an indicator to represent the filterability of MFT.

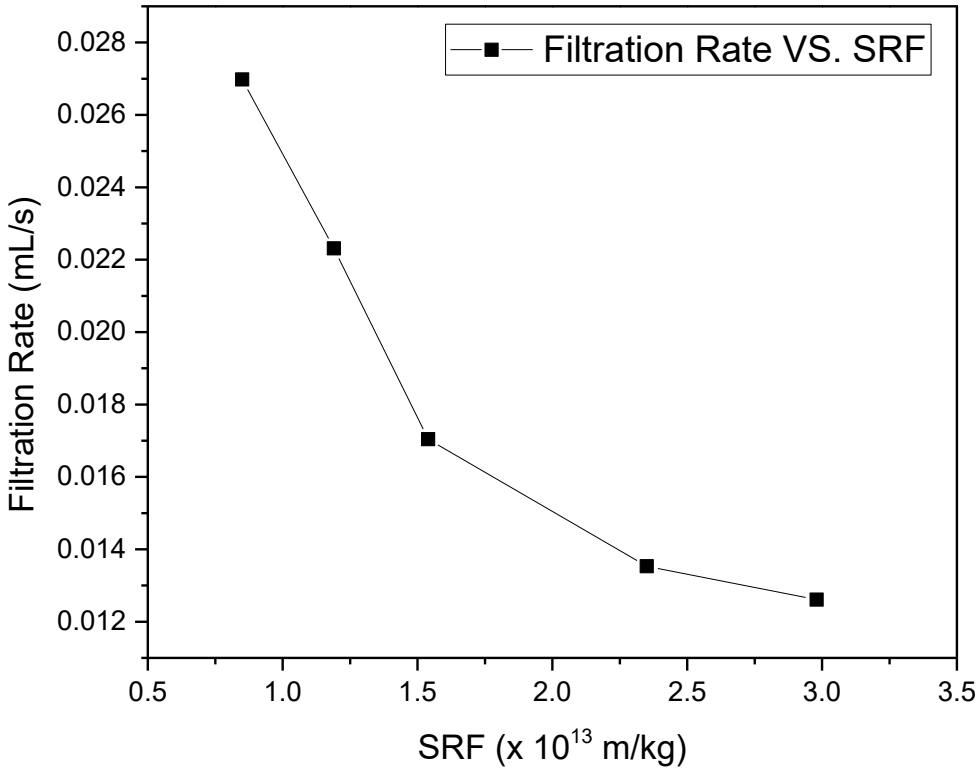

Figure 4.3 Filtration rate versus SRF.

4.1.2 Effect of Polymer Dosages

Polymer flocculation improves the dewatering performance of tailings [100]–[102]. Polymer dosage is important. If the dosage is too low, there will be insufficient amount of polymers to bridge the particles. On the other hand, too high a dosage not only increases cost but worse, it could lead to steric stabilization.

As shown in Figure 4.1, the filtration rate increased as the dosage of Alcomer 7115 was increased from 0.5 kg/t to 4 kg/t. Higher dosage of Alcomer 7115 may generate more flocs thus form more porous structures in the sediment which led to faster filtration rates.

In the following repeating filtration tests under 150 kPa, the dosage of Alcomer 7115 was varied between 1 kg/t and 5 kg/t while the dosage of A3335 was kept at 1 kg/t. The CST and SRF results are shown in Figure 4.4, and the change of net water release volume with time is presented in Figure 4.5.

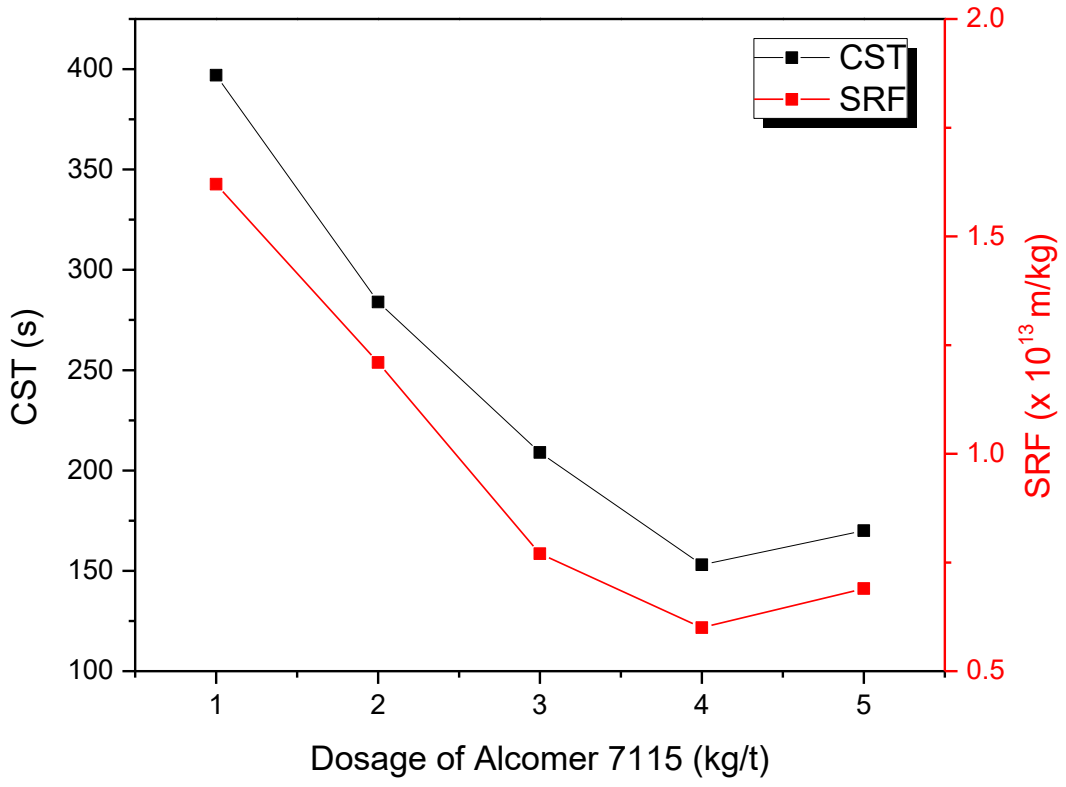

Figure 4.4 CST & SRF results for MFT treated with different Alcomer 7115 dosages and 1 kg/t A3335, and filtered under a pressure of 150 kPa.

As can be seen, the CST and SRF results of the repeating experiments have shown similar trends which were observed previously (Figures 4.2 and 4.3). Figure 4.4 also shows that both CST and SRF decrease with the increasing dosage of Alcomer 7115, reaching the lowest value at the dosage of 4 kg/t. At higher dosage, there was a slight increase in both

CST and SRF. The optimum dosage seems to be between 3 kg/t and 5 kg/t. The results indicated that the SRF correlated well with CST.

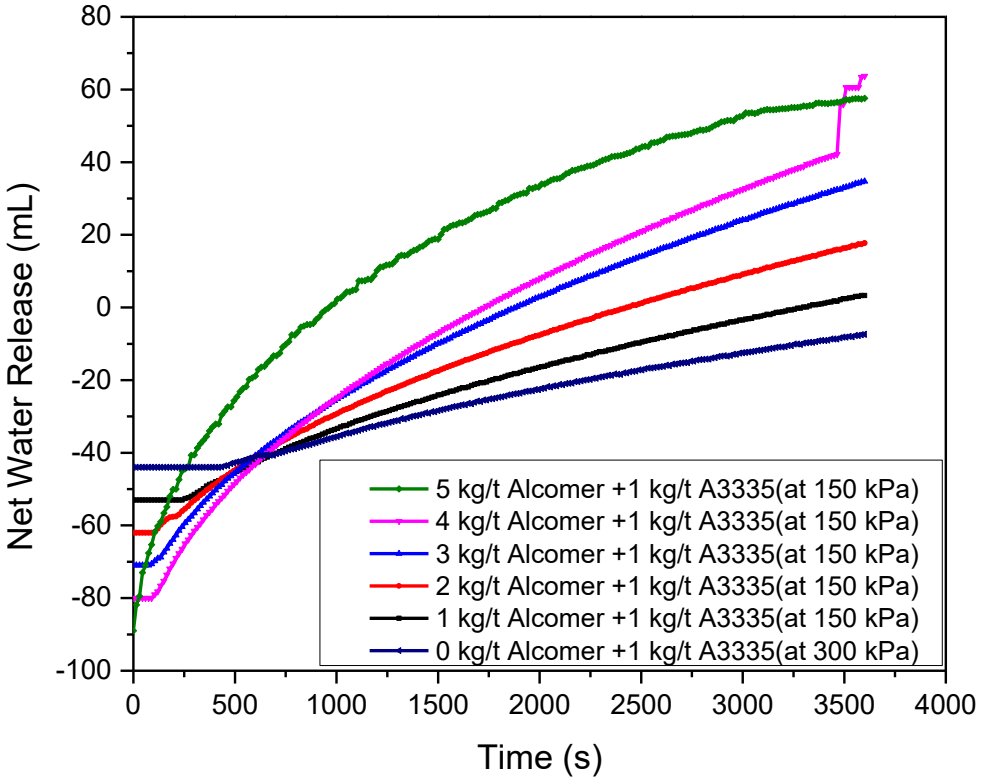

Figure 4.5 Net water release volume as a function of time for MFT treated with stated polymer dosages and filtered under a pressure of 150 kPa.

Figure 4.5 shows that despite the slightly higher CST and SRF results of test using 5 kg/t Alcomer 7115 and 1 kg/t A3335, it has very similar net water release volume using 4 kg/t Alcome r 7115 amd 1 kg/t A3335. And for comparison, a test of MFT treated with only 1 kg/t A3335 and then filtered under 300 kPa was conducted. As shown in Figure 4.5, even though filtered under a higher pressure, single polymer treated MFT has lower filtration rate and less net water release compared with dual polymer treatment. Overall, the combination of 4 kg/t Alcomer 7115 and 1 kg/t A3335 seems to be the optimum dosages.

It is to be noted that although the filtration behavior of the above two sets of tests, using two batches of different MFT samples, was similar, the measured CST were quite different, as shown in Table 4.3.

Table 4.3 Comparison of CST results of two batches of MFT samples.

Dosage of polymers	CST (s)	
	Batch 1	Batch 2
0.5 kg/t Alcomer 7115 + 1 kg/t A3335	494	---
1 kg/t Alcomer 7115 + 1 kg/t A3335	454	397
2 kg/t Alcomer 7115 + 1 kg/t A3335	717	284
3 kg/t Alcomer 7115 + 1 kg/t A3335	336	209
4 kg/t Alcomer 7115 + 1 kg/t A3335	311	153
5 kg/t Alcomer 7115 + 1 kg/t A3335	---	170

The data in Table 4.3 shows that the absolute values of CST differed significantly even at the same polymer dosages, although the trend of the CST was the same, i.e., the higher the dosage of the Alcomer 7115, the shorter the CST.

4.1.3 Effect of Pressure on Filtration Rate

Although the CST was very low, the 500 g MFT sample only had a net water release of less than 10 mL in 24 h when it was placed on a 150 μm aperture sieve to dewater following treatment with 1 kg/t Alcomer 7115 and 1 kg/t A3335. The application of pressure significantly improved the dewaterability. Therefore, filtration tests were conducted under different pressures.

Two series of tests were performed. Each test series consisted of four experiments with the dosage of Alcomer 7115 changed from 1 kg/t to 4 kg/t while the dosage of A3335 was

fixed at 1 kg/t. In series 1 (described in 4.1.2) the treated MFT was filtered under a pressure of 150 kPa; while in series 2 the treated MFT was filtered under a pressure of 600 kPa. The accumulation of filtrate volume with time are shown in Figure 4.6 and Figure 4.7.

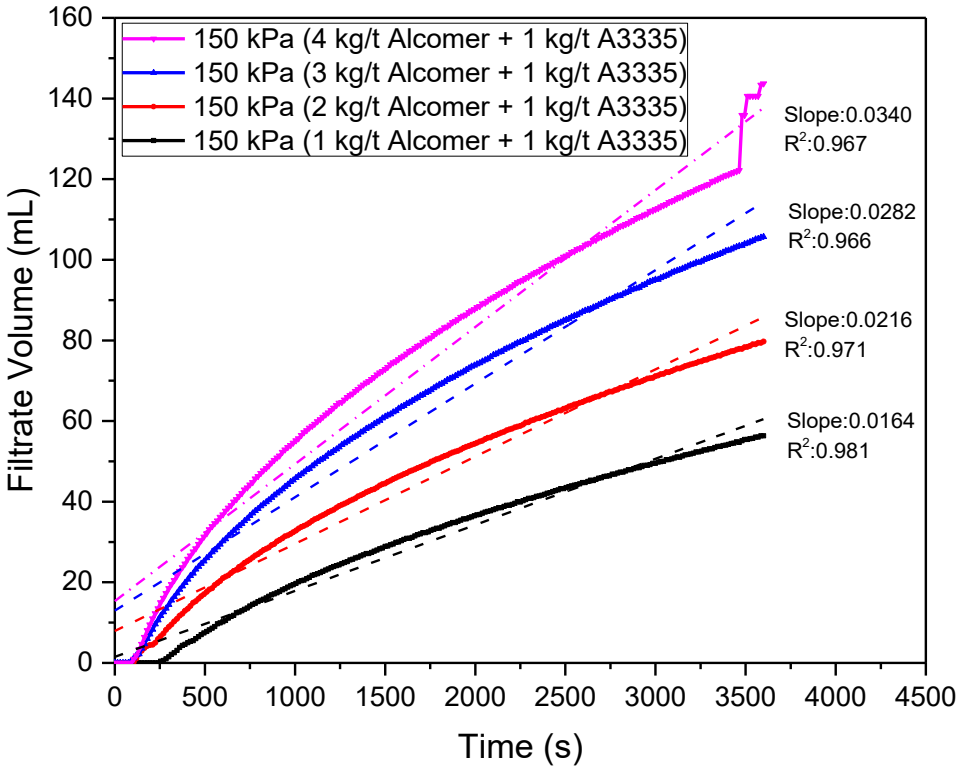

Figure 4.6 Filtrate volume as a function of time under a pressure of 150 kPa.

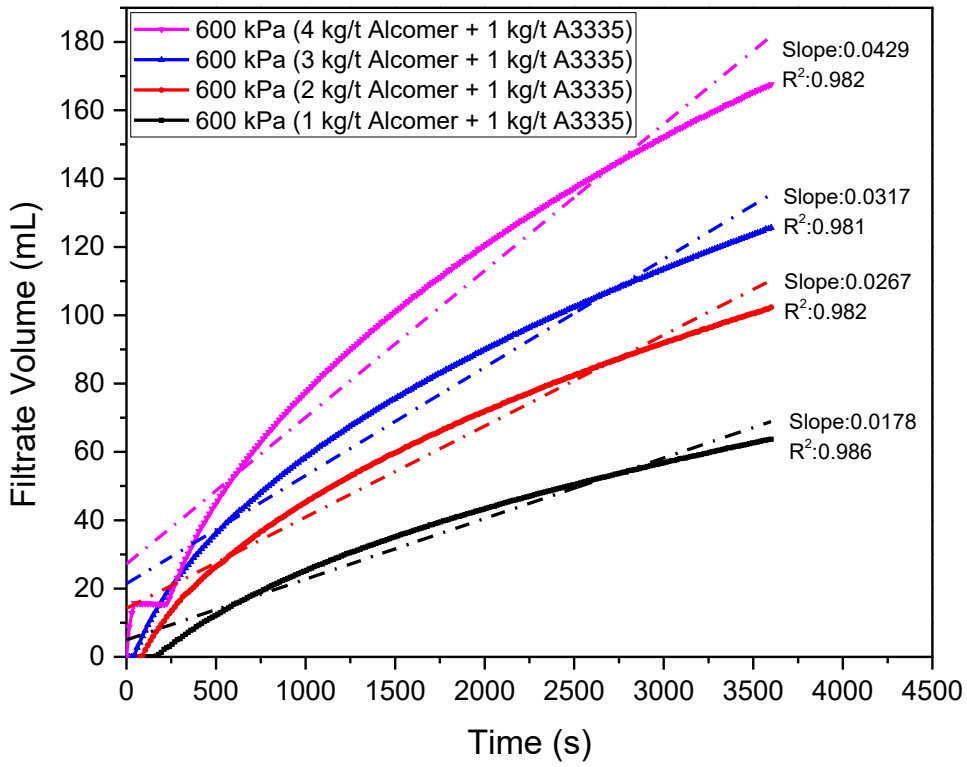

Figure 4.7 Filtrate volume as a function of time under a pressure of 600 kPa.

The comparison of net water release after filtration (obtained based on Figure 4.6 and Figure 4.7) is presented in Table 4.4. As shown, higher pressure gives a higher net water release when the MFT was treated with the same polymer dosages.

Table 4.4 Comparison of net water release under 150 kPa and 600 kPa

Dosage of polymers	Net water release (mL)	
	150 kPa	600 kPa
1 kg/t Alcomer 7115 + 1 kg/t A3335	3.3	10.7
2 kg/t Alcomer 7115 + 1 kg/t A3335	17.7	40.3
3 kg/t Alcomer 7115 + 1 kg/t A3335	34.7	54.6
4 kg/t Alcomer 7115 + 1 kg/t A3335	63.7	87.6

In Figure 4.8, the filtration rate was compared at the two pressures as a function of Alcomer 7115 dosage. A linear relationship was observed between the filtration rate and Alcomer 7115 dosage, for both pressures.

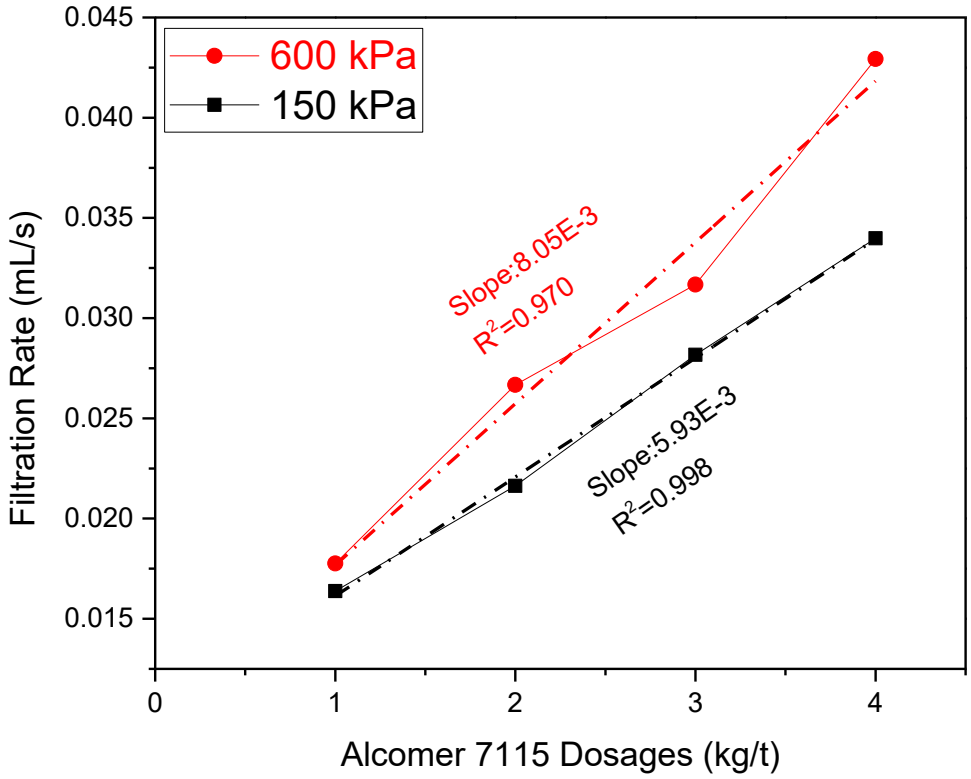

Figure 4.8 Comparison of filtration rate under different pressures.

Figure 4.8 also illustrated that higher pressure brings faster filtration rates. The faster filtration rates here were due to higher external driving force. Connected structures of particles (flocs) were produced with the addition of the polymers. This connected structure could behave like a solid [103] and has the ability to support itself. For a flocculated system which has a certain initial volume fraction of solids, it can support a certain external applied pressure, called compressive yield stress. Once the external

pressure exceeds the compressive yield stress, a collapse of the structure and increase of local solid volume fraction happen, thus the water inside the pores are squeezed out by the external force. Moreover, the higher the volume fraction of solids, the higher the compressive yield stress [20] [21] [104]. Therefore, higher pressure can compress flocculated system to a higher volume fraction of solids than lower pressure, thus can result in shorter filtration times and higher filtration output quantitatively.

The SRF values were calculated for each experiment and are presented in Figure 4.10 as a function of the dosage of Alcomer 7115. It can be seen from this figure that when filtered under a pressure 600 kPa, the specific resistance was much higher than that under the lower pressure of 150 kPa. This increase in SRF is likely caused by the increase in the volume fraction of the solids, which resulting in more compacted structure and higher resistance [80].

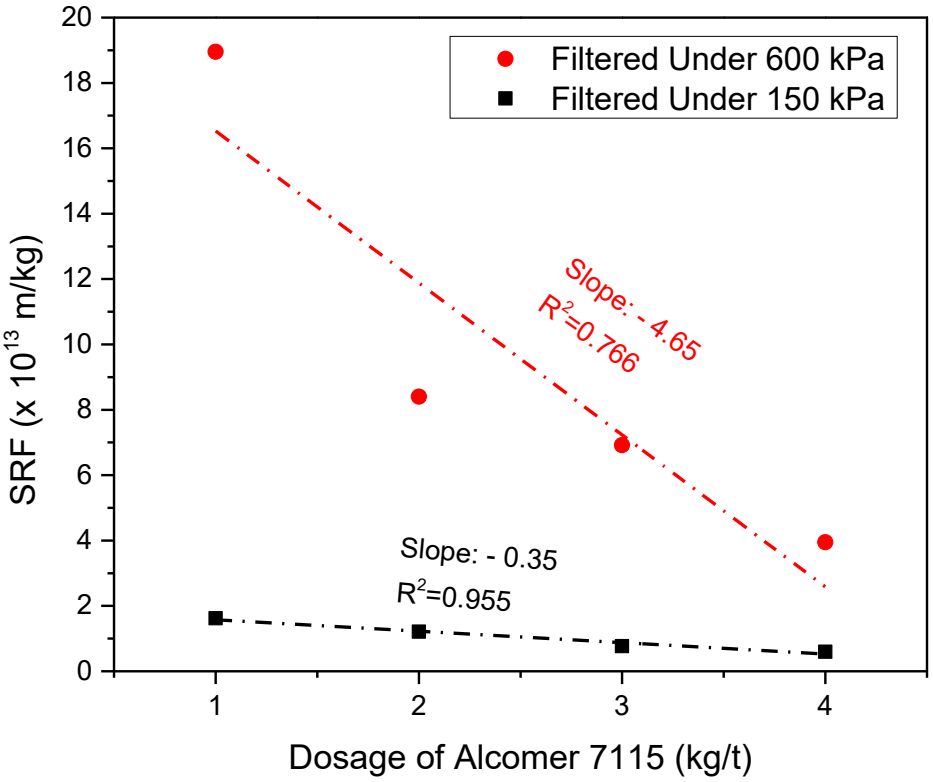

Figure 4.9 Comparison of SRF under different pressures.

Results of these two series of experiments showed that 4 kg/t Alcomer 7115 + 1 kg/t A3335 treated MFT filtered under a pressure of 600 kPa gave the highest filtration rate and filtrate volume.

The filtrate volume plots in Figure 4.6 and Figure 4.7 show that the pressure filtration was still ongoing after one hour. Therefore, the filtration time of experiments in series 2 was extended to around 2 hours. The filtrate volume of test with 4 kg/t Alcomer 7115 and 1 kg/t A3335 is plotted versus time in Figure 4.10.

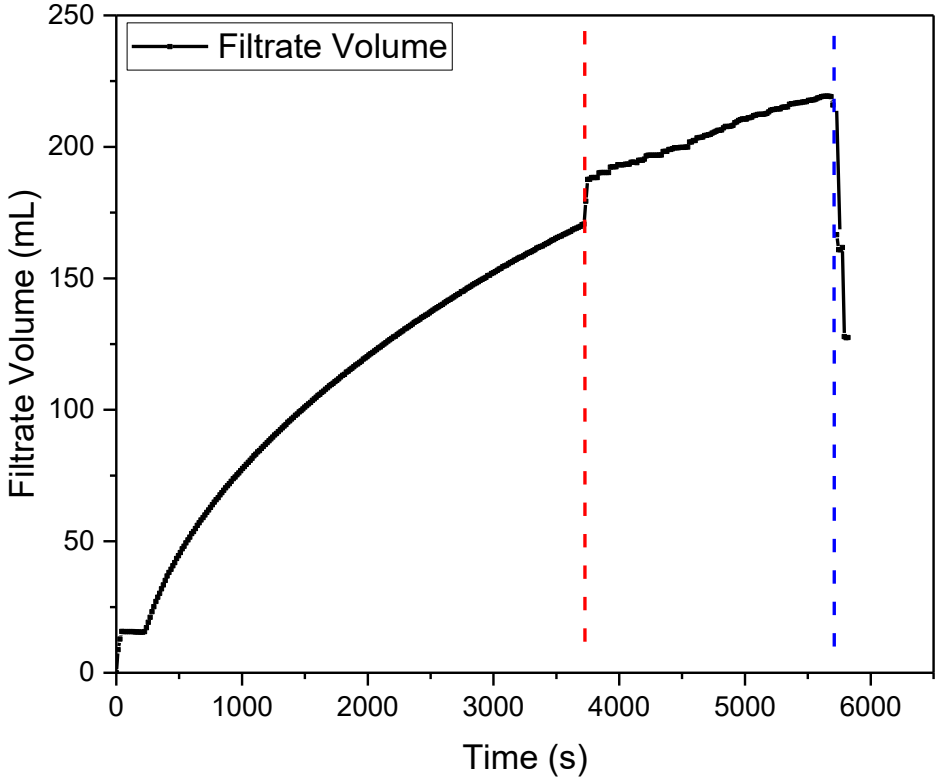

Figure 4.10 Filtrate volume as a function of time under 600 kPa (4 kg/t Alcomer 7115 and 1 kg/t A3335).

As can be seen from Figure 4.10, the filtrate volume increased to 217 mL after 1.5 hours of filtration, compared with the 167 mL after one hour of filtration. Interestingly, there was a "jump" in filtrate volume at about 1 hour (vertical red dash line). This was caused by the formation of cracks (Figure 4.11). Once cracks formed, the pressure dropped but it became easier for water in the immediate vicinity of the cracks to pass through.

Figure 4.11 Cracks on filter cake at 600 kPa (4 kg/t Alcomer 7115 and 1 kg/t A3335).

The blue vertical line in Figure 4.10 marked the formation of more cracks, which caused a significant drop in pressure. The experiment had to be stopped at this point. Indeed the formation of cracks in the filtration cake is the limiting factor to the efficiency of pressure filtrations when the pressure was induced by compressed air.

The pressure filtration tests in series 2 ended after 2 hours. The net water release volume is plotted against time in Figure 4.12, and the corresponding CST and solid contents in the filter cake are shown in Table 4.5.

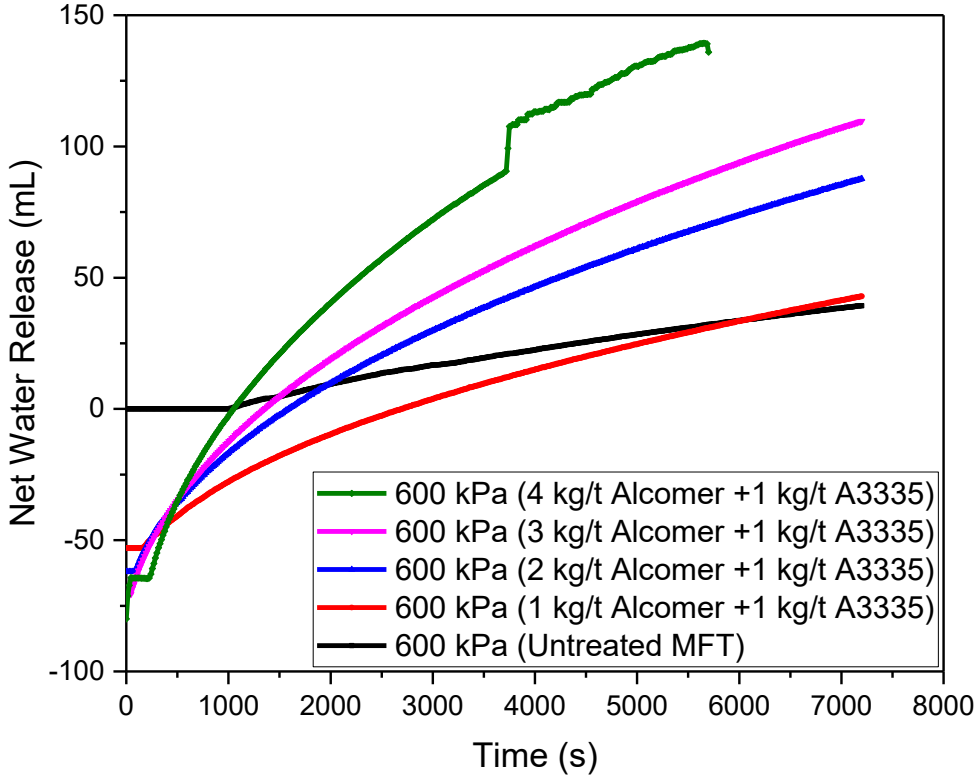

Figure 4.12 Net water release under 600 kPa.

Table 4.5 CST and solid contents of filter cake (pressure: 600 kPa).

Dosage of polymers	CST (s)	Solid Content (wt%)
1 kg/t Alcomer 7115+1 k/t A3335	611	46.2
2 kg/t Alcomer 7115+1 kg/t A3335	330	55.7
3 kg/t Alcomer 7115+1 kg/t A3335	250	58.0
4 kg/t Alcomer 7115+1 kg/t A3335	217	64.1

Table 4.5 shows that, an increase in Alcomer 7115 dosage results in lower CST and higher solid contents in the filter cake. This verified again that CST is a good parameter to assess the dewaterability of polymer treated MFT. The highest solid content in the filter cake was 64.1 wt%, with the addition of 4 kg/t Alcomer 7115 and 1 kg/t A3335.

4.2 Vacuum Filtration

Vacuum filtration is more economically feasible for industries than pressure filtration, due to its low cost and high unit capacity [105]. Also, because of the lower driving force, it is expected that crack formation may not happen or may be delayed, so that the filtration may proceed more smoothly.

4.2.1 Comparison of Vacuum and Pressure Filtration

A vacuum filtration test was carried out on 500 g MFT treated with 4 kg/t Alcomer 7115 and 1 kg/t A3335. After measuring the CST, the treated MFT was transferred to the vacuum filtration system and filtered under 3.5 kPa. Filtrate volume was read every minute in the first 10 minutes, and then every five minutes until one hour. After one hour, the filtration rate was very slow, so the readings then were read every 30 minutes until two and half hours when the filtration test was stopped. The net water release volume versus time curve is shown in Figure 4.13, and compared with the curve obtained from MFT filtered under 600 kPa after treating with the same dosage of polymers. Figure 4.13 also shows the vacuum filtration test results when the Alcomer 7115 dosage was increased to 10 kg/t.

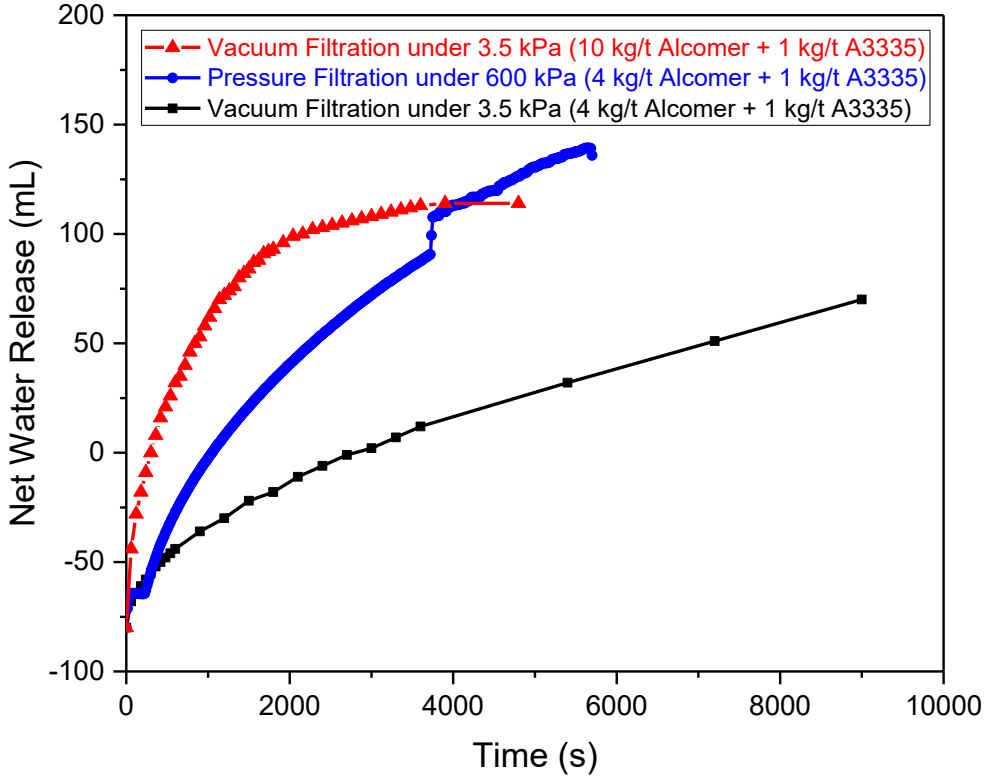

Figure 4.13 Comparison of filtrate volume of vacuum filtration (at 3.5 kPa) and pressure filtration (at 600 kPa).

The filtration rate of vacuum filtration (indicated by the black line) was very low compared with that of pressure filtration (indicted by the blue line). Extending the filtration time resulted in an increase in filtrate volume at a very slow rate. No cracks were observed during vacuum filtration process.

When the dosage of Alcomer 7115 was raised to 10 kg/t followed by 1 kg/t A3335, the treated MFT looked extremely thick, and a low average CST of about 60 seconds was obtained. The treated MFT was subjected to both pressure and vacuum filtration. However, the filter cake cracked very quickly in the pressure filtration tests. On the other hand, there is a significant increase in filtration rate under vacuum filtration (note that

the Alcomer 7115 stock solution concentration was increased so that at the 10 kg/t dosage, the amount of added water was the same as at the Alcomer 7115 dosage of 4 kg/t), and the filtration seems to have finished after about 1 hour. The solid content in the filter cake was 58.6 wt%.

The calculated SRF for both vacuum filtration and pressure filtration is compared in Table 4.6. As can be seen, the SRF of vacuum filtration are slightly smaller than that of pressure filtration under 600 kPa. But when compared vacuum filtration with pressure filtration under 150 kPa, the SRF values are about the same order (Table 4.1). This implies that vacuum filtration does not give an easier filtration than pressure filtration in terms of SRF.

Table 4.6 SRF of pressure filtration and vacuum filtration.

	Dosage of Alcomer 7115 (kg/t)	Solid Content (wt%)	SRF ($\times 10^{13}$ m/kg)
Pressure	4	64.1	3.95
Vacuum	4	48.9	1.23
	10	58.6	0.17

4.3 Correlation between CST and SRF for MFT Treatment

As the two most commonly used parameters to evaluate the dewaterability of sludge, CST and SRF have their own advantages and shortcomings. As it was mentioned in previous sections, CST measurement is simple, fast, and inexpensive, and requires no special skills. In contrast, SRF determination is time-consuming, complex, and expensive to conduct and calculate. Yet on the other hand, unlike SRF which is theoretically modeled with parameters to determine the permeability of sludge, CST is a practical but empirical

method for the determination of filterability, mainly used after the addition of coagulant/flocculent aids with no theoretically complete mathematical model [106]. Moreover, sludge filterability predominantly governs the output of almost all commonly used type of dewatering equipment including filter presses, vacuum filters, drying beds, and centrifuges [72] [106]. For these reasons, these two parameters should not substitute each other [71], but instead should be evaluated in different aspects of dewatering performance. Furthermore, if SRF is correlated with CST, then by measuring CST of a sample the SRF value can be estimated quickly using the correlations [107].

When studying the mechanisms for polymer overdosing in sludge conditioning, researchers proposed a two-phase concept to characterize the dewaterability, and developed the relationship between CST and SRF [83]:

$$SRF \times w = c_1 \times \frac{1}{\mu} CST + c_2 \qquad (4.1)$$

Where c_1 and c_2 are empirical coefficients related to CST, μ (Pa·s) is the viscosity of the filtrate, and w (kg/m^3) is the solid content per unit volume of the filtrate. Jimmy et al [19] suggested that the resistance was from both the sludge (first part on the right of Eq. (4.1)) and the apparatus (second part on the right of Eq. (4.1)).

Different views on CST-SRF correlation were made by researchers. One school of thoughts suggested that for specified suspended solids contents, CST and SRF values usually correlate well for sludge from water treatment plants, but not for biological sludge containing organic matter, such as flocs [71] [106].

The correlation between CST and SRT for MFT treated with dual polymers is investigated here. CST and SRF data shown in Table 4.7 are from experiment series 1 described in section 4.1.3, where the MFT was treated with different dosages of Alcomer 7115 from 1 kg/t to 5 kg/t with an increment of 1 kg/t, followed by filtration at 150 kPa.

Table 4.7 CST and SRF results of dual polymer treatment with different dosages of Alcomer 7115, 1 kg/t A3335, and filtered at 150 kPa pressure

Dosage of polymers	CST (s)	SRF ($\times 10^{13}$ m/kg)	SRF $\times w$ ($\times 10^{15}$ m^{-2})
1 kg/t Alcomer 7115+1 kg/t A3335	397	1.62	6.63
2 kg/t Alcomer 7115+1 kg/t A3335	284	1.21	4.85
3 kg/t Alcomer 7115+1 kg/t A3335	209	0.77	3.02
4 kg/t Alcomer 7115+1 kg/t A3335	153	0.60	2.31
5 kg/t Alcomer 7115+1 kg/t A3335	170	0.69	2.61

As can be seen from Table 4.7 and Figure 4.14, the trends of CST and SRF values change with the incremental increase of polymer dosage are the same. According to Eq. (4.1), assume that the filtrate viscosity was constant, CST and SRF×w should follow a linear correlation. SRF×w values for this test series are shown in Table 4.7.

SRF×w versus CST scatter graph was plotted, as shown in Figure 4.14. As can be seen, the data points fell very well on a straight line. A linear fitting was generated to verify the correlation. As can be seen from Figure 4.14, the R^2 value for the fitting is 0.988, indicating that these two parameters correlate with each other well in the linear relation:

$$\text{SRF}\times w = (0.018\times\text{CST}-0.524)\times 10^{15} \qquad (4.2)$$

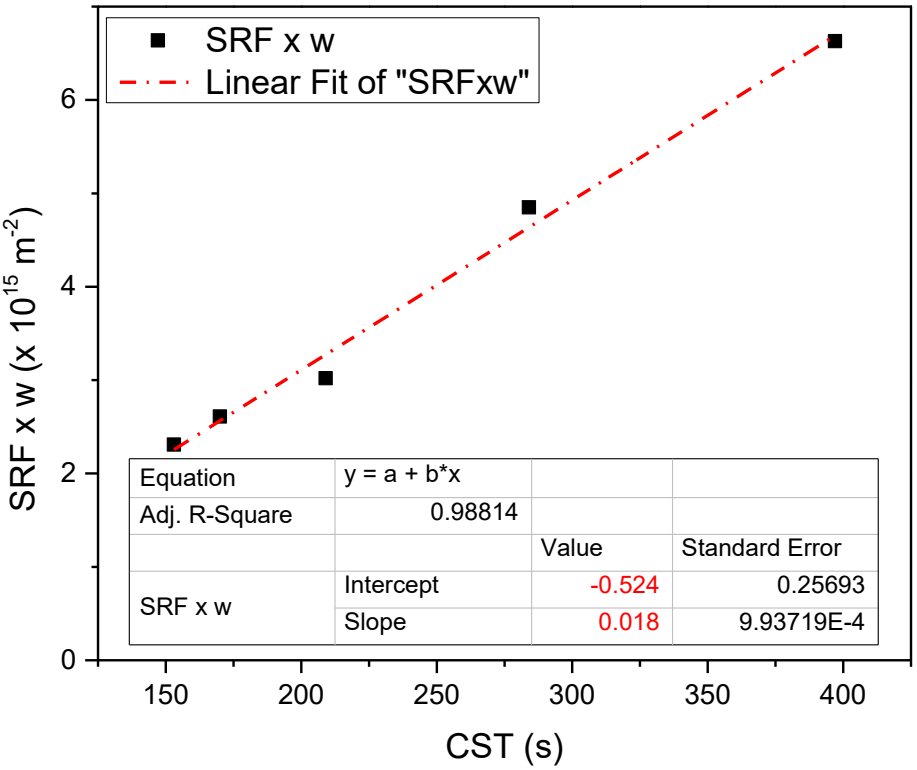

Figure 4.14 CST versus SRF×w plot.

To verify the general applicability of this linear relation, it was used to predict the SRF values of MFT treated with different polymer dosages and filtered under a pressure of 150 kPa (described in section 4.1.1). The CST results and measured SRF×w results ((SRF×w)$_{\text{series 1}}$) are shown in Table 4.8, together with the predicted SRF×w results ((SRF×w)$_{\text{predicted}}$). Figure 4.15 shows a correlation between the measured SRF×w and the predicted SRF×w.

Table 4.8 CST and measured/predicted SRF×w results of MFT treated with different polymer dosages and filtered under 150 kPa.

Dosage of polymers	CST (s)	$(SRF \times w)_{series\ 1}$ ($\times 10^{15}$ m^{-2})	$(SRF \times w)_{predicted}$ ($\times 10^{15}$ m^{-2})
0.5 kg/t Alcomer 7115+1 kg/t A3335	494	12.3	8.37
1 kg/t Alcomer 7115+1 kg/t A3335	454	9.62	7.65
3 kg/t Alcomer 7115+1 kg/t A3335	336	4.68	5.52
4 kg/t Alcomer 7115+1 kg/t A3335	311	3.27	5.07

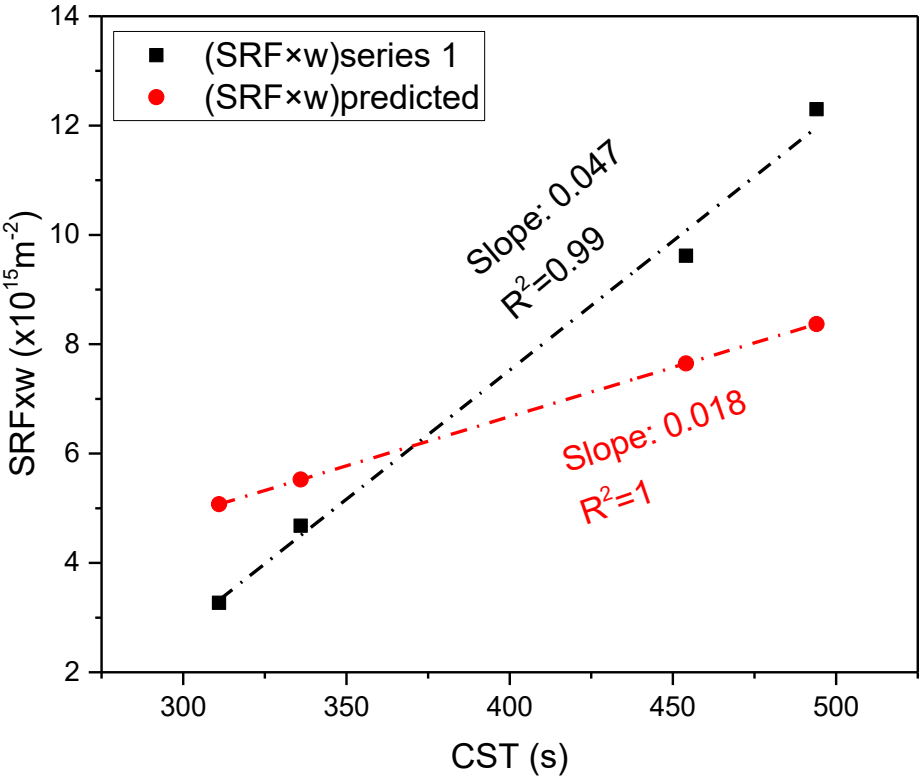

Figure 4.15 Measured and predicted SRF×w versus CST.

Figure 4.15 shows that the predicted SRF×w values differed from measured values, though they were in the same order of magnitude. Figure 4.15 also shows that the measured SRF×w values correlate well with CST results.

The measured $(\text{SRF}\times w)_{\text{series1}}$ is plotted against CST for this series of samples in Figure 4.16.

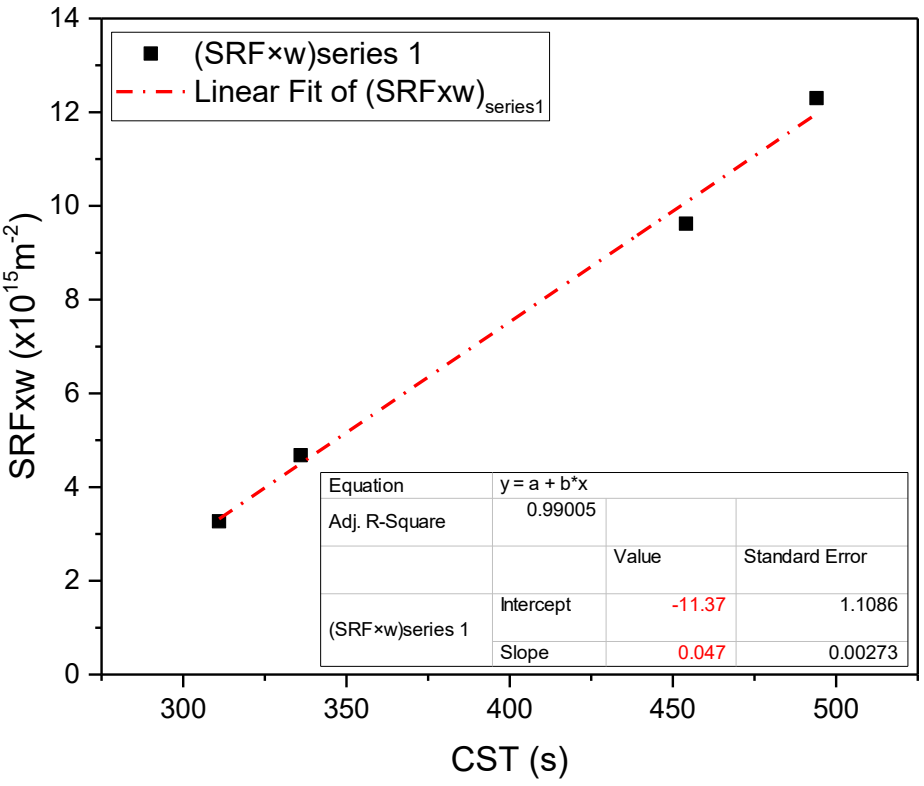

Figure 4.16 CST and SRF×w correlation.

Figure 4.16 shows that in this series of experiments, CST has a good linear correlation with SRF×w values. The correlation can be written in an equation:

$$\text{SRF}\times w = (0.047\times\text{CST} - 11.37)\times 10^{15} \qquad (4.3)$$

The possible reason that Eq. (4.2) and Eq. (4.3) do not have the same coefficients is that these were from two different batch of MFT samples (from different buckets). However, the linear relations established by both Eq. (4.2) and Eq. (4.3) indicates that CST correlates well with SRF in dual polymer treatment for MFT within a same batch of sample.

For the filtration experiments (filtered under 600 kPa) described in section 4.1.3, CST, SRF and SRF×w values are shown in Table 4.9.

Table 4.9 CST, SRF and SRF×w values for experiments treated with different polymer dosages and filtered under 600 kPa.

Dosage of polymers	CST (s)	SRF ($\times 10^{13}$ m/kg)	SRF×w ($\times 10^{15} m^{-2}$)
1 kg/t Alcomer 7115+1 k/t A3335	611	18.95	77.6
2 kg/t Alcomer 7115+1 kg/t A3335	330	8.40	33.7
3 kg/t Alcomer 7115+1 kg/t A3335	250	6.92	27.21
4 kg/t Alcomer 7115+1 kg/t A3335	217	3.95	15.23

The CST value is plotted against SRF×w values for filtration experiments at 600 kPa, as shown in Figure 4.17. And it shows that within one batch of MFT, the CST again correlates well with SRF.

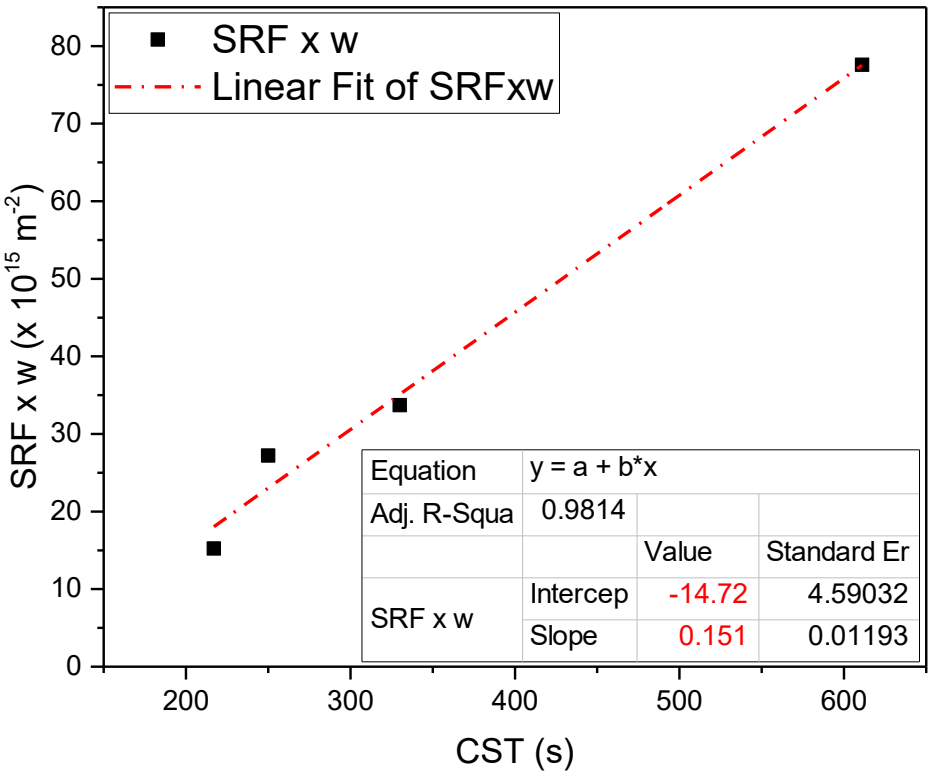

Figure 4.17 Correlation of CST and SRF×w of filtration experiments at 600 kPa.

Recently, more studies were carried out to establish the model to correlate CST and SRF [72] [107]–[109]. However, the models all have limitations. Therefore, more accurate correlations between CST and SRF are yet to be sought [109]. On the other hand, when correlating CST with SRF for different sludge, a best model needs to be chosen through many trials. As for dual-polymer treated MFT here, the model shown in Eq. (4.1) was the best fitted one. And based on the established correlation between CST and SRF, relatively easy-to-obtain CST results can be used to predict SRF results.

4.4 Cryo-SEM Images of Flocs Structure

Single polymer treated MFT samples (MFT treated with 1 kg/t A3335 or 4 kg/t Alcomer 7115), dual polymer treated MFT samples (MFT treated with 4 kg/t Alcomer 7115 and 1 kg/t A3335) as well untreated MFT samples were prepared as cryo-SEM samples through freezing, fracture, sublimation and coating. The cryo-SEM images are showed in Figure 4.18-(a), (b), (c), (d).

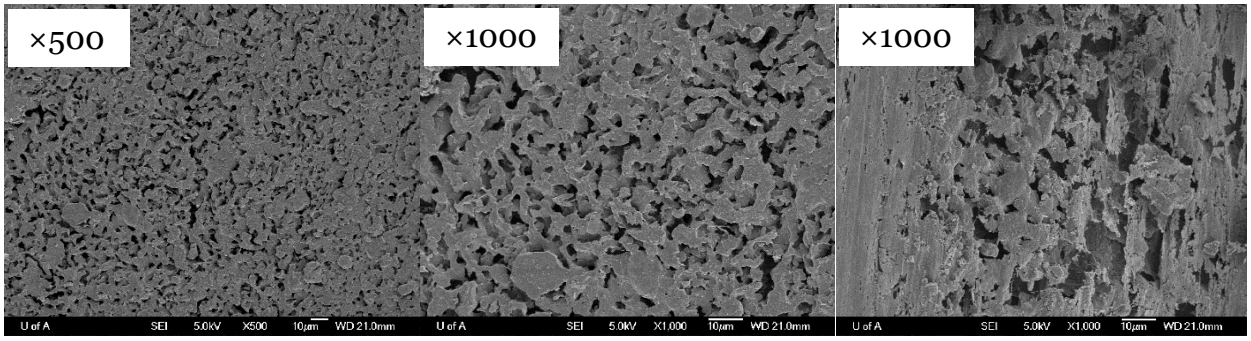

Figure 4.18-(a) Cryo-SEM images of untreated MFT at different magnifications.

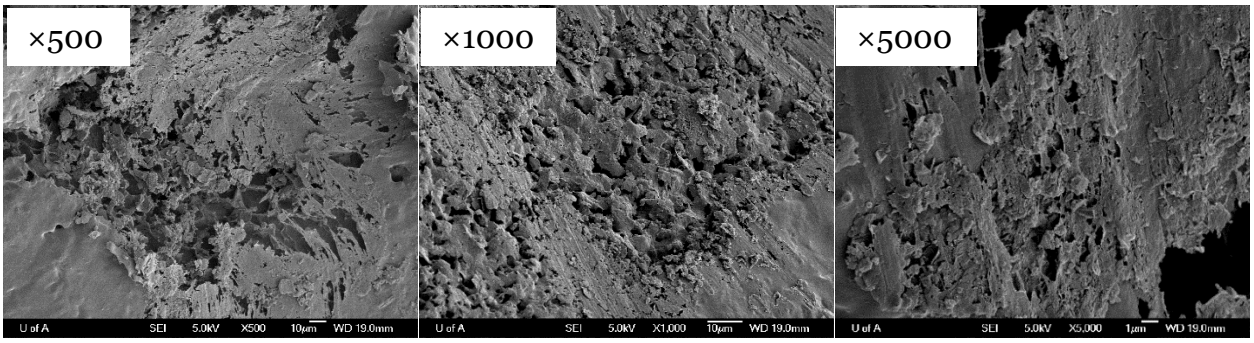

Figure 4.18-(b) Cryo-SEM images of MFT treated with 1 kg/t A3335 at different magnifications.

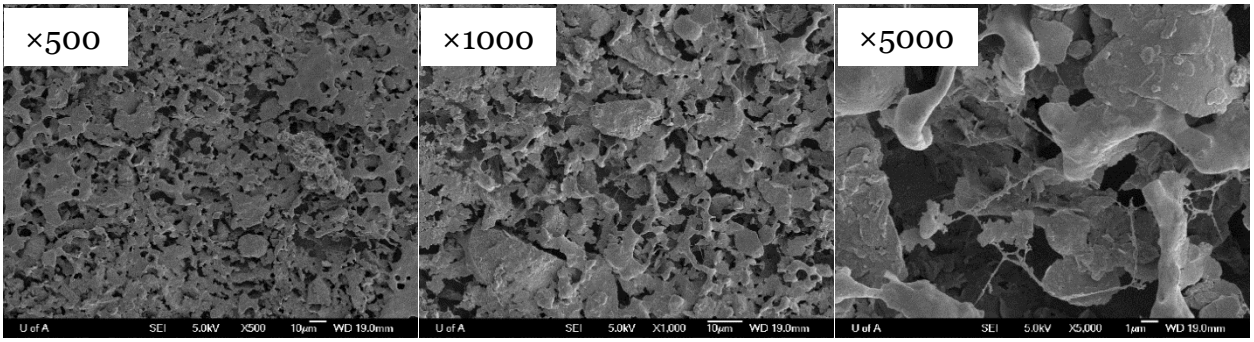

Figure 4.18-(c) Cryo-SEM images of MFT treated with 4 kg/t Alcomer 7115 at different magnifications.

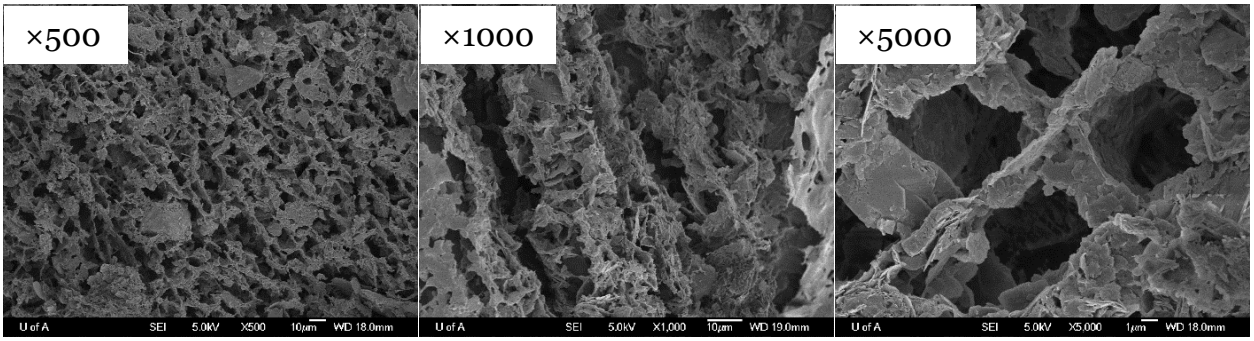

Figure 4.18-(d) Cryo-SEM images of MFT treated with 4 kg/t Alcomer 7115 and 1 kg/t A3335 at different magnifications.

From the images of untreated MFT (Figure 4.18-(a)), it can be seen that the fine particles are connected to each other forming small "cages" to trap water inside. With the help of A3335 (Figure 4.18-(b)), fine particles were bridged together, and small "cages" disappeared and in the meantime some pores were formed, which helped dewater MFT. For 4 kg/t Alcomer 7115 treated MFT, small pores were generated (Figure 4.18-(c)). When MFT was treated with 4 kg/t Alcomer 7115 and 1 kg/t A3335 (Figure 4.18-(d)), more organized porous structure were produced, and the pore sizes were large and water channel can be observed. As an estimation based on the scale bars in the image, the pore size of original MFT is about 5~5.5 μm; after treatment with 4 kg/t Alcomer 7115, the pore

size has been enlarged to 13~13.3 μm; and with the dual polymer treatment, the pore size are in the order of 14~24 μm.

These images somewhat validate the hypothesis about dual polymer treatment of the MFT. And when correlating the cryo-SEM images with experimental results, it can be concluded that the porous structure is the main reason that accelerated dewatering of MFT in dual-polymer treatment process. And larger, more organized pores accounted for better dewaterability of the treated MFT.

4.5 The effect of polymer addition sequence

Due to the relatively low molecular weight of Alcomer 7115, it was added first to generate small flocs. To further study the treatment with Alcomer 7115 and A3335 on their dewatering effect for MFT, the sequence of polymer addition was reversed.

In preliminary experiments, 500 g MFT was treated with 0.5 kg/t A3335 and 0.5 kg/t Alcomer 7115 or 1 kg/t Alcomer 7115, respectively, following the dual polymer treatment protocol described earlier (Figure 3.11). The CST results of these two tests are shown in Table 4.10.

Table 4.10 CST of MFT treated with 0.5 kg/t A3335 and 0.5 kg/t or 1 kg/t Alcomer 7115.

Dosage of A3335 (kg/t)	Dosage of Alcomer 7115 (kg/t)	CST (s)
0.5	0.5	1910
	1	992

The appearances of the MFT after the treatment were shown in Figure 4.19. From the pictures, it can be seen that the treated MFT were over sheared, indicating that 15 seconds stirring past the peak torque was beyond the optimum operating window of this treatment.

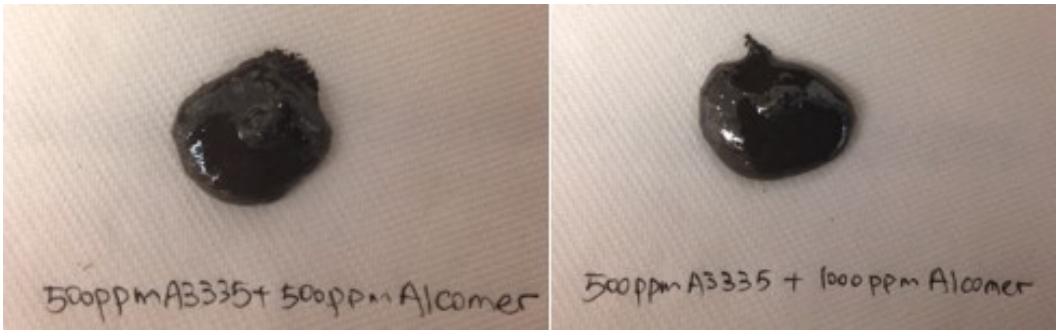

Figure 4.19 Pictures of MFT treated with 1 kg/t A3335 and different dosages of Alcomer 7115.

To determine the optimum window of treatment with the addition of A3335 first followed by Alcomer 7115, different stirring times, 5, 10 and 15 seconds after reaching the peak torque were used after treating the MFT with 1 kg/t A3335 and 3 kg/t Alcomer 7115. The CST results are shown in Table 4.11.

Table 4.11 CST of MFT after treatment using A3335 and Alcomer 7115 with different stirring time after reaching peak torque.

Stopping Time (s)	5	10	15
CST (s)	51	148	175

It can be seen from the CST results that a stirring time of 5 s gave the lowest CST and thus possibly best filterability of MFT. Longer stirring would cause over shear of MFT. Furthermore, The CST value observed by adding A3335 first followed by Alcomer 7115 gave a very low CST value, indicating potentially very good dewaterability of MFT. Filtration tests under a pressure of 600 kPa were conducted to quantify the dewaterability

of MFT treated with 1 kg/t A3335 and 3 kg/t Alcomer 7115, and the results are compared in Figure 4.20 with previous results where the Alcomer 7115 was added first.

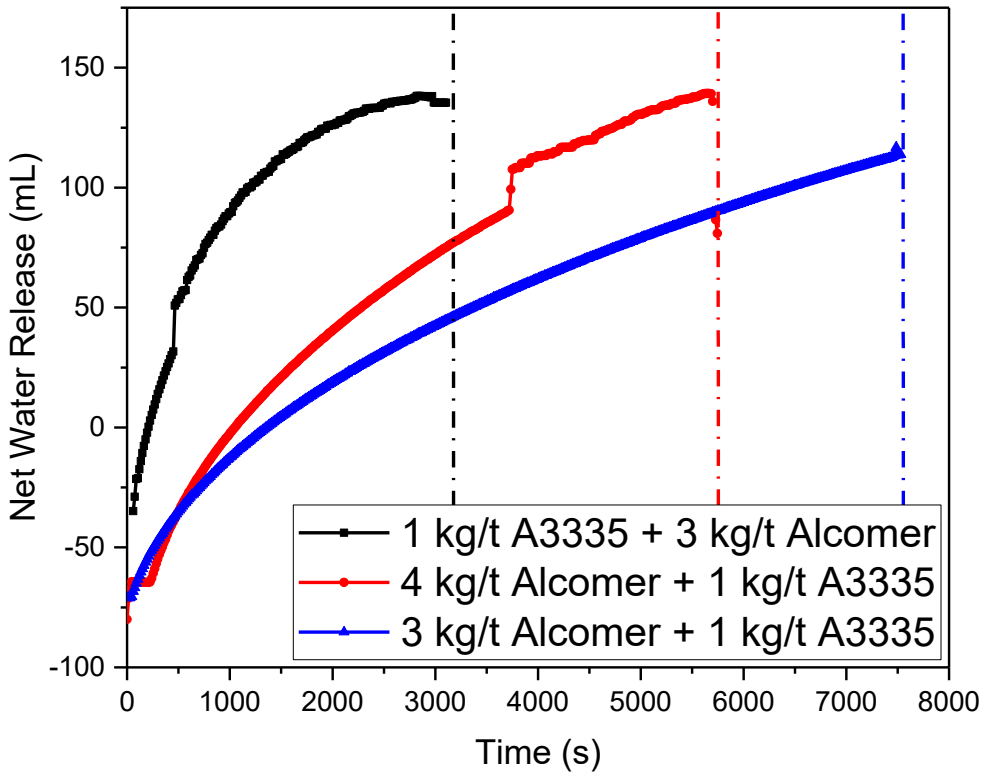

Figure 4.20 Comparison of net water release of MFT treated by dual polymers with different addition sequence.

The red curve and blue curve show the net water release from previous experiments, in which the MFT was treated with Alcomer 7115 first, followed by 1 kg/t A3335 and a pressure filtration at 600 kPa. Compared with the black curve which shows the results when A3335 was added first, it can be seen that the filtration rate indeed became much faster when A3335 was added first, consistent with the low CST. When adding A3335 first, even using a lower dosage of Alcomer 7115 (3 kg/t), it gave a much faster filtration rate

than adding a higher dosage of Alcomer 7115 (4 kg/t) first. The dashed vertical lines in the figure marked the onset of filter cake cracking. As can be seen, cracks formed much earlier when A3335 was added before Alcomer 7115. Therefore, although the filtration rate was faster, the earlier formation of cracks caused the filtration to terminate earlier, so that the final solid content in the filter cake (58.5 wt%) was similar to the test when the same dosage of Alcomer 7115 was added before A3335 (58.0 wt%). However, the significant shortening of the filtration cycle is something that may be desirable in any practical application of the process.

To further investigate the effect of addition sequence on dewatering of MFT, test work was conducted in which the MFT was treated with 1 kg/t A3335 followed by different dosages of Alcomer 7115 (1 to 4 kg/t), and then filtered either under 600 kPa or under vacuum. The results are shown in Table 4.12.

Table 4.12 Filtration results of MFT treated using dual polymers with A3335 injected first

	Dosage of Alcomer 7115 (kg/t)	CST (s)	Time of filtration (s)	Net water release (mL)	Solid Content (wt %)
Pressure Filtration (600 kPa)	1	547	---	---	---
	2.5	229	2835	105.1	55.5
	3	51	2820	138.2	58.5
	4	68	2985	112.1	58.8
Vacuum Filtration	4	91	3600	100	55.1

As the filtration results showed, injecting A3335 first followed by Alcomer 7115 resulted in the lower CST and faster filtration rate (compared with Table 4.5). However, the final solid content did not change significantly. This may have been caused by the

aforementioned formation of cracks in the filter cakes, and the limitations of using compressed gas in pressure filtration.

It was also observed that when the MFT was treated with same polymer dosages, the torque increased to a much higher value when A3335 was added first followed by Alcomer 7115 (Figure 4.21). This seems to signify a better flocculation performance, which may have contributed to the faster filtration rate. However, the mechanism of two-stage polymer treatment is still not clear, and further study is needed to thoroughly understand the mechanism thus to reach a higher solid content.

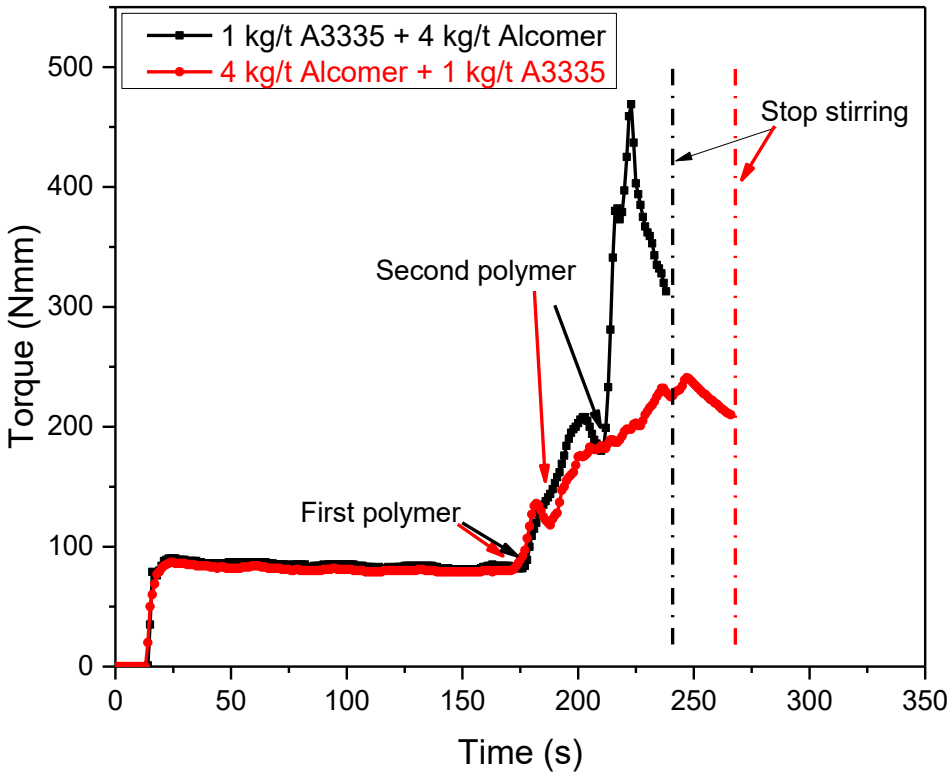

Figure 4.21 Torque change of MFT treatment using same polymer dosage with different addition sequence.

4.6 Auxiliary Chemicals to Strengthen Floc Structures

One common problem that was encountered in both pressure filtration and vacuum filtration was that the cake shrinkage resulting from the collapse of floc structure caused a decrease in pressure during pressure filtration or an increase of pressure during vacuum filtration. This happened before the formation of cracks in the filter cake, and caused a reduction of filtration efficiency.

To control the collapse of the floc structure and the shrinkage of pores, two main methods are: 1) increasing the content of non-spherical particles as the relative displacement of facets and edges requires shear of inter-particle contacts instead of pure rotations, and 2) increasing the friction between particles, for example, the strength between inter-particle bonds [110].

In this study, several chemicals/polymers were tested with the objective to strengthen the floc structures and to maintain dewaterability when the filter cake was under strain.

4.6.1 α-cellulose

Cellulose is the most abundant natural organic polymers on the Earth [111]. α-cellulose is of the highest degree of polymerization and possess the most stable structures of the three classes of cellulose (the other two classes are β-cellulose and γ-cellulose). It is a polysaccharide composed of long chains of β (1, 4) linked D-glucose units. α-cellulose has been widely used as structural backbone or structural media. Utilizing its stable structure as a frame to support flocs, it is expected that by adding a proper amount of α-cellulose, the effective filtration time will be prolonged before the flocs collapse.

In the following experiments, 5 g α-cellulose was mixed with 500 g MFT, followed by sequential polymer treatment with 4 kg/t Alcomer 7115 and 1 kg/t A3335. In control experiment, the MFT was treated with Alcomer 7115 and A3335 only. After treatment, vacuum filtration was conducted on both the control and the α-cellulose treated samples. CST and SRF data are shown in Table 4.13, and the net water release is plotted as a function of time in Figure 4.22.

Table 4.13 CST results and SRF results of experiment with or without α-cellulose

	CST (s)	SRF ($\times 10^{13}$ m/kg)	Solid Content (wt %)
Without α-cellulose	453	0.044	48.9
With 5 g α-cellulose	332	0.026	54.5

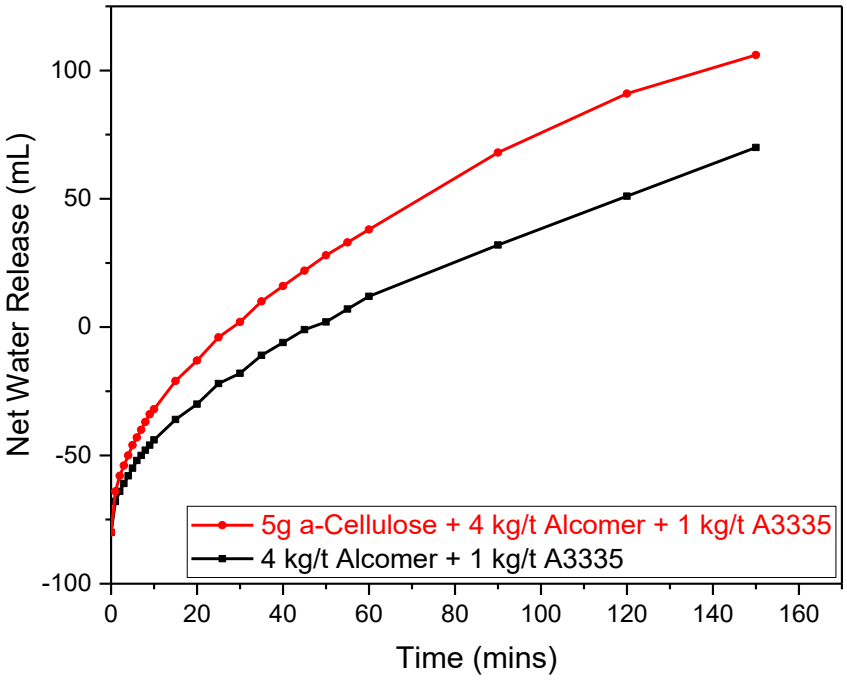

Figure 4.22 Filtrate volume comparison of experiments with or without α-cellulose.

After adding α-cellulose, lower CST and SRF values were obtained in comparison with the control test. Figure 4.22 also shows a faster filtration rate when α-cellulose was added, consistent with a higher final solid content. During the vacuum filtration, no obvious crack or shrinkage were noticed.

4.6.2 Geopolymers

The term geopolymer was coined by Joseph Davidovits to define alkali aluminosilicate binders formed by the alkali silicate activation of aluminosilicate materials [112]. Due to the formation of an inorganic structural network, geopolymers possess high mechanical strength [113].

In another study [114], sodium hydroxide and sodium silicate were used as activators to treat MFT, and the resulting MFT quickly acquired sufficient mechanical strength that meets regulatory requirements.

The idea to combine the geopolymerization activators with the dual polymer treatment was then tested with the expectation that the addition of the activators would help enhance the strength of the floc structure. For 500 g MFT sample, 7.12 g NaOH, 10.68 g Na_2SiO_3, 4 kg/t Alcomer 7115 (stock solutions at 2.0 wt%) and 1 kg/t A3335 (stock solutions at 0.4 wt%) were used. The reagents were added in different manners as described below.

In experiment (1), the activators were added first, and the polymers were added in sequence in 5 minutes after the addition of the activators. The MFT was transferred to the vacuum filtration system immediately after the treatment; in experiment (2), the

treatment procedure was the same with experiment (1), but the treated MFT was left overnight prior to the vacuum filtration test; in experiment (3), after treatment with the activators, the MFT was cured overnight for 24 hours before the sequential addition of the two polymers. Vacuum filtration was followed immediately after the polymer treatment; in experiment (4), polymers were first added into MFT in sequence, followed by activators. Filtration was conducted immediately after the treatment.

The CST was measured immediately after the treatment, and the vacuum filtration time for each experiment was 2 hours. Table 4.14 shows the average CST and the solid contents in the filter cake of each experiment.

Table 4.14 CST and solid content of experiments (1)-(4)

Experiment No.	CST (s)	Solid Content (wt %)
(1)	296	51.3
(2)	694	49.7
(3)	407	52.0
(4)	574	50.6

As can be seen, the overall effect of geopolymers are not noticeable. When comparing the CST and solid content, it can be seen that the formation of geopolymers, experiment (2), yielded a higher CST value and lower solid content. The increase in CST implies that the introduction of geopolymerization activators actually reduced the efficiency of polymer treatment to some degree.

4.6.3 Chitin

Chitin is a biopolymer of high molecular weight. it is often found to compose the exoskeletons of arthropods and the cell walls of fungi and yeasts, and contains naturally ordered crystalline microfibers which can act as reinforcing agents [115]. It is the second-most abundant and important natural polymer in nature [116] [117].

Chitin was used in a similar way as cellulose to strengthen the floc structures in this study. The MFT sample (500 g) was treated with 2.5 g chitin, followed by 4 kg/t Alcomer 7115 and 1 kg/t A3335. A control experiment was conducted in which the MFT was only treated with 4 kg/t Alcomer 7115 and 1 kg/t A3335. Results of pressure filtration tests showed a very mediocre behavior of chitin (Table 4.15).

Table 4.15 Filtration results of treatment with or without chitin.

	CST (s)	Net Water Release (mL)	Crack formation time (s)
Without Chitin	150	136.6	5400
With Chitin	169	117.8	5520

4.6.4 Combinations of Bacteria and Polymers

The mechanism for the bacteria to work on MFT strengthening is based on a process called microbial induced calcite precipitation (MICP). This is a process in which the presence of excess calcium ions lead to the precipitation of carbonate as calcite ($CaCO_3$) in situ [118]. The formation of calcite on the surface of microbial cells bonds soil particles cohesively. The bacteria used in this case, sporosarcina pasteurii, a urea-hydrolyzing

bacterium can induce $CaCO_3$ precipitation as well as act as nucleation sites to facilitate the precipitation of $CaCO_3$ on bacteria surfaces. The combination of bacteria and polymers is expected to form porous structure while the bacteria can strengthen the structure.

A series of experiments were carried out as follows: a) 9 mL bacterial solutions were used to treat the MFT. After 24 hours, the CST of the treated MFT was measured and pressure filtration was carried out at 600 kPa; b) MFT was treated with 4 kg/t Alcomer 7115 and 1 kg/t A3335, followed by CST measurement and then pressure filtration at 600 kPa; c) 9 mL bacterial solutions were injected into MFT first, after stirring for 90 seconds, 4 kg/t Alcomer 7115 and 1 kg/t A3335 were added sequentially. CST was measured both immediately after the treatment and after 24 hours. Filtration test was conducted after 24 hours following the treatment; d) 4 kg/t Alcomer 7115 and 1 kg/t A3335 were added to MFT in sequence first, 9 mL bacterial solutions were injected in 30 seconds after the addition of A3335. CST was measured both immediately after the treatment and in 24 hours. Filtration test was conducted in 24 hours after treatment. For the experiments above, bacterial solutions were at a concentration of 10^9 cells per mL. Filtration tests were carried until cracks formed and pressure dropped quickly. The measured CST and solid contents are shown in Table 4.16, and the net water release volume as a function of time is shown in Figure 4.23.

Table 4.16 Comparison of immediate and 24 hour CST results and solid content results of MFT treated with polymers and bacteria

Addition Sequence	Immediate CST (s)	CST in 24 hours (s)	Solid content (wt %)	SRF ($\times 10^{13}$m/kg)
(a) Bacteria only	---	939	46.8	25.1
(b) Polymers only	150	---	64.1	4.7
(c) Bacteria + Polymers	109	155	56.5	3.7
(d) Polymers + Bacteria	168	148	59.8	5.1

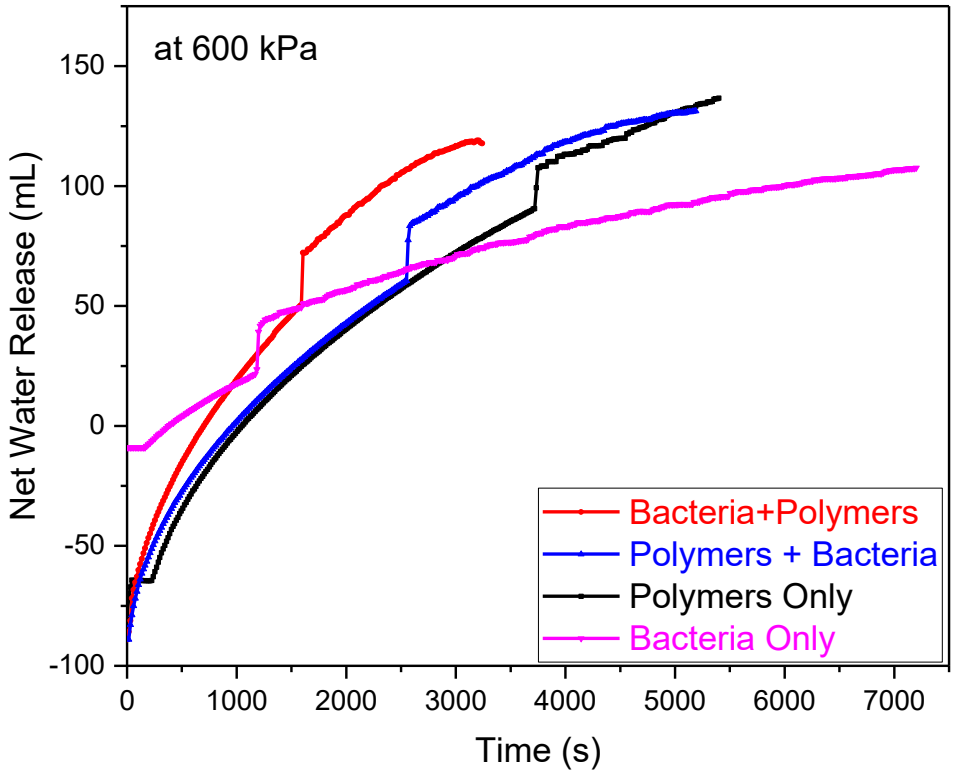

Figure 4.23 Filtrate volume comparison of MFT treated with polymers and bacteria sporosarcina pasteurii.

The CST after 24 hours following the bacteria treatment of MFT was much lower than that of untreated MFT (which is around 3000 s), indicative of a better filterability after bacterial treatment. The CST's of MFT treated with polymers with or without the bacteria are very close. So are the SRF results. This implies that the addition of bacterial solutions did not significantly change the effect of polymers. However, as can be seen from Figure 4.23, the addition of bacterial solutions caused the earlier occurrence of both the collapse and the cracks formation in the filter cakes. The addition of bacteria also increased the filtration rate slightly but without affecting the final filtrate volume significantly.

In general, bacterial solutions did not help with prolonging the effective filtration time before cracks were formed.

4.7 Summary

The filtration tests and data analysis demonstrate that CST and SRF are two meaningful indicators to predict the filterability or dewaterability of MFT with dual polymer treatment. And the correlation between these two parameters is linear within the same MFT batch tests.

In the range of 1 kg/t to 4 kg/t with an increment of 1 kg/t, with the increasing Alcomer 7115 dosage, a lower CST and better dewaterability of MFT can be obtained. And if filtered under the same pressure, SRF decreases as the dosage of Alcomer 7115 increases. The highest solid content obtained was 64.1 wt% when the MFT was treated with 4 kg/t Alcomer and 1 kg/t A3335, followed by pressure filtration at 600 kPa. A weak strength of the filter cake is the limitation to reach higher solid content. And treated with same polymer dosage, MFT filtered under 600 kPa has a larger final filtrate volume and faster

filtration rate than under 150 kPa. However, SRF values of MFT filtered under 600 kPa are higher than those under 150 kPa.

Vacuum filtration is very promising due to the much lower SRF values (compared to pressure filtration) it generates, and can procced without bringing cracks to filter cakes. But the filtration rate was much lower than pressure filtration.

The cryo-SEM images provide evidence to the validity of the hypothesis of the mechanisms underlying the dual-polymer treatment. Dual-polymer treatment led to larger pores in the filter cake and consequently, better dewaterability.

5 Conclusions

5.1 General findings

The general findings of this thesis research are presented in the following two sections.

5.1.1 Methodology

(1) Capillary suction time (CST) is a meaningful indicator to assess the dewaterability in dual polymer treatment for oil sands mature fine tailings (MFT). Lower CST value indicates better dewaterability.

(2) Specific resistance to filtration (SRF) is also a suitable parameter to evaluate the dewaterability of MFT for dual polymer treatment. Higher SRF value means it is more difficult to filter MFT. Moreover, SRF correlates well with CST in MFT treatment within the same batch of samples, i.e., both of them can give an accurate prediction of the dewaterability of MFT. The easily obtained CST results can be used to predict SRF values.

(3) The cryogenic scanning electron microscopic (cryo-SEM) images validated the hypothesis of the mechanism underlying the dual-polymer treatment. For polymer treatment, porous structure of the sludge is the main cause of the change of dewaterability. Larger pore size and more organized porous structures account for better dewaterability of MFT. Also, the cryo-SEM images show the advantage of dual polymer treatment over single polymer treatment. The former can produce more organized porous structures with larger pore size, which contribute to much better dewaterability of MFT.

5.1.2 Dewatering Results using Dual Polymers Alcomer 7115 and A3335

(1) The use of dual polymer system consisting of a cationic polyDADAMAC polymer Alcomer 7115 and an anionic polyacrylamide polymer A3335 gives a lower CST and higher final filtrate volume, indicating a better dewatering performance of MFT, compared with single polymer A3335 alone or Alcomer 7115 alone. Using compressed air pressure filtration under 600 kPa, a filter cake solid content of 64 wt% could be obtained after 2 hours of filtration.

(2) In the range of 1 kg/t to 4 kg/t with an increment of 1 kg/t, with the increasing of Alcomer 7115 dosage, a lower CST and better dewaterability of MFT can be obtained. Further increase in Alcomer 7115 dosage to 5 kg/t causes the CST to increase, indicative of decreasing dewaterability. Therefore, the optimum dosage to treat MFT is 4 kg/t Alcomer 7115 and 1 kg/t A3335.

(3) If MFT treated with different polymer dosages was filtered under the same pressure, the specific resistance to filtration (SRF) decreases as the dosage of Alcomer 7115 increases. SRF is higher under 600 kPa than under 150 kPa when other conditions are the same. A possible explanation is that high pressure causes the porous pore structure to collapse, leading to a higher volume fraction of the solids and thus higher resistance of the filter cake to filtration. However, treated with same polymer dosage, MFT filtered under 600 kPa gives larger final filtrate volume and faster filtration rate than under 150 kPa, despite the higher SRF. This is obviously caused by the larger driving force.

(4) A weak strength of flocs is the limiting factor to obtain higher solid content in tailings for MFT treatment with Alcomer 7115 and A3335. To strengthen the flocs, various additives, including α-cellulose, chitin, geopolymer activators (sodium hydroxide and sodium silicate), a calcite-forming bacterium sporosarcina pasteurii, are tested with the expectation to work as backbone structure to increase the strength of flocs generated by Alcomer 7115 and A3335. However, no significant benefits were observed in overall evaluation for dewaterability of MFT except for α-cellulose. On the other hand, vacuum filtration can significantly reduce or eliminate the formation of cracks. When increase the dosage of Alcomer to 10 kg/t, vacuum filtration gives fast filtration rate and the filter cake reaches a high solid content (58.6 wt%) in one hour.

5.1.3 Suggestions to future work

(1) More research is needed to further study the properties and compositions of MFT, and their effects on the performance of different polymers.

(2) The combination of Alcomer 7115 and A3335 has promising performances in MFT treatment, further work regarding the mechanism should be conducted, and more Alcomer series of cationic polymers need to be studied to find polymers that have similar advantages and also can generate flocs with high strength.

References

[1] "Oil Sands," *Alberta Energy, Government of Alberta*, 14-Jun-. [Online]. Available: http://www.energy.alberta.ca/oilsands/oilsands.asp. [Accessed: 14-Oct-2015].

[2] J. Robbins, "The Dilbit Hits the Fan: Alberta Oil," *Places J.*, Oct. 2015.

[3] "About the Oil Sands," *Government of Alberta*, 10-Aug-2010. [Online]. Available: http://oilsands.alberta.ca/about.html. [Accessed: 14-Oct-2015].

[4] "Facts and Statistics," *Alberta Energy, Government of Alberta*, 20-Jun-2007. [Online]. Available: http://www.energy.alberta.ca/OilSands/791.asp. [Accessed: 14-Oct-2015].

[5] CAPP, "Recovering the Oil - Oil Sands Today," *Canadian Association of Petroleum Producers*. [Online]. Available: http://www.oilsandstoday.ca/whatareoilsands/Pages/RecoveringtheOil.aspx. [Accessed: 08-Nov-2015].

[6] "Oil Sands Development," *Canadian Association of Petroleum Producers*. [Online]. Available: http://www.capp.ca/canadian-oil-and-natural-gas/oil-sands/oil-sands-development. [Accessed: 14-Oct-2015].

[7] G. Stringham, "Chapter 2 - Energy Developments in Canada's Oil Sands," in *Alberta Oil Sands*, 1st ed., vol. 11, Elsevier Ltd., 2012, pp. 19–34.

[8] "About the resource," *Alberta's Oil Sands, Government of Alberta*, 11-Aug-2010. [Online]. Available: http://www.oilsands.alberta.ca/resource.html. [Accessed: 14-Oct-2015].

[9] "2015 Crude Oil Forecast, Markets and Transportation - Canadian Association of Petroleum Producers," *Canadian Association of Petroleum Producers*. [Online]. Available: http://www.capp.ca/publications-and-statistics/crude-oil-forecast. [Accessed: 14-Oct-2015].

[10] R. J. Chalaturnyk, J. Don Scott, and B. Özüm, “Management of Oil Sands Tailings,” *Pet. Sci. Technol.*, vol. 20, no. 9–10, pp. 1025–1046, 2002.

[11] J. Masliyah, Z. J. Zhou, Z. Xu, J. Czarnecki, and H. Hamza, “Understanding Water-Based Bitumen Extraction from Athabasca Oil Sands,” *Can. J. Chem. Eng.*, vol. 82, no. 4, pp. 628–654, 2004.

[12] G. J. Cymerman and T. Kwong, “Improvements in the oil recovery flotation process at Syncrude Canada Ltd,” in *Processing of Hydrophobic Minerals and Fine Coals: Proceedings of the 1st UBC-McGill Bi-Annual International Symposium on Fundamentals of Mineral Processing, Vancouver, BC*, 1995, pp. 20–24.

[13] K. L. Kasperski, “A review of properties and treatment of oil sands tailings,” *AOSTRA J. Res.*, vol. 8, p. 11, 1992.

[14] R. a Carter, “Oil sands operators tackle tailings management challenges,” *E&MJ - Eng. Min. J. VO - 210*, no. 4, p. 54, 2009.

[15] “Tailings Ponds - Oil Sands Today.” [Online]. Available: http://www.oilsandstoday.ca/topics/Tailings/Pages/default.aspx. [Accessed: 15-Oct-2015].

[16] P. G. Nix and R. W. Martin, “Detoxification and reclamation of Suncor’s oil sand tailings ponds,” *Environ. Toxicol. Water Qual.*, vol. 7, no. 2, pp. 171–188, 1992.

[17] Alberta chamber of commerce, “Oil Sands Technology Roadmap,” *Technol. Soc.*, vol. 26, pp. 455–468, 2004.

[18] C. C. Small, S. Cho, Z. Hashisho, and A. C. Ulrich, “Emissions from oil sands tailings ponds: Review of tailings pond parameters and emission estimates,” *J. Pet. Sci. Eng.*, vol. 127, pp. 490–501, 2015.

[19] J. Long, H. Li, Z. Xu, and J. H. Masliyah, “Role of colloidal interactions in oil sand tailings treatment,” *AIChE J.*, vol. 52, no. 1, pp. 371–383, 2006.

[20] K. a. Landman, C. Sirakoff, and L. R. White, “Dewatering of flocculated suspensions by pressure filtration,” *Phys. Fluids A Fluid Dyn.*, vol. 3, no. 1991, p. 1495, 1991.

[21] K. a Landman, L. R. White, and M. Eberl, “Pressure Filtration of Flocculated Suspensions,” vol. 41, no. 7, pp. 1687–1700, 1995.

[22] L. S. Kotlyar, “Effect of Particle Size on the Flocculation Behaviour of Ultra-Fine Clays in Salt Solutions,” *Clay Miner.*, vol. 33, no. 1, pp. 103–107, 1998.

[23] Y. Tu, J. B. O’Carroll, L. S. Kotlyar, B. D. Sparks, S. Ng, K. H. Chung, and G. Cuddy, “Recovery of bitumen from oilsands: Gelation of ultra-fine clay in the primary separation vessel,” *Fuel*, vol. 84, no. 6 SPEC. ISS., pp. 653–660, 2005.

[24] L. S. Kotlyar, B. D. Sparks, J. Woods, C. E. Capes, and R. Schutte, “Biwetted ultrafine solids and structure formation in oil sands fine tailings,” *Fuel*, vol. 74, no. 8, pp. 1146–1149, Aug. 1995.

[25] J. Don Scott, M. B. Dusseault, and W. David Carrier, “Behaviour of the clay/bitumen/water sludge system from oil sands extraction plants,” *Appl. Clay Sci.*, vol. 1, no. 1–2, pp. 207–218, Jul. 1985.

[26] L. S. Kotlyar, B. D. Sparks, R. Schutte, and J. R. Woods, “Understanding of fundamentals. Key to process modification for tailings reduction,” *J. Environ. Sci. Heal. Part A Environ. Sci. Eng.*, vol. 28, no. 10, pp. 2215–2224, 1993.

[27] J. D. O. N. Scott, M. B. Dusseault, and W. D. C. Iii, “Behaviour of The Clay/Bitumen/Water Sludge System From Oil Sands Extration Plants,” vol. 1, pp. 207–218, 1985.

[28] J. D. S. Nagula N. Suthaker, “Measurement of hydraulic conductivity in oil sand tailings slurries,” *Can. Geotech. J.*, vol. 33, no. 4, pp. 642–653, 1996.

[29] C. Klein, D. Harbottle, L. Alagha, and Z. Xu, “Impact of fugitive bitumen on polymer-based flocculation of mature fine tailings,” *Can. J. Chem. Eng.*, vol. 91, no. 8, pp. 1427–1432, 2013.

[30] F. T. F. Consortium, *Advances in oil sands tailings research.* Edmonton, Alta. : Alberta Dept. of Energy, 1995., 1995.

[31] J. G. Matthews, W. H. Shaw, M. D. MacKinnon, and R. G. Cuddy, “Development of Composite Tailings Technology at Syncrude,” *Int. J. Surf. Mining, Reclam. Environ.*, vol. 16, no. 1, pp. 24–39, 2002.

[32] D. W. Devenny, “Oil Sand Tailings Technologies and Practices,” *Report*, no. March, pp. 1–131, 2010.

[33] E. S. Hall and E. L. Tollefson, “Stabilization and Destabilization of Mineral Fines Bitumen Water Dispersions in Tailings from Oil Sand Extraction Plants That Use the Hot Water Process,” *Can. J. Chem. Eng.*, vol. 60, no. 6, pp. 812–821, 1982.

[34] G. Cymerman, T. Kwong, E. Lord, H. Hamza, and Y. Xu, “Thickening and disposal of fine tails from oil sand processing,” in *38th Annual Conference of Metallurgists of CIM, Quebec City, Quebec, August*, 1999, pp. 22–26.

[35] J. Sobkowicz, “Oil Sands Tailings Technology Deployment Roadmap Volume 2: Component 1 Results,” vol. 2, pp. 1–102, 2012.

[36] J. C. Sobkowicz, “History and developments in the treatment of oil sands fine tailings BT - 14th International Conference on Tailings and Mine Waste’10, October 17, 2010 - October 20, 2010,” 2011, pp. 11–30.

[37] R. J. Mikula, V. A. Munoz, and O. Omotoso, “Centrifugation options for production of dry stackable tailings in surface mined oil sands tailings management,” *J. Can. Pet. Technol.*, vol. 48, no. 9, pp. 19–23, 2009.

[38] P. D. Vorob, N. P. Krut, E. V Vorob, and N. Strnadova, “Successive Adsorption of Polyacrylamide Compounds from Electrolyte Solutions on the Surface of Kaolinitic Clay Particles,” vol. 70, no. 2, pp. 171–174, 2008.

[39] J. Gregory, “Flocculation by polymers and polyelectrolytes,” *Solid/liquid dispersions*, pp. 163–181, 1987.

[40] G. John, “Polymer adsorption and flocculation in sheared suspensions,” *Colloids and Surfaces*, vol. 31, no. 0, pp. 231–253, 1988.

[41] N. J. D. Graham, “Orthokinetic flocculation rates for amorphous silica microspheres with cationic polyelectrolytes,” *Colloids and Surfaces*, vol. 3, no. 1, pp. 61–77, 1981.

[42] R. Slater and J. Kitchener, “Characteristics of flocculation of mineral suspensions by polymers,” *Discuss. Faraday Soc.*, 1966.

[43] A. McFarlane, K. Y. Yeap, K. Bremmell, and J. Addai-Mensah, “The influence of flocculant adsorption kinetics on the dewaterability of kaolinite and smectite clay mineral dispersions,” *Colloids Surfaces A Physicochem. Eng. Asp.*, vol. 317, no. 1–3, pp. 39–48, 2008.

[44] C. Gordon and G. Klein, “Effect of Residual Bitumen on Polymer-assisted Flocculation of Fluid Fine Tailings,” University of Alberta, 2014.

[45] a. Sworska, J. S. Laskowski, and G. Cymerman, “Flocculation of the Syncrude fine tailings Part II. Effect of hydrodynamic conditions,” *Int. J. Miner. Process.*, vol. 60, no. 2, pp. 153–161, 2000.

[46] A. Blanco, C. Negro, E. Fuente, and J. Tijero, “Effect of Shearing Forces and Flocculant Overdose on Filler Flocculation Mechanisms and Floc Properties,” *Ind. Eng. Chem. Res.*, vol. 44, no. 24, pp. 9105–9112, 2005.

[47] R. Hogg, “Collision efficiency factors for polymer flocculation,” *J. Colloid Interface Sci.*, vol. 102, no. 1, pp. 232–236, 1984.

[48] Y. Adachi, “Dynamic aspects of coagulation and flocculation,” *Adv. Colloid Interface Sci.*, vol. 56, pp. 1–31, 1995.

[49] R. Hogg, “The role of polymer adsorption kinetics in flocculation,” *Colloids Surfaces A Physicochem. Eng. Asp.*, vol. 146, no. 1–3, pp. 253–263, 1999.

[50] X. S. Yuan and W. Shaw, “Novel Processes for Treatment of Syncrude Fine Transition and Marine Ore Tailings,” *Can. Metall. Q.*, vol. 46, no. 3, pp. 265–272, 2007.

[51] C. Klein, “Effect of Residual Bitumen on Polymer-assisted Flocculation of Fluid Fine Tailings,” University of Alberta, 2014.

[52] L. Alagha, S. Wang, L. Yan, Z. Xu, and J. Masliyah, “Probing adsorption of polyacrylamide-based polymers on anisotropic Basal planes of kaolinite using quartz crystal microbalance.,” *Langmuir*, vol. 29, no. 12, pp. 3989–98, 2013.

[53] M. H. Haroon, “Flocculation and dewatering of kaolinite suspensions and oil sands mature fine tailings using dual polymers,” University of Alberta, 2014.

[54] Y. Zhou and G. V. Franks, “Flocculation mechanism induced by cationic polymers investigated by light scattering,” *Langmuir*, vol. 22, no. 16, pp. 6775–6786, 2006.

[55] R. P. Singh, S. Pal, S. Krishnamoorthy, P. Adhikary, and S. K. Ali, “High-technology materials based on modified polysaccharides,” *Pure Appl. Chem.*, vol. 81, no. 3, pp. 525–547, 2009.

[56] S. Krishnamoorthi and R. P. Singh, “Synthesis, characterization, flocculation, and rheological characteristics of hydrolyzed and unhydrolyzed polyacrylamide-grafted poly(vinyl alcohol),” *J. Appl. Polym. Sci.*, vol. 101, no. 4, pp. 2109–2122, 2006.

[57] X. W. Wang, X. Feng, Z. Xu, and J. H. Masliyah, “Polymer aids for settling and filtration of oil sands tailings,” *Can. J. Chem. Eng.*, vol. 88, no. 3, pp. 403–410, 2010.

[58] Y. Xu, T. Dabros, and J. Kan, “Filterability of oil sands tailings,” *Process Saf. Environ. Prot.*, vol. 86, no. 4, pp. 268–276, 2008.

[59] a. Sworska, J. S. Laskowski, and G. Cymerman, “Flocculation of the Syncrude fine tailings Part I. Effect of pH, polymer dosage and Mg2q and Ca2q cations,” *Int. J. Miner. Process.*, vol. 60, no. 2, pp. 153–161, 2000.

[60] C. H. Lee and J. C. Liu, “Sludge dewaterability and floc structure in dual polymer conditioning,” *Adv. Environ. Res.*, vol. 5, no. 2, pp. 129–136, 2001.

[61] P. R. Senthilnathan and R. G. Sigler, “Improved Sludge Dewatering by Dual Polymer Conditioning,” *Water Sci. Technol.*, vol. 28, no. 1, pp. 53–57, 1993.

[62] S. M. Glover, Y. Yan, G. J. Jameson, and S. Biggs, “Dewatering properties of dual-polymer-flocculated systems,” *Int. J. Miner. Process.*, vol. 73, no. 2–4, pp. 145–160, 2004.

[63] R. S. Gale and B. RC, “CAPILLARY SUCTION METHOD FOR DETERMINATION OF FILTRATION PROPERTIES OF A SOLID/LIQUID SUSPENSION,” *Chemistry & Industry*, no. 9. SOC CHEMICAL INDUSTRY 14 BELGRAVE SQUARE, LONDON SW1X 8PS, ENGLAND, p. 355, 1967.

[64] J. D. Swanwich, “Theoretical and Practical Aspects of Sludge Dewatering,” Munich, Germany, 1972.

[65] P. A. Vesilind, “Capillary measure suction of time sludge as a fundamental dewaterability,” *Water Pollut. Control Fed.*, vol. 60, no. 2, pp. 215–220, 1988.

[66] D. K. Sengupta, H. A. Hamza, and K. A. Hashmi, “Role of Cationic and Anionic Flocculants in the Filtration of an Industrial Sludge,” *Annu. Conf. Metall. Metall. Soc. Can. Inst. Min. Metall.*, vol. CONF 33, p. 357, 1994.

[67] D. K. Sengupta, J. Kan, A. M. AlTaweel, and H. A. Hamza, “Dependence of separation properties on flocculation dynamics of kaolinite suspension,” *INTERNATIONAL JOURNAL OF MINERAL PROCESSING*, vol. 49, no. 1–2. pp. 73–85.

[68] D. Lee and Y. H. Hsu, “Use of Capillary Suction Apparatus for Estimating the Averaged Specific Resistance of Filtration Cake,” *J. Chem. Technol. Biotechnol.*, vol. 59, pp. 45–51, 1994.

[69] L. Besra, D. K. Sengupta, B. P. Singh, and S. Bhattacharjee, “A novel method based on Capillary Suction Time (CST) for assessment of dispersion characteristics of suspensions,” *J. Am. Ceram. Soc.*, vol. 88, no. 1, pp. 109–113, 2005.

[70] B. P. Singh, S. K. Swain, S. K. Dash, and S. Bhattacharjee, “Correlation between Dispersion Stability of Concentrated Ceramic Suspension and Capillary Suction Time,” *J. Dispers. Sci. Technol.*, vol. 27, no. 2, pp. 251–258, 2006.

[71] M. Smollen, “Dewaterability of municipal sludge 1: a comparative study of specific resistance to filtration and capillary suction time as dewaterability parameters,” *Water SA*, vol. 12, no. 3. pp. 127–132, 1986.

[72] O. Sawalha and M. Scholz, “Modeling the Relationship between Capillary Suction Time and Specific Resistance to Filtration,” *J. Environ. Eng.*, vol. 136, no. 9, pp. 983–991, 2010.

[73] A. Ayol, “Enzymatic treatment effects on dewaterability of anaerobically digested biosolids-I: Performance evaluations,” *Process Biochem.*, vol. 40, no. 7, pp. 2427–2434, 2005.

[74] S. K. Teoh, R. B. H. Tan, and C. Tien, “A new procedure for determining specific filter cake resistance from filtration data,” *Chem. Eng. Sci.*, vol. 61, no. 15, pp. 4957–4965, 2006.

[75] H. Yukseler, I. Tosun, and U. Yetis, “A new approach in assessing slurry filterability,” *J. Memb. Sci.*, vol. 303, no. 1–2, pp. 72–79, 2007.

[76] B. F. Ruth, G. H. Montillon, and R. E. Montonna, “Studies in Filtration I. Critical Analysis of Filtration Theory,” *Ind. Eng. Chem.*, vol. 25, no. 1, pp. 76–82, 1933.

[77] B. F. Ruth, G. H. Montillon, and R. E. Montanna, “Studies in Filtration II. Fundamentals of constant pressure filtration,” *Ind. Eng. Chem.*, vol. 25, no. 2, pp. 153–161, 1933.

[78] B. F. Ruth, “Studies in Filtration III. Derivation of General Filtration Equations,” *Ind. Eng. Chem.*, vol. 27, no. 6, pp. 708–723, Jun. 1935.

[79] B. Ruth, “Correlating Filtration Theory with Industrial Practice.,” *Ind. & Eng. Chem.*, 1946.

[80] P. C. Carman, “Fundamental principles of industrial filtration,” *Trans. Inst. Chem. Eng*, vol. 16, no. 4, pp. 168–188, 1938.

[81] M. L. Agerbaek and K. Keiding, “On the origin of specific resistance to filtration,” *Water Sci. Technol.*, vol. 28, no. 1, pp. 159–168, 1993.

[82] R. C. Viadero, X. Wei, and K. M. Buzby, “Characterization and Dewatering Evaluation of Acid Mine Drainage Sludge from Ammonia Neutralization,” *Environ. Eng. Sci.*, vol. 23, no. 4, pp. 734–743, 2006.

[83] B. Jimmy, R. Christensen, P. B. Srensen, G. L. Christensen, and J. A. Hansen, “Mechanisms for Overdosing in Sludge Conditioning,” vol. 119, no. 1, pp. 159–171, 1993.

[84] Y. Endo and M. Alonso, “Physical meaning of specific cake resistance and effects of cake properties in compressible cake filtration,” *Filtr. Sep.*, vol. 38, no. 7, pp. 42–46, 2001.

[85] A. Rushton, A. S. Ward, and R. G. Holdich, *Solid-liquid filtration and separation technology*. Weinheim ; New York : VCH, 1996, PP. 33-83, 1966.

[86] W. W. Eckenfelder, D. L. Ford, and A. J. Englande, *Sludge Handling and Disposal*. McGraw-Hill Professional, 2009.

[87] X. Cao and M. Jahazi, “Examination and verification of the filtration mechanism of cake mode during the pressure filtration tests of liquid Al-Si cast alloys,” *Mater. Sci. Eng. A*, vol. 408, no. 1–2, pp. 234–242, 2005.

[88] M. J. Matteson and C. Orr, *Filtration : principles and practices.*, Second. New York : M. Dekker, c1987., 1987.

[89] N. P. Cheremisinoff, *Liquid filtration. [electronic resource].* Boston : Butterworth-Heinemann, ©1998, pp. 59-87, 1998.

[90] C. E. Eckert, R. E. Miller, D. Apelian, and R. Mutharasan, “Light metals 1984,” *TMS, Warrendale*, p. 1281, 1984.

[91] C. O. Bennett and J. E. Myers, *Momentum, heat, and mass transfer*. New York : McGraw-Hill, c1982., 1982.

[92] A. P. Coackley and B. R. S. Jones, “VACUUM SLUDGE FILTRATION I . INTERPRETATION OF RESULTS BY THE CONCEPT,” vol. 28, no. 8, pp. 963–976, 2015.

[93] G. L. Christensen and R. I. Dick, “Specific Resistance Measurements: Methods and Procedures,” *J. Environ. Eng.*, vol. 111, no. 3, pp. 258–271, 1985.

[94] W. L. McCabe and J. C. Smith, *Unit operations of chemical engineering*. McGraw-Hill, 1976.

[95] R. Lotzien, D. Hansel, S. G. Ozkan, A. Onur, I. Kursun, and K. Cinku, “Batch filtration studies of fine calcites,” *CHEMICAL AND BIOCHEMICAL ENGINEERING QUARTERLY*, vol. 19, no. 3. pp. 263–267.

[96] E. S. Tarleton and R. J. Wakeman, *Solid/liquid separation. [electronic resource] : equipment selection and process design*. Oxford : Butterworth-Heinemann, 2007., 2007.

[97] J. B. Pawley, *Handbook of biological confocal microscopy. [electronic resource]*. New York, NY : Springer, c2006., 2006.

[98] R. J. Mikula, V. A. Munoz, and V. W. Lam, “MICROSCOPIC CHARACTERIZATION OF OIL SANDS PROCESSING EMULSIONS,” *Fuel Sci. Technol. Int.*, vol. 7, no. 5–6, pp. 727–749, Jan. 1989.

[99] R. J. Mikula and V. a. Munoz, “Characterization of emulsions and suspensions in the petroleum industry using cryo-SEM and CLSM,” *Colloids Surfaces A Physicochem. Eng. Asp.*, vol. 174, no. 1–2, pp. 23–36, 2000.

[100] P. Mpofu, J. Addai-Mensah, and J. Ralston, “Investigation of the effect of polymer structure type on flocculation, rheology and dewatering behaviour of kaolinite dispersions,” *Int. J. Miner. Process.*, vol. 71, no. 1–4, pp. 247–268, 2003.

[101] L. Besra, D. K. Sengupta, S. K. Roy, and P. Ay, “Influence of polymer adsorption and conformation on flocculation and dewatering of kaolin suspension,” *Sep. Purif. Technol.*, vol. 37, no. 3, pp. 231–246, 2004.

[102] M. J. Pearse, “Historical use and future development of chemicals for solid-liquid separation in the mineral processing industry,” *Miner. Eng.*, vol. 16, no. 2, pp. 103–108, 2003.

[103] R. Buscall, T. Heath, C. Wa, and L. R. White, “The Consolidation of Concentrated Suspensions,” pp. 873–891, 1987.

[104] K. a. Landman and L. R. White, “Predicting filtration time and maximizing throughput in a pressure filter,” *AIChE J.*, vol. 43, no. 12, pp. 3147–3160, 1997.

[105] D. a. Sievers, L. Tao, and D. J. Schell, “Performance and techno-economic assessment of several solid-liquid separation technologies for processing dilute-acid pretreated corn stover,” *Bioresour. Technol.*, vol. 167, pp. 291–296, 2014.

[106] M. Scholz, “Review of recent trends in Capillary Suction Time (CST) dewaterability testing research,” *Ind. Eng. Chem. Res.*, vol. 44, no. 22, pp. 8157–8163, 2005.

[107] T. J. Hwa and S. Jeyaseelan, “Conditioning of oily sludges with municipal solid wastes incinerator fly ash,” *Water Science and Technology*, vol. 35, no. 8. pp. 231–238, 1997.

[108] J. R. Pan, C. Huang, M. Cherng, K. C. Li, and C. F. Lin, “Correlation between dewatering index and dewatering performance of three mechanical dewatering devices,” *Adv. Environ. Res.*, vol. 7, no. 3, pp. 599–602, 2003.

[109] W. Ma, Y. Q. Zhao, and P. Kearney, “A study of dual polymer conditioning of aluminum-based drinking water treatment residual.,” *J. Environ. Sci. Health. A. Tox. Hazard. Subst. Environ. Eng.*, vol. 42, no. 7, pp. 961–968, 2007.

[110] D. Antelmi, B. Cabane, M. Meireles, and P. Aimar, “Cake collapse in pressure filtration,” *Langmuir*, vol. 17, no. 22, pp. 7137–7144, 2001.

[111] D. Klemm, B. Heublein, H. P. Fink, and A. Bohn, “Cellulose: Fascinating biopolymer and sustainable raw material,” *Angew. Chemie - Int. Ed.*, vol. 44, no. 22, pp. 3358–3393, 2005.

[112] J. Davidovits, “Geopolymers,” *J. Therm. Anal.*, vol. 37, no. 8, pp. 1633–1656, 1991.

[113] P. Duxson, J. L. Provis, G. C. Lukey, S. W. Mallicoat, W. M. Kriven, and J. S. J. Van Deventer, “Understanding the relationship between geopolymer composition,

microstructure and mechanical properties," *Colloids Surfaces A Physicochem. Eng. Asp.*, vol. 269, no. 1–3, pp. 47–58, 2005.

[114] S. Nusri, "Using Surface Geopolymerisation Reactions to Strengthen Athabasca Oil Sands Mature Fine Tailings," University of Alberta, 2015.

[115] A. de Sousa Mol, I. Martins, and R. L. Oréfice, "Surface-pegylated chitin whiskers as an effective additive to enhance the mechanical properties of recycled ABS," *J. Appl. Polym. Sci.*, vol. 132, no. 35, p. n/a–n/a, 2015.

[116] A. T. Paulino, J. I. Simionato, J. C. Garcia, and J. Nozaki, "Characterization of chitosan and chitin produced from silkworm crysalides," *Carbohydr. Polym.*, vol. 64, no. 1, pp. 98–103, 2006.

[117] M. N. . Ravi Kumar, "A review of chitin and chitosan applications," *React. Funct. Polym.*, vol. 46, no. 1, pp. 1–27, 2000.

[118] J. T. DeJong, B. M. Mortensen, B. C. Martinez, and D. C. Nelson, "Bio-mediated soil improvement," *Ecol. Eng.*, vol. 36, no. 2, pp. 197–210, 2010.

Appendix A

Proper mixing is the key factor to flocculation process. To test if the mixing is appropriate, capillary suction time (CST) measurement, and the volume of water released after placing the treated MFT on a 150 μm aperture sieve, were used to evaluate the flocculation performance under different mixing conditions.

In earlier trials, a stainless steel tank with four baffles at 90° angle was used as the stirring vessel, as shown in Figure A.1, which has a diameter of 10.9 cm. The impeller is a curved blade turbine (CBT) with three blades, with an angle of 120° between two near blades, as shown in Figure A.2. The diameter of the impeller is 6.4 cm.

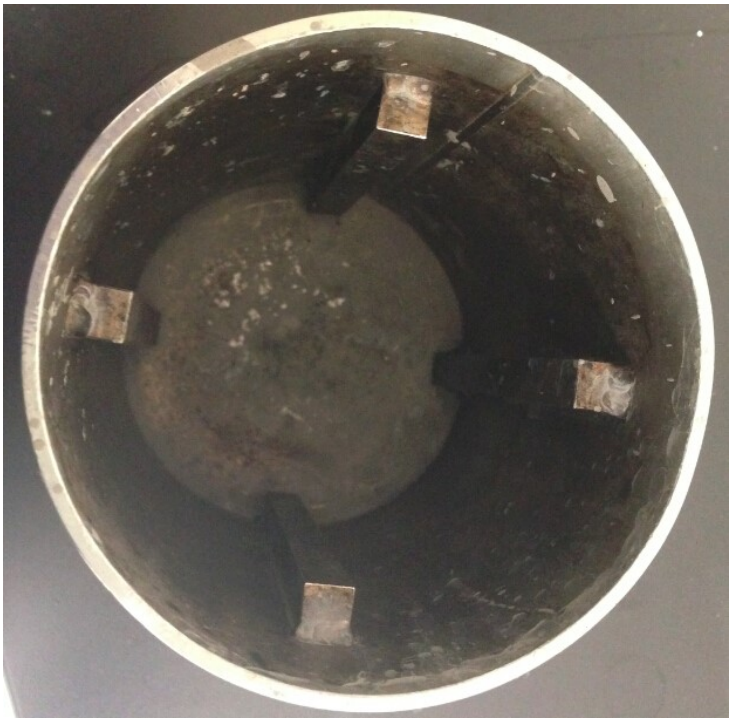

Figure A.1 Top view of the stainless steel tank with baffles.

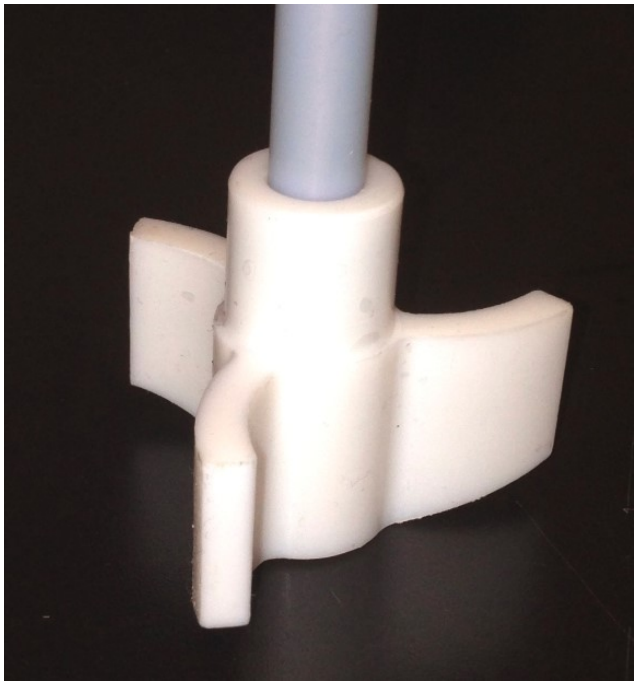

Figure A. 2 the CBT impeller.

In these tests, 500 g MFT was treated with A3335 (stock solution was at 0.4 wt%) and lignosulfonate (stock solution was at 2.0 wt%), and the dosage of both polymers was fixed at 1 kg/t. After a series of experiments performed by a previous graduate student, it was shown that 600 rpm was the optimal stirring speed and the best result was observed by adding lignosulfonate first followed by A3335.

However, during the tests it was observed that the flocculation process was not efficient as there was significant amount of what seemed to be unreacted gel-like MFT left on the surface. It quickly turned out that the agitator set up could not adequately agitate the MFT. It was possible that the level of MFT in the stainless steel tank was too high for the impeller as the CBT type impeller can only generate radial flow. Several experiments were then conducted to assess the efficiency of the mixing in the stainless steel tank using the CBT impeller.

In the control experiment, the impeller was set at a fixed position, which was about 25 mm from the bottom of the tank. In the next test that followed, the position of the impeller was first placed at 25 mm from the bottom of the tank. After adding A3335, the impeller was raised to the position just beneath the surface of MFT until treatment ended. The water release results for both experiments were listed in Table A.1.

Table A.1 Comparison of water release of experiments with impeller in different positions

	Water Release (mL)		
	24h	48h	72h
Control Experiment (impeller at 25 mm from bottom)	54	---	---
Experimental Group (impeller moved from bottom to top)	103	136	155

In the control experiment, there was very a small volume of water released in day 1, with no more water release in the next two days. However, after moving the impeller to the top, there was less gel-like MFT on the top and more water release. Higher stirring speed had been tested under the same conditions, and found unsuitable.

Therefore, for better flocculation outcomes, a 2 L beaker with a diameter of 12.6 cm and a pitch blade impeller (PBT, as shown in Figure A.3) with a diameter of 10 cm which can generate both radial and axial flow were used. The ratio of impeller diameter to beaker diameter is D_i/D_b= 0.79.

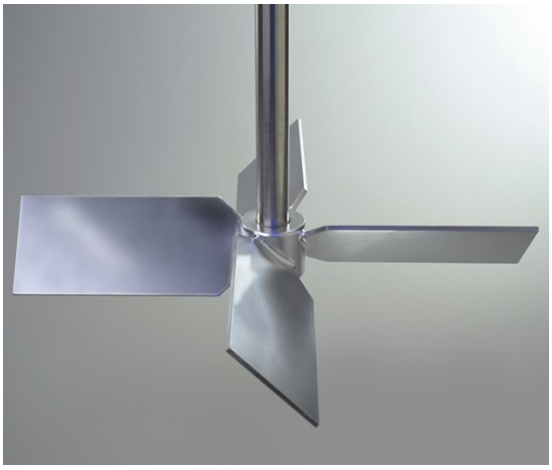

Figure A. 3 PBT impeller.

When placed into the 2 L beaker, the 500 g MFT sample filled to a height of 4.9 cm, which was inside the effective agitation range of the impeller. The agitation efficiency was significantly improved compared to the stainless steel tank and CBT impeller.

Appendix B

The drain pipe under pressure filtration system was a straight plastic pipe. When filtration proceeded to a time that the filter cake started collapsing, the compressed air blew out with filtrate fluid and hit the bottom of the beaker, which led to random fluctuations in the readings of the weighing balance. To avoid the effect of air flow and to maintain accurate readings of filtrate volume, a "T" glass joint was used to help release the impact of air flow, as shown in Figure B.1. After the adjustment, the random fluctuation of readings due to the air flow was eliminated.

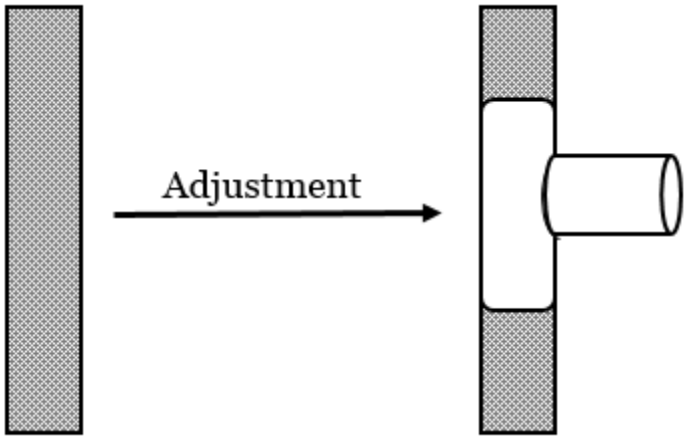

Figure B.1 Adjustment of drain pipe.